UNIVERSITÀ DEGLI STUDI DI PALERMO

PhD Course in Chemical, Environmental, Biomedical, Hydraulic and Materials Engineering
Dipartimento di Ingegneria
S.S.D. CEAR-01/A

CRITICALITY ANALYSIS IN WATER DISTRIBUTION NETWORKS BASED ON A MINIMUM PRESSURE CRITICALITY INDICATOR

PhD Candidate:

Ing. Daniele Puleo

PhD Course Coordinator:

Prof. Ing. Giorgio Domenico Maria Micale

Supervisor:

Prof. Ing. Tullio Tucciarelli

Co-Supervisors:

Ing. Marco Sinagra

Ing. Calogero Picone

XXXVIII CYCLE
GRADUATION YEAR 2025

ABSTRACT

Water distribution networks (WDNs) represent an urban infrastructure essential for a safe and reliable water supply, whose management is complex and fundamental for public health. Growing urbanization and the increase in global water demand (estimated to rise by 20-30% by 2050) exacerbate the challenges posed by often outdated infrastructure, causing supply interruptions, excessive losses, and water quality problems.

Traditional numerical models for WDNs, that are crucial for predicting network behavior, are influenced by considerable limitations in some specific scenarios: the demand driven (DD) approach produces unrealistic results under conditions of water deficiency or failures of network components, as it assumes that demand is always met. The head driven (HD) approach, while considering a relation between flow rate and pressure, overlooks the intrusion of air into the pipes. Air entrainment, which can occur at zero relative pressure, converts parts of the pressurized flow into free surface flow, altering hydraulic dynamics and potentially increasing velocities and degrading water quality (e.g. turbidity). All traditional models ignore the possibility of air intrusion, and this consequently impacts the computed results in terms of flow regime and pressures.

The drawbacks of these models directly impact the validity of performance and criticality indicators, especially in pressure reduction scenarios. Many current indicators rely solely on network's topological characteristics or hydraulic performance, without holistic integration and ignoring realistic scenarios such as air intrusion. A more accurate and comprehensive assessment of the weaknesses of each network element is therefore needed.

To address these challenges, this thesis focuses on two main objectives: first, development of a new numerical model (Minimum Pressure - MP) for WDNs. This model aims to overcome the limitations of the DD and HD approaches by assuming pipe permeability to air and a zero minimum relative pressure in all nodes of the network. The MP model will be able to identify pipes where free surface flow, due to

air intrusion, may occur, providing more accurate and realistic results, especially under water scarcity conditions.

The thesis also focuses on the definition of a new criticality indicator (Minimum Pressure Criticality Indicator - MPCI). The MPCI will innovatively integrate the network's topological characteristics, derived from the "structural hole" theory, with the hydraulic solution provided by the numerical model used (MP or traditional). This indicator will offer a strategic perspective for prioritizing pipe maintenance, supporting water managers in their decision-making and asset management of WDNs.

Results computed on the real WDNs selected as test cases showed that, while the output values calculated by MP model in normal functioning conditions of the network are similar to the ones provided by DD and HD approaches, in pressure deficiency conditions instead the results vary significantly and MP is able to correctly predict the hydraulic dynamics of the network, differently from conventional approaches. MPCI was calculated in the chosen networks to establish a prioritized maintenance for pipes, and it proved to be able to give priority both to pipes subject to hydraulic stress and to pipes crucial for network functioning, whereas other criticality indicators available in the literature could fail to identify critical pipes, especially in water reduction conditions.

In conclusion, by providing a more physically grounded numerical model and a more accurate criticality indicator, this thesis aims to fill the current gaps in simulation models and assessment tools, crucial for the resilient management of WDNs in the era of increasing challenges related to water scarcity and water quality control, accentuated by climate change.

Keywords: numerical modeling, head driven, free surface flow, open channel flow, criticality indicator, criticality assessment, structural hole, prioritized maintenance

List of Contents

List of Figures

List of Tables

Acronyms

Acronym	**Description**
CI	Criticality Indicator
DD	Demand Driven
EPS	Extended Period Simulation
GGA	Global Gradient Algorithm
HD	Head Driven
ISO	Isolation valve
IVS	Isolation Valve System
MP	Minimum Pressure
MPCI	Minimum Pressure Criticality Indicator
PI	Performance Indicator
PRV	Pressure Regulating Valve
WDN	Water Distribution Network
WEC-Network	Water Engineering Consulting - Network (software developed by hydraulic research group at UNIPA)

1. Introduction

1.1. Background

Water is the main resource for sustainability and economic growth of human communities. Water distribution networks (WDNs) represent one of the most important assets of urban infrastructures, with the purpose of guaranteeing a safe, stable and efficient water supply to consumers. Its functionality is directly related to public health and to the quality of urban life. However, the management of these highly complex and interconnected systems, which can extend for kilometers with an elevated number of elements such as pipes, junctions, isolation and pressure reduction valves, pumps, turbines, reservoirs and tanks, represents a significative challenge that has to be faced from different points of view.

Nowadays, several problems affect the quality and efficiency of water distribution service. Water discoloration events, characterized by the systematic detachment of accumulated material on pipes' walls, are one of the main reasons for customer complaint (Boxall & Saul, 2005, Braga *et al.*, 2020). These events can be the result of high shear stress on pipe walls, exceeding regular operating values, due for example to high flow rates or pipe failures (Braga *et al.*, 2020). Besides discoloration, WDNs are notoriously susceptible to leakages that entail large economic losses and environmental impacts; water losses have become a severe global issue that in some urban areas can reach up to 80% of the total supplied water (Hommes & Boelens, 2016). The damage of leakage is not only restricted to the hydric resource itself, but it includes also the energy involved in the process: about 7%-8% of global energy production is used for domestic water production and distribution and 67% of the energy consumed in the water industry is related to pump stations (Pabi *et al.,* 2013).

This implies that the impact of an efficient management of WDNs will drastically rise in the upcoming future, also as a consequence of the intensive and enlarging urbanization: in fact, more than half of the world's population already inhabit urban regions and this ratio is expected to reach about 68% by 2050 (UN-DESA, 2018).

Demographic expansion, also due to the increasing pressures exerted by climate change, requires large scale investments by water managers, in order to provide uninterrupted and safe water with sufficient pressure.

Moreover, global water demand is expected to constantly increase until 2050 (Fig. 1), with an estimated total rise between 20%-30% with respect to actual levels, mainly guided by increasing requests in industrial and domestic sectors (Eggimann, 2017). Currently more than 2 billion people live in countries with elevated water stress and about 4 billion people experience serious water scarcity for at least one month per year (Mekonnen and Hoekstra, 2016). In this context, resilience and operational efficiency of water distribution networks have become primary concerns for water industry operators.

The actual outlook, characterized by aging hydraulic infrastructures and increasing sensibility of customers towards the quality of water service entails the adoption of innovative and proactive approaches. Several WDNs operate beyond their expected lifespan, often lacking the necessary maintenance and without any adaptation to the increasing demands, with frequent supply interruptions, excessive leakages and water quality issues. In the past traditional design and management of WDNs were often based on practical experience more than rigorous scientific principles, focused mainly on satisfying water demand and neglecting important aspects such as water quality (Vreeburg *et al.*, 2009); moreover, aspects such as the role of isolation valve systems (IVS) were not accounted for in the design process of WDNs, as well as the consequences of their possible failures. These issues are combined with those related to difficult leakage localization, scarcity of sensors and overall networks complexity.

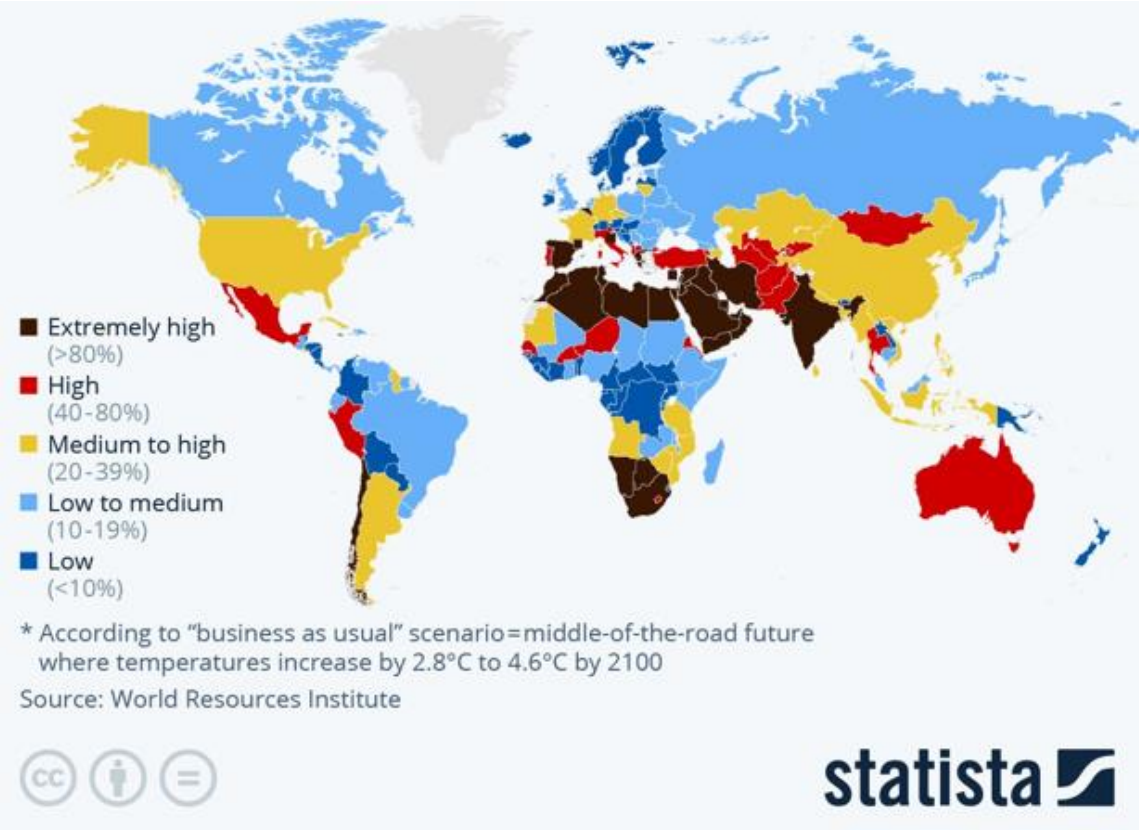

Figure 1. Projected ratio of human water demand to water availability (water stress level) in 2050 (source: World Resources Institute)

1.2. Statement of the problem

To effectively deal with these challenges it is essential to use advanced numerical modelling and optimization tools, that are crucial to link the WDN geometry and materials to key parameters such as nodal flow rates and pressures. However, traditional numerical modeling approaches for WDNs are affected by significant criticalities, which limit their ability to correctly represent the real operating conditions, especially in complex or water scarcity scenarios (Khadr *et al.* 2022, Fontanazza *et al.*, 2013, Fortunato, 2012). Demand-Driven (DD) approach assumes that nodal demand in each node is always satisfied regardless of the available pressure in the same node: while this hypothesis is valid in regular operating conditions and in properly designed networks, it becomes unrealistic and produces unrealistic results in water scarcity conditions or in the event of network elements' failure (pipes, pumps), leading to negative pressures in some nodes and consequently to serious errors in flow rate results in the whole WDN (Fortunato, 2012, Tucciarelli *et al.*, 2025). To overcome these issues, several Head-Driven (HD) approaches were developed (Khadr *et al.* 2022, Pacchin, *et al.*, 2017) in which the actual flow rate in each node depends on the available pressure, based on algorithms that provide the mathematical relation assumed between delivered flow rate and head. Despite these improvements, all these models share the critical assumption that air cannot enter the distribution network (Khadr *et al.* 2022, Tucciarelli *et al.*, 2025): this hypothesis is not always true and it can be shown that air intrusion in WDNs can be caused, for example, by small fractures or by vents in transport pipes when water pressure attains the zero relative value. A more in-depth analysis of air intrusion hypothesis can be found in section 3. Air entrainment changes part of the pressurized flow in pipes into free surface flow, significantly modifying flow dynamics in the WDN and its mathematical representation (Tucciarelli *et al.*, 2025). This issue is crucial and of utmost importance for WDNs, especially during pipes' maintenance or water scarcity scenarios, where pressures reduction, due to intermittent distribution, can seriously affect the network: in fact, it can be shown that the occurrence of free surface flow can lead to increased velocities in pipes and to a turbidity raise and water quality degradation (Boxall and Saul, 2005, Husband *et al.*, 2016, Shin *et al.*, 2023). All traditional numerical models for WDNs neglect air intrusion and the eventuality of open channel flows, overestimating piezometric gradients and underestimating velocities in these conditions (Tucciarelli *et al.*, 2025).

1.3. Research Objectives

The limits in traditional numerical models for WDNs directly impact the performance and criticality indicators used to respectively evaluate the efficiency and the resilience of water networks. Since the outcomes of these indicators are mainly based on the hydraulic simulations, they consequently inherit the same limitations: in fact, when hydraulic simulations cannot accurately represent the analyzed physical problem, particularly in water scarcity conditions, the outcome given by performance and criticality indicators cannot be completely reliable. Moreover, a large number of actual criticality indicators consider only some specific characteristics of the network: some studies are based essentially on the topological features of the network, such as its nodes' connectivity described by graph theory, without adequately integrating hydraulic calculations; other studies instead focus on the hydraulic performances, expressed e.g. by the rate of satisfied water demand, but without an appropriate integration with the WDN topological features or using hydraulic models that neglect realistic air intrusion scenarios, as described in section 3. For these reasons it is clear that a holistic and accurate evaluation of vulnerability and criticality of each single element in the network is required.

On the basis of these problems occurring in currently available numerical models and evaluation tools for WDNs, this thesis focuses on two main objectives:

1. Development of a new numerical model for water distribution networks, based on the Minimum Pressure (MP) approach. The new model aims at overcoming the actual limitations of demand driven (DD) and head driven (HD) approaches through the assumption of a more realistic hypothesis, i.e. pipe permeability to the air and the subsequent minimum zero relative pressure in all the nodes of the network. The MP model, unlike traditional models, is able to detect pipes where free surface flow can occur, due to air intrusion in the WDN. It will be shown how air intrusion hypothesis leads to more accurate and closer to reality results, in particular in water shortage conditions, compared to DD and HD approaches.

2. Development of a new criticality indicator, able to include the new MP model. The new criticality indicator (Minimum Pressure Criticality Indicator - MPCI) integrates in an innovative way topological characteristics of the network, provided by the "structural hole" theory, with the hydraulic solution provided by the adopted numerical model, including also the new one (MP or HD or DD). Results will show how the MPCI is able to give a different perspective for a prioritized maintenance of pipes, compared to other criticality indicators, providing water managers an accurate and comprehensive tool useful for asset

management and decision-making for WDNs. The adoption of the new MP solver leads to significantly different results when water scarcity scenarios become a realistic event for the analyzed WDN.

In summary, the present thesis aims to provide a new definition of the criticality indices for WDNs, taking full advantage of the most recent techniques for hydraulic simulation occurring in water scarcity scenario conditions, to provide a more physically based numerical model and a more accurate criticality indicator, essential for a resilient administration of water distribution networks, especially in an age characterized by the rising challenges, driven by climate change, of water scarcity management and water quality control.

1.4. Thesis Outline

The present thesis has been divided into five main chapters as follows:

- **Chapter One**: *Introduction* describes the background of the research and identifies the main issues in present numerical methodologies and criticality indicators for water distribution networks; research objectives are then presented.
- **Chapter Two**: *Literature Review* explores the state of the art about WDNs numerical modeling, focusing both on topological and on hydraulic modeling; successively, a description of the main evaluation tools such as performance and criticality indicators, available in the literature, is provided.
- **Chapter Three**: *Materials and Methods* presents the new numerical model (MP) and the newly developed criticality indicator (MPCI), elaborating on founding hypotheses and mathematical formulations.
- **Chapter Four**: *Results and Discussion* shows the results of the numerical tests carried out on real WDNs, comparing them with results obtained through other numerical methodologies and/or criticality indicators.

- **Chapter Five**: *Conclusion* summarizes the main findings and limitations of the present study; future research and improvements on the proposed methodology are finally suggested.

1.4.1. Related Publications

Part of the methodology and the results presented in this thesis can also be found in the following papers:

- Tucciarelli, T.; Puleo, D.; Nasello, C.; Sinagra, M. Air intrusion in Water Distribution Network (WDN) modelling. *Journal of Hydroinformatics* **2025**, 27 (9): 1371–1389. https://doi.org/10.2166/hydro.2025.027.
- Puleo, D.; Sinagra, M.; Picone, C.; Tucciarelli, T. Criticality assessment of pipes in water distribution networks based on the minimum pressure criterion, *Water* **2025**, 17(22), 3185; https://doi.org/10.3390/w17223185

2. Literature Review

2.1. Water distribution networks' components and characteristics

Water distribution networks are an integrated set of components, each with a specific function for the control, delivery or management of water flows: reservoirs generally represent the primary water supplier and are often linked to natural water sources as lakes or rivers, while tanks work as stock elements, aiming to provide balance in the variations between water supply and consumption, guaranteeing service continuity even during demand peaks or temporary water service interruptions.

Pipes constitute the physical network through which water flows and are usually classified into trunk or primary mains, usually the largest transport pipes which carry the higher flow rates, secondary mains, linking primary mains to local districts, and service lines or distribution pipes, branching towards user delivery points (Mays, 2000). Valves, located in specific areas of the networks, can regulate water flow and pressure (pressure regulating valves, PRV) or interrupt water flow in a given portion of the WDN (isolation valves, ISO); pumps are used to increase water pressure to guarantee sufficient pressure to the most distant parts of the network or to ensure service in high-altitude areas and are often controlled by automated systems to optimize energy consumption. Finally, WDNs are generally equipped with hydrants for emergencies, vents to free the transport pipes from air, and flow and pressure meters, which are fundamental for management and monitoring of the network, allowing leakages detection and useful for numerical models' calibration.

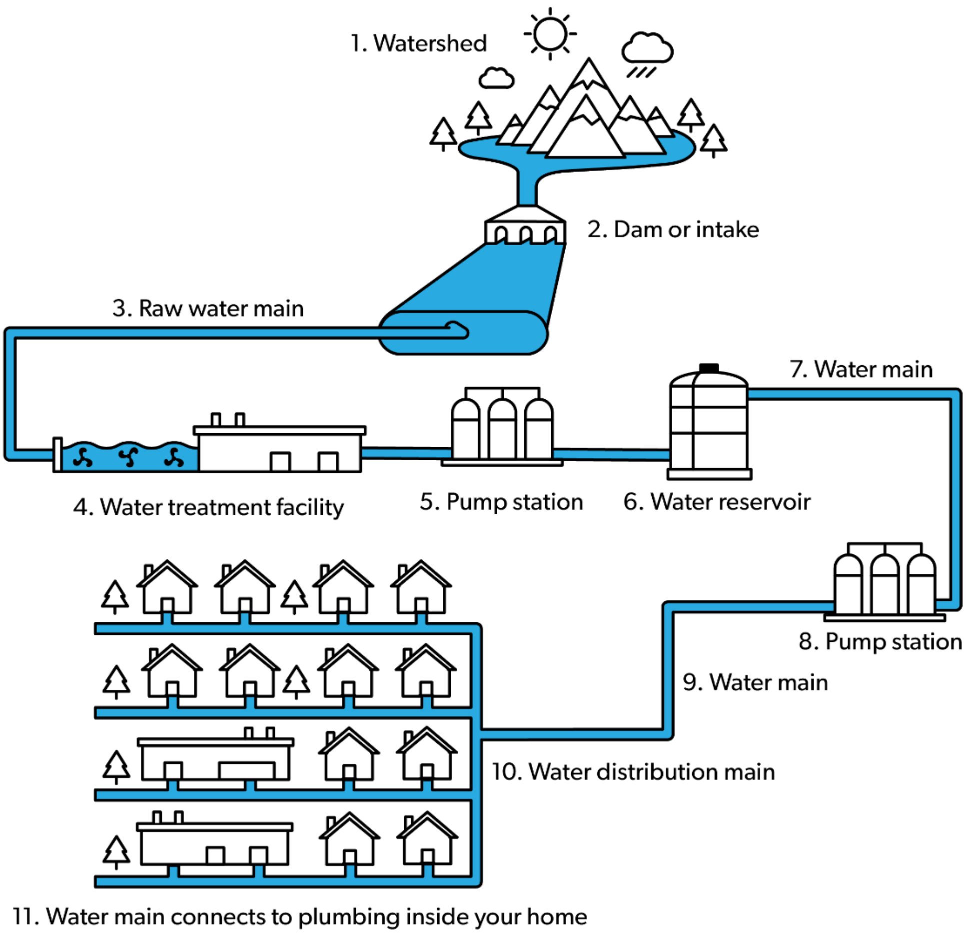

Figure 2. Typical schematization of a water distribution network, from main reservoir to consumers/homes (source https://pressbooks.bccampus.ca/plumbing3b/chapter/describe-water-services/#id1)

2.2. Recent developments and issues in WDNs management

The constant global population growth and the consequent water demand increment have forced water managers to invest and modify WDN systems in order to meet the requirements in terms of water quality and quantity: in fact, about 80% of total cost of water supply projects, for a given population, is invested in distribution system. In the last years, WDNs' evolution has been driven by the rising attention to sustainability, digitalization and infrastructural resilience, and this led to the development of:

- Smart Water Networks, with integrated sensors and actuators to allow a real-time monitoring of the WDN, making predictive maintenance easier and providing automatic response to abnormal events (pipe failure or contaminant intrusion).

- Variable control valves and variable-speed pumps to improve pressure management, dynamically adapting to functioning conditions.
- Advanced leakage detection systems, using artificial-intelligence-assisted hydraulic models (e.g. machine learning).
- Resilient approach to WDN design, incorporating redundancy criteria to better face extreme events such as earthquakes or water scarcity caused by drought, according to a multi-parameter logic.

However, several WDNs are nowadays complex and aged systems and are affected by multiple deterioration issues including:

- High water losses, with an average 40% of the total flow rate from the reservoir and peaks up to 73%.
- Frequent pipes failures, related to the average age of many WDNs which is often more than 30 years, against an average operational lifespan of about 40-50 years which suggests the need for significant maintenance interventions.
- Water quality issues, influenced by network condition, by the material accumulated over pipes internal wall and by the residual disinfectant concentration.

Finally, the performance management of WDNs is particularly challenging in developing countries, where most networks operate intermittently with reduced water service: in these situations, networks often fail to satisfy water demand and guarantee adequate water quality.

2.3. Numerical modeling of water distribution networks

Software for simulating hydraulic variables inside pipeline networks are fundamental for design and maintenance of water supply systems. The mathematical models, upon which these software are based, solve the discretized form of the governing equations of the physical phenomena occurring inside the pipes, and are able to identify in real time both the actual operating conditions and the network's behavior in future scenarios.

Usually, numerical modeling of a water supply system consists of two main phases:

1) Topological modeling
2) Hydraulic modeling

While the first phase includes only the connectivity information about the main elements of the WDN, which are the pipes and the water supply or delivery points (represent by nodes), in the second phase all the necessary hydraulic information are provided, including: geometric and hydraulic information about pipes (diameters, lengths, roughness) and about nodes (elevations, nodal demands), pressure-reducing valves and isolation valves' opening degree, reservoirs levels and other network's characteristics (pumps and/or turbines curves, tanks levels etc.).

The reliability of the outcomes provided by the numerical simulation is therefore highly influenced by the precision of the WDN input parameters: the analysis of a water distribution network presents different layers of complexity and several simplifying hypotheses are necessary to solve the problem.

2.3.1. Topological modeling

Topological modeling focuses on defining structural and connectivity characteristics of the WDN, representing the relations between network's components.

Graph theory constitutes an extremely natural and efficient approach to represent spatially distributed elements and their mutual connections and it is widely used in WDNs analysis to model contiguity and analyze network's structure. According to graph theory, a water distribution network can be expressed through a node – arc system representing the physical components, in which:

- **Arcs/edges** represent pipes, with their respective lengths, diameters.

- **Nodes** represent the network locations in which two or more pipes are connected. Nodes are typically divided into supply nodes (e.g. reservoirs, tanks) and demand nodes (e.g. consumers). They can also represent intermediate nodes, with neither water supply nor water demand, that facilitate connectivity between other nodes.

Graph theory's applications include adjacency modeling, realized through a segment graph, as the one proposed by Walski (1993), where valves are the connection points between two or more segments.

The interconnections between nodes make them extremely vulnerable to systemic risks and cascade failures, and graph theory becomes a useful instrument to quantify nodes and pipes' failure impact on the whole WDN, as well as the network's capacity to face the event of failures. Several studies about resilience analysis and performance evaluation use metrics provided by graph theory, as meshedness coefficient, clustering coefficient and co-spanning edge betweenness (Tornyeviadzi *et al.*, 2021), to finally identify key topological elements in the network and their attributes, which are responsible of the networks' resilience.

2.3.1.1. Topological classification of WDNs

The identification of a network's structure is essential to predict hydraulic behavior and distinguish key elements in the network. In the topological modeling of water supply systems several common configurations can be identified, depending on recurring connectivity features.

Looped networks are among the most frequent WDN configurations, appreciated for their redundancy and capability to provide alternative paths for water fluxes, especially in failure scenarios. The simple layout of looped networks often allows the use of indicators to characterize, according to a heuristic approach, network's resilience.

These networks can be distinguished into densely looped or hybrid-type networks, where the former are generally able to provide water even when failed pipes are closed, while the latter are more susceptible to long service interruptions. Optimization of looped networks can be realized by minimizing costs and at the same time guaranteeing adequate resilience. Hanoi WDN (Fujiwara & Khang, 1990), represented in Fig. 3, is a common example of looped network (source node depicted in blue):

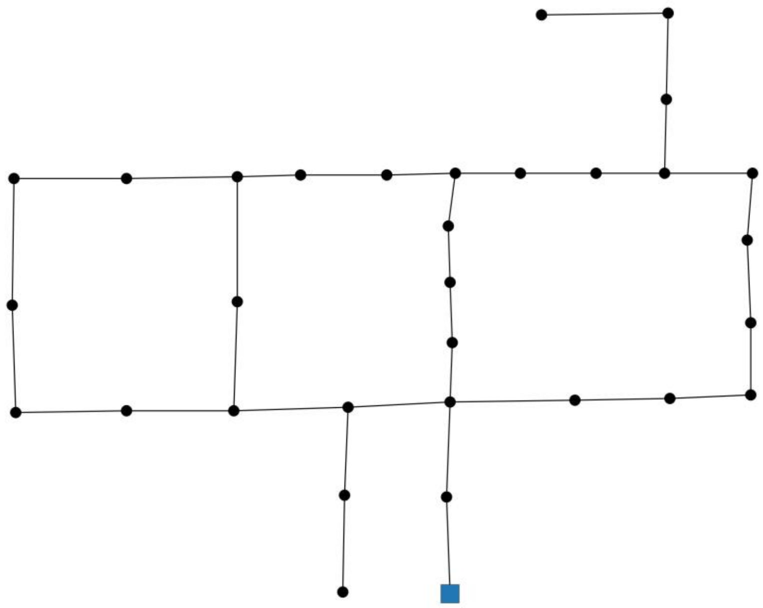

Figure 3. Hanoi water distribution network

Branched networks, unlike looped networks, present a tree-like structure, where branches (i.e., smaller pipes) spread from the main pipe directly linked to water reservoir; these networks therefore generally have no loops, occurring instead in hybrid looped-branched networks. Branched networks usually respond differently to element failures: in fact, failures in the main branch can affect all the downstream pipes and the connected nodes, directly impacting water supply to customers. Medina Bank WDN, in Belize (Abbott, 2012), presents a typical branched structure as it can be observed in Fig. 4:

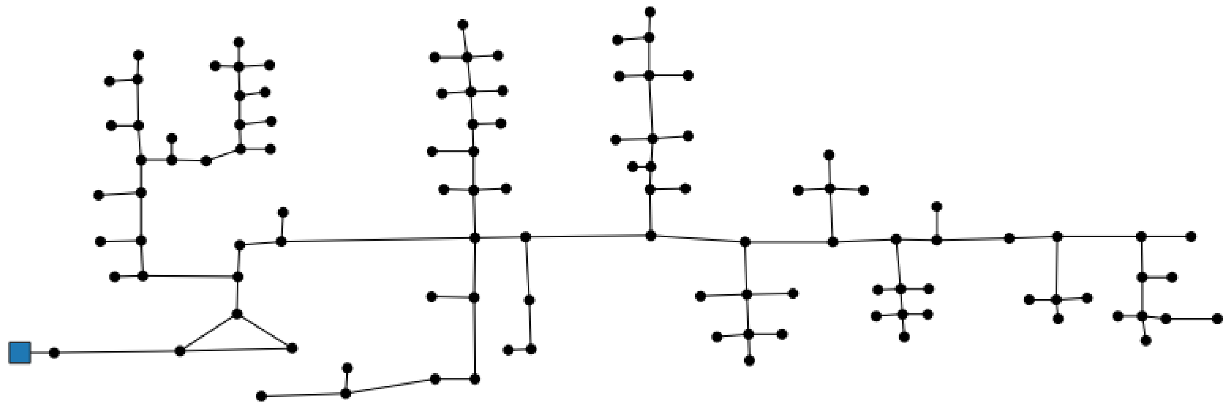

Figure 4. Medina Bank water distribution network

Observe that Medina Bank WDN does not represent a fully branched network, due to the presence of one simple loop composed of three nodes in the bottom-left area of the network.

Besides looped and branched networks, other common configurations can be identified, including:

- **Grid systems**: globally adopted for many WDNs due to their capability to offer multiple paths to water sources (see Fig. 5)
- **Ring systems**: a central ring surrounds service areas, delivering water from multiple directions and improving pressure and redundancy.
- **Radial systems**: generally extending from a central source towards the external areas, they are similar to a tree but where all branches originate from the same central point.
- **Dead-end systems**: while presenting a simple design, these WDNs can be affected by water quality issues, due to water stagnation, and limited reliability (only one path to water source).

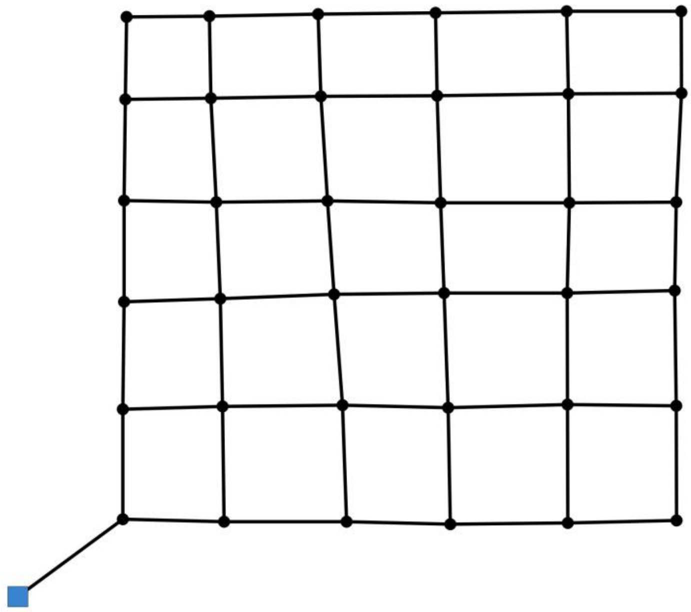

Figure 5. Typical grid network schematization

2.3.1.2. Segments identification

Segments identification is a crucial concept in WDNs management, especially for maintenance and rehabilitation planning. A segment is defined as the minimum isolated area of the WDN formed after valve closing (Walski, 1993): in fact, by closing the appropriate isolation valves, a part of the network containing one or more pipes becomes isolated and both planned and unplanned maintenance can be carried out on it, e.g. to repair a broken pipe.

All the segments in a network can be represented in a planar and undirected graph G=(N,E), called segment-valve (SV) graph by Walski (1993), where N are the segments and E are the isolation valves connecting segments.

In Fig. 6 a typical conversion from network graph to segment-valve graph is shown:

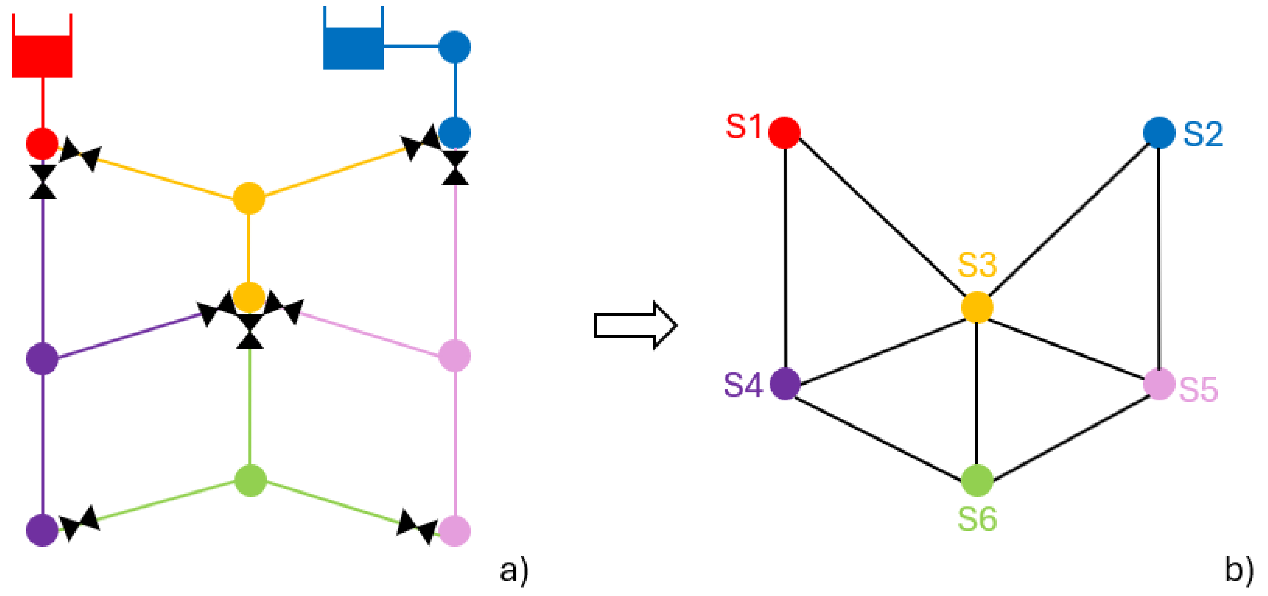

Figure 6. a) Real WDN with 9 isolation valves (in black) and b) conversion to segment-valve graph

Clearly, in the best possible case, every pipe in the whole network should have two isolation valves (one near each of their two nodes) so that, in order to isolate only one pipe, it would be necessary to close solely the two corresponding valves at its nodes, without affecting other parts of the network. However, in reality this is not the case for many WDNs and only a limited number of valves is installed: therefore, when even a single broken pipe needs to be isolated for maintenance, all the other functioning pipes belonging to the same segment will consequently be isolated; finally, depending on the specific topology of the network, it is also possible that the isolation of one segment leads to the unintended isolation from the water sources of other segments of the WDN.

In Fig. 7 the effects of the voluntarily isolation for maintenance of segments S3 and S5 (dotted segments in Fig. 7a) are shown. Observe that, due to isolation of these two segments, segment S2 (represented inside dotted box in Figs. 7a and 7b) remains unintentionally isolated from the only water source (segment S1).

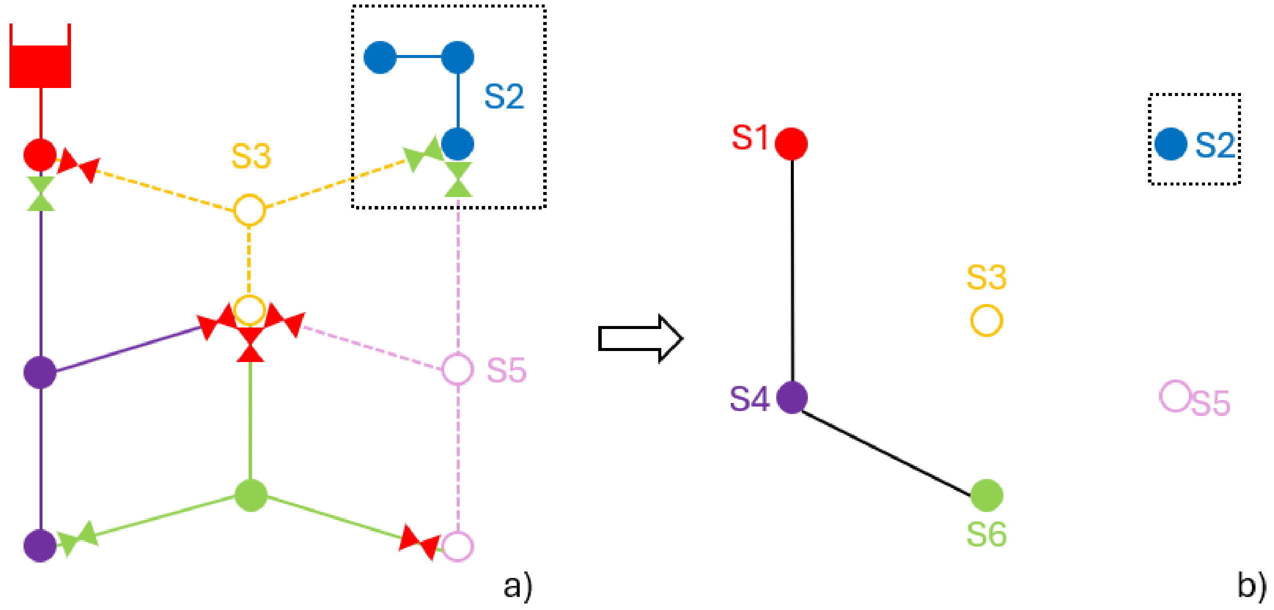

Figure 7. a) Isolation for maintenance of segments S3 and S5 leads to unintended isolation of segment S2 (opened valves in green, closed valves in red) and b) corresponding segment-valve graph

It is then evident how segments identification is essential to identify key valves that delimitate large segments in the network, in order to provide maintenance and guarantee their regular functioning; when all segments in the network have been identified, it is possible to define clusters of segments and determine which are the ones to prioritize for maintenance, but also to understand which segments, when isolated, affect others by unintentionally isolating them.

Segments identification is also useful for the design of new WDNs, given that it provides the possibility to identify strategic positions for new isolation valves that, when installed, allows to minimize the affected area of the network when a failure occurs, consequently minimizing the number of affected customers and reducing water leakage.

Several algorithms were proposed to realize segments identification in a WDN, such as the Breadth-First-Search (BFS) and the Depth-First-Search (DFS) algorithms (Walski 1993), the seed-filling algorithm and other methods based on topology matrices or adjacency matrices. In addition, efficient algorithms like the SVLU (segment valve local update) were developed to be integrated into optimization models, where a repeated segments identification process is necessary to evaluate each optimized configuration of the analyzed network.

2.3.2. Hydraulic modeling - steady state conditions

Hydraulic modeling is a pivotal aspect in water supply systems analysis and management, allowing to integrate connectivity information about the network's components, provided by topological modeling, with the real hydraulic parameters.
In order to get reliable results from hydraulic modeling, it is also essential to evaluate the unknown characteristics of the system by means of calibration, which consists in elaborating pressure and flow rates measurements in different operational conditions, and in specific points of the network, to compare them with the output values provided by the numerical model, in order to reduce, as much as possible, the differences between the measured and the simulated values.
Steady state modeling refers to water distribution networks analysis in steady state flow conditions, where flow rates and pressures are assumed to be time independent. This numerical approach is useful to simulate specific and fixed scenarios of the network, as for example during the peak hour of the day with the maximum consumption of the year, and it represents the most common modeling approach for WDNs.
The related systems of equations are solved to calculate the flow rate values in each pipe, the piezometric head and the actual flow rate delivered in each node of the WDN. The two basic physical principles upon which the equations are based are mass and energy conservation, expressed respectively by continuity equation for each node in the network and momentum equation for each pipe in the network:

$$\sum_{l=1}^{L} a_{il} q_l = Q_{a,i} \tag{1}$$

$$h_i - h_j = r_l q_l^m \tag{2}$$

where a_{il} is the element of the i^{th} row and i^{th} column of the incidence matrix A, describing connections between nodes and pipes, and is equal to 1, -1 or 0 respectively if flow rate q_l of pipe *l* enters in, exits from or if pipe *l* is not connected to node *i*. $Q_{a,i}$ is the actual flow rate extracted from node *i* (if positive, it represents a consumer's demand, otherwise it represents a water external supply). h_i and h_j are respectively the nodal head in node *i* and *j*, which are the two extreme nodes of pipe *l*, *m* is a coefficient depending on flow regime (usually between 1.75 and 2) and r_l is the hydraulic resistance of pipe *l*, given by:

$$r_l = K_l \frac{l_l}{D_l^n} \tag{3}$$

where K_l depends on pipe *l* roughness and l_l and D_l^n are respectively the length and diameter of pipe *l*, with *n* usually approximated as constant. Given a network composed of L pipes, N internal nodes, S external nodes or reservoirs, the following relation is valid:

$$L = M + N + S - 1 \tag{4}$$

M is the number of independent loops, where a loop is defined as any path having the same starting and ending nodes and independent loops are only those not corresponding to the combination of other simple loops; *S*-1 is the number of virtual loops, constituted by paths linking two external nodes (reservoirs). Momentum equation of Eq. (2) can also be written as follows:

$$-\sum_{i=1}^{N+S} a_{il} h_i = r_l q_l^m \tag{5}$$

And in matrix form as:

$$-\boldsymbol{A} \cdot \boldsymbol{h} = \boldsymbol{D} \cdot \boldsymbol{q} \tag{6}$$

where $\boldsymbol{A}$ is the incidence matrix [L x (N+S)] related to pipe-node connections, whose elements are the a_{il} terms, $\boldsymbol{h}$ represents nodal head vector [N+S], $\boldsymbol{q}$ represents the vector of pipe flow rates and $\boldsymbol{D}$ is the diagonal matrix containing the non-zero elements d_l, each related to one pipe *l*, given by:

$$d_l = r_l |q_l|^{m-1} \tag{7}$$

The non-linear system (1) – (5) consists of L+N equations where the unknowns, if we assume the actual flow rate (Eq. 1) in each node to be equal to the demand, i.e. $Q_{a,i} = Q_{d,i}$, are the L flow rate q_l and the N piezometric head h_i. It is useful to separate, in Eq. (6), the vector $\boldsymbol{h}$ into the two vectors $\boldsymbol{h_N}$ [N] and $\boldsymbol{h_S}$ [S], related respectively to internal nodes and reservoirs; applying the same procedure to matrix $\boldsymbol{A}$ we can write:

$$-(\boldsymbol{A_N} \cdot \boldsymbol{h_N} + \boldsymbol{A_S} \cdot \boldsymbol{h_S}) = \boldsymbol{D} \cdot \boldsymbol{q} \tag{8}$$

Continuity equations of Eq. (1) can also be expressed as:

$$\boldsymbol{A_N}^T \cdot \boldsymbol{q} = \boldsymbol{Q} \tag{9}$$

where $\boldsymbol{Q}$ represents the vector of nodal demand $Q_{d,i}$ in all internal nodes. The system can be finally written as:

$$\begin{cases} -(\boldsymbol{A_N} \cdot \boldsymbol{h_N} + \boldsymbol{A_S} \cdot \boldsymbol{h_S}) = \boldsymbol{D} \cdot \boldsymbol{q} \\ \boldsymbol{A_N}^T \cdot \boldsymbol{q} = \boldsymbol{Q} \end{cases} \tag{10}$$

2.3.2.1. Solution of water distribution network numerical modeling

Numerical solution of water distribution network problem consists in calculating the L flow rates in pipes and the N piezometric heads in internal nodes, once the geometric and hydraulic parameters of pipes and nodes, representing customers, are given. Observe that usually the nodal demands at each node incorporate the possible water demand along the pipes connected to the node: this implies that water demands along pipes' length are converted and added to the nodal demand of their respective nodes; this is, in fact, the most common case in real WDNs, where water delivery points are actually located along the length of each pipe.

Water distribution network numerical problem, expressed by system (10), is completely determined, given that the total number of equations [L+N] is equal to the total unknowns; however, due to the non-linearity of momentum equations, it is necessary the adoption of an iterative solution scheme. In the following sections we briefly present the most common numerical solution methods for WDNs.

2.3.2.1.1. Global gradient algorithm

Global gradient algorithm (GGA), proposed by Todini (1979) and based on the minimization of the total energy dissipated in the network, is implemented in many WDNs simulation models and commercial software such as EPANET.

In GGA continuity and momentum equations are first merged into a non-linear algebraic system with the same number of equations and unknowns. With simple algebraic manipulation, GGA splits the solution search into the solution of a non-linear system with a number of unknowns and equations equal to the number of interior nodes, plus the solution of a number of uncoupled equations equal to the number of pipes. The non-linear system is solved by applying the Newton-Raphson method, where the corresponding Jacobian matrix is diagonally dominant and positive definite.

First, consider the momentum equation, related to each pipe *l*, expressed as follows:

$$h_i - h_j = r_l q_l |q_l|^{\alpha-1} \tag{11}$$

where q_l is assumed positive if its direction is the same direction going from the first node i to the second node j. Combining Eq. (11) with the continuity equation (1), the system is completely defined in the L+N unknowns given by the flow rates in the pipes and the head levels in the interior nodes. According to Todini and Pilati (1987) the system can be written in matrix form as:

$$\boldsymbol{F}(\boldsymbol{\xi}) = \begin{bmatrix} \boldsymbol{D} & \boldsymbol{A} \\ \boldsymbol{A}^T & \boldsymbol{0} \end{bmatrix} \begin{bmatrix} \boldsymbol{q} \\ \boldsymbol{h} \end{bmatrix} - \begin{bmatrix} \boldsymbol{A_S h_0} \\ \boldsymbol{Q} \end{bmatrix} = 0 \tag{12}$$

where $\boldsymbol{\xi}$ is the vector composed by the vectors $\boldsymbol{q}$ and $\boldsymbol{h}$ previously defined. If we assume constant the r_l coefficients, the system can be solved by applying Newton-Raphson method. Observe that deriving Eq. (12) with respect to the generic component ξ_j of $\boldsymbol{q}$ or $\boldsymbol{h}$ vectors is equivalent to write:

$$\frac{\partial \boldsymbol{F}}{\partial \xi_j} = \frac{\partial}{\partial \xi_j} \begin{bmatrix} \boldsymbol{D} & \boldsymbol{A} \\ \boldsymbol{A}^T & \boldsymbol{0} \end{bmatrix} \begin{bmatrix} \boldsymbol{q} \\ \boldsymbol{h} \end{bmatrix} + \begin{bmatrix} \boldsymbol{D} & \boldsymbol{A} \\ \boldsymbol{A}^T & \boldsymbol{0} \end{bmatrix} \frac{\partial}{\partial \xi_j} \begin{bmatrix} \boldsymbol{q} \\ \boldsymbol{h} \end{bmatrix} \tag{13}$$

The matrix derivative calculated with respect to the vector of flow rate q_l is:

$$\frac{\partial}{\partial q_l} = \begin{bmatrix} \boldsymbol{D} & \boldsymbol{A} \\ \boldsymbol{A}^T & \boldsymbol{0} \end{bmatrix} = \begin{bmatrix} \boldsymbol{D'} & 0 \\ 0 & \boldsymbol{0} \end{bmatrix} \tag{14}$$

where every element in $\boldsymbol{D'}$ is zero unless for those along the diagonal, equal to:

$$D'_{ll} = \frac{|q_l|}{q_l} (\alpha - 1) r_l |q_l|^{\alpha-2} \tag{15}$$

The upper left matrix of the Jacobian will therefore be a diagonal matrix, where non-zero elements are equal to:

$$J_{ll} = \frac{\partial F_l}{\partial q_l} = (\alpha - 1) r_l |q_l|^{\alpha-1} + r_l |q_l|^{\alpha-1} = \alpha r_l |q_l|^{\alpha-1} \tag{16}$$

And the Jacobian matrix can be written as:

$$\boldsymbol{J} = \begin{bmatrix} \alpha\boldsymbol{D} & \boldsymbol{A} \\ \boldsymbol{A}^T & \boldsymbol{0} \end{bmatrix} \tag{17}$$

It can be shown that the generic *k* iteration of Newton-Raphson method can be expressed as:

$$\begin{bmatrix} \alpha\boldsymbol{D} & \boldsymbol{A} \\ \boldsymbol{A}^T & \boldsymbol{0} \end{bmatrix} \begin{pmatrix} \boldsymbol{q}^k - \boldsymbol{q}^{k+1} \\ \boldsymbol{h}^k - \boldsymbol{h}^{k+1} \end{pmatrix} = \begin{pmatrix} \boldsymbol{D}\boldsymbol{q}^k + \boldsymbol{A}\boldsymbol{h}^k + \boldsymbol{A}_S\boldsymbol{h}_0 \\ \boldsymbol{A}^T\boldsymbol{q}^k - \boldsymbol{Q} \end{pmatrix} \tag{18}$$

System (18) can be solved without other modifications; however, in this case, the system would be characterized by a symmetric but not positive definite matrix and it would have to be solved by direct methods. Otherwise, after some simple manipulations we obtain:

$$\alpha\boldsymbol{D}(\boldsymbol{q}^k - \boldsymbol{q}^{k+1}) - \boldsymbol{A}\boldsymbol{h}^{k+1} = \boldsymbol{D}\boldsymbol{q}^k + \boldsymbol{A}_S\boldsymbol{h}_0 \tag{19}$$

$$\boldsymbol{A}^T\boldsymbol{q}^{k+1} = \boldsymbol{Q} \tag{20}$$

Observe that the two systems (19) and (20) are coupled since the number of pipes L is generally higher than the number of internal nodes. By multiplying the left-hand side and right-hand side of Eq. (19) for the matrix $\boldsymbol{A}^T\boldsymbol{D}^{-1}$ and replacing the right-hand side of Eq. (20) to the product $\boldsymbol{A}^T\boldsymbol{q}^{k+1}$ obtained in the left-hand side of Eq. (19), the following equations for calculating piezometric heads at iteration *k*+1 are attained:

$$\boldsymbol{h}^{k+1} = -(\boldsymbol{A}^T\boldsymbol{D}^{-1}\boldsymbol{A})^{-1}[\boldsymbol{A}^T(\boldsymbol{q}^k + \boldsymbol{D}^{-1}\boldsymbol{A}_S\boldsymbol{h}_0) + \alpha(\boldsymbol{Q} - \boldsymbol{A}^T\boldsymbol{q}^k)] \tag{21}$$

Once the $\boldsymbol{h}^{k+1}$ vector is known, $\boldsymbol{q}^{k+1}$ can be calculated from Eq. (19) that can be now written as:

$$\boldsymbol{q}^{k+1} = \frac{\alpha - 1}{\alpha}\boldsymbol{q}^k - \frac{1}{\alpha}\boldsymbol{D}^{-1}(\boldsymbol{A}\boldsymbol{h}^{k+1} + \boldsymbol{A}_S\boldsymbol{h}_0) \tag{22}$$

Observe also that $\boldsymbol{h}^{k+1}$ can be obtained by Eq. (21) independently from the calculation of $\boldsymbol{q}^{k+1}$ and by solution of the following linear system:

$$\begin{cases} \boldsymbol{G}\boldsymbol{h}^{k+1} = \boldsymbol{B} & (23a) \\ \boldsymbol{G} = \boldsymbol{A}^T\boldsymbol{D}^{-1}\boldsymbol{A} & (23b) \\ \boldsymbol{B} = -[\boldsymbol{A}^T(\boldsymbol{q}^k + \boldsymbol{D}^{-1}\boldsymbol{A}_S\boldsymbol{h}_0) + \alpha(\boldsymbol{Q} - \boldsymbol{A}^T\boldsymbol{q}^k)] = (\alpha - 1)\boldsymbol{A}^T\boldsymbol{q}^k - \boldsymbol{A}^T\boldsymbol{D}^{-1}\boldsymbol{A}_S\boldsymbol{h}_0 - \alpha\boldsymbol{Q} & (23c) \end{cases}$$

Similarly, the flow rates $\boldsymbol{q}^{k+1}$ can be obtained through the uncoupled Eqs. (22) without the necessity to solve any algebraic system. $\boldsymbol{G}$ matrix is positive definite, given that $\boldsymbol{D}^{-1}$ is a diagonal matrix where every element is strictly positive. It can be shown that the generic element G_{ij}, where *i* and *j* are the two nodes of pipe *l*, is given by:

$$G_{ij} = -\frac{1}{r_{ij}\left|q_{ij}\right|^{\alpha-1}} \qquad if\ i \neq j\ and\ i\ is\ connected\ to\ j \tag{24}$$

$$G_{ij} = -\sum \frac{1}{r_{ij}\left|q_{ij}\right|^{\alpha-1}} \tag{25}$$

where the sum is related to all the pipes connected to node *i*; if *i* is not connected to *j* then clearly $G_{ij} = 0$.

Observe that the final flow rates distribution could not satisfy continuity equations at internal nodes. The initial pipe flow rates and nodal piezometric heads (respectively $\boldsymbol{h}^0$ and $\boldsymbol{q}^0$) can be determined in a different way: a first criterion consists in assuming, only at the first iteration, $\alpha = 1$, that is equivalent to a laminar flow regime. This implies that $\boldsymbol{G}$ and $\boldsymbol{B}$ will not depend anymore on the pipe flow rate of the previous iteration, the problem becomes linear and can be solved with a single iteration of Newton-Raphson method. The computed flow rate distribution will satisfy continuity equation and will be often close to the final one; however, piezometric heads distribution will be affected by a significant error, due to the completely incorrect estimation of head losses. It is therefore better to assume, as initial piezometric heads, the simple arithmetic mean of the reservoirs' piezometric heads or calculating the piezometric heads starting from any reservoir and following an arbitrary path until reaching every node.

Finally, convergence is guaranteed independently from the first iteration solution: in fact, it is not necessary to define the problem in terms of number of loops, and this avoids the possibility to obtain a non-convergent scheme.

2.3.2.2. Demand Driven Approach

Demand driven (DD) approach is the traditional approach for WDNs numerical simulation, and it is based on the assumption that the actual supplied flow rate $Q_{a,i}$ in each node is always assigned and equal to the respective nodal demand $Q_{d,i}$, regardless of the actual available pressure $h_{a,i}$ in the node:

$$Q_{a,i} = Q_{d,i} \tag{26}$$

The assumption of Eq. (26) implies that nodal heads are always sufficient to guarantee the requested demand.

Continuity and momentum equations are consequently solved considering fixed demand $Q_{d,i}$ in every node, without considering any pressure-flow rate relation.

Demand driven approach provides accurate results only when the actual nodal head is more than the nodal head required to meet the sought after nodal demand ($h_{a,i} > h_{r,i}$).

While the approach is quite simple because there is no relation between the flow rate and the pressure in a node, the founding hypothesis is no longer valid in pressure reduction scenarios, where the effective pressure in a node is not sufficient to guarantee the requested nodal demand. These scenarios are quite common in the event of pipe break, maintenance, water scarcity or when the total demand in the WDN rises due to additional water needed for firefighting: in all these circumstances, the demand driven approach is not able to identify nodes where nodal demand is not completely or even partially satisfied and the computed flow rates are not coherent with the respective nodal pressures; besides, results can also lead to unrealistic negative pressures.

Demand driven model can be useful especially for the design of new networks or to verify a regular operating condition of existing networks, where pressure and flow rates are expected to be equal to the design ones; however, in the pressure deficit cases described above, it provides unreliable results. Furthermore, demand driven approach is unable to represent water leakages in the network, which often affect real WDNs and induce significant variations in pressures and actual nodal flows delivered to consumers. Due to these limitations, several head driven approaches were developed to obtain reliable and accurate results even in pressure reduction events.

2.3.2.2.1. Numerical convergence of Demand Drivend models

The demand driven model provides the basis for deriving various simultaneous equation algorithms, such as the Global Gradient Algorithm (GGA), already presented in section 2.3.2.1.1, which, unlike the early local modeling approaches (Cross, 1936) that considered only one equation at time, use instead Newton-Raphson (NR) and Linear Theory (LT) methods to manage the non-linearity of equations. Demand driven model can be also represented by its transformed formulations such as pipe flows (PF) algorithms, loop flows (LF) algorithms and loop nodes (LN) algorithms, obtained by linear and non-linear transformations, as described in Todini & Rossman (2013).

The choice of algorithm influences the convergence characteristics of the numerical solution: Todini & Rossman (2013) showed that all formulations derived via linear transformation (such as GGA, PF, LF and LN) have exactly the same convergence rate and the only factor influencing convergence rate is the solution method used (NR or LT). Generally, NR algorithms based on linear transformations converge faster than LT algorithms. However, LT algorithms (such as LT-GGA) can converge quickly for low-precision requirements (e.g., 10^{-2} to 10^{-3} l/s, considering the logarithm of the maximum error in terms of discharges) making them comparable to linear NR approaches for practical problems.

The exception to this rapid convergence is found in algorithms derived via nonlinear transformation of the GGA, such as the Nodal Head (NH) approach: in fact, the NR algorithm applied to the NH formulation (NR-NH) exhibits poorer convergence properties. This is due to the non-linearity of the equations, which are of the square root type when they are expressed in terms of nodal heads, and can lead to slow alternating convergence. To mitigate this problem, it is sometimes necessary to include an under-relaxation coefficient. This highlights the risks of the nodal head-based NR approach, as conditions may arise that require a very large number of iterations to converge.

Finally, among the algorithms derived from the DD formulation, the NR-GGA and the LT-GGA (for low tolerance requirements) emerge as the most preferred due to their computational properties, such as the use of symmetric and sparse matrices, and because they do not depend on the loops chosen.

2.3.2.3. Head Driven Approach

Unlike the demand driven approach, the head driven (HD) approach is based on the assumption that a one-to-one numerical relation between the available nodal pressure and the respective nodal flow rate, in every node of the WDN, does exist:

$$Q_{a,i} = f(h_{a,i}) \tag{27}$$

For this reason, the actual nodal flow $Q_{a,i}$ may differ from the demand $Q_{d,i}$, although clearly in regular operating scenarios, where pressure is sufficient, the two flows are the same. Thus, head driven model is a more consistent and valid approach for WDN modeling, and, while more complex than the demand driven model, it is able to overcome the main limitation of the DD approach, especially in pressure reduction scenarios, identifying nodes with unsatisfied demands and providing reliable results also in the evaluation of the network in failure events. Head driven model is also essential in WDN rehabilitation planning because supplementary water supplies, due to leakages, significantly influence the performance of the network. In Fig. 8 the flow rate and pressure relations, according to DD and HD models, are shown:

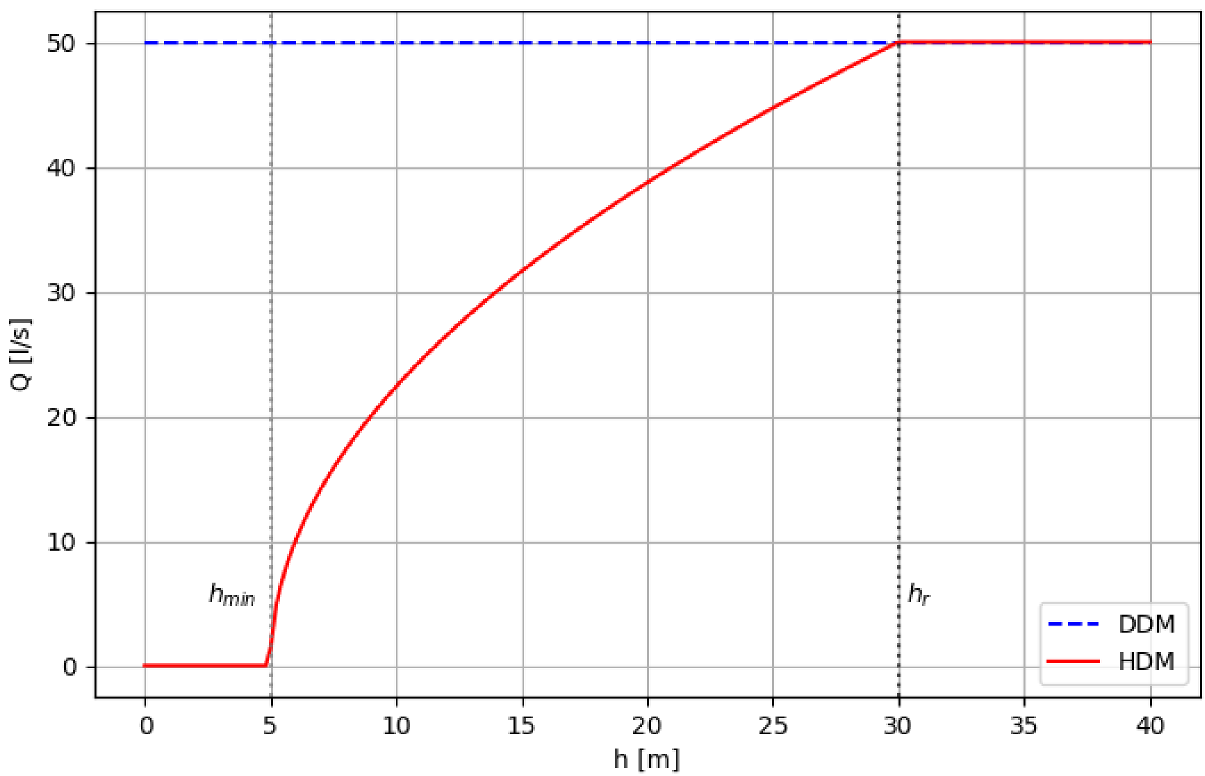

Figure 8. Nodal flow rate curves for DD model (in blue) and HD model (red)

Usually, the definition of a numerical relation between pressure and flow rate is considerably challenging, because it depends on several factors including network's configuration and nodes' planimetric distribution.

All these elements are highly variable for each node and a complete and detailed knowledge of them is almost never available for a typical network. Hence, only an approximated relation $Q_{a,i} = f\left(h_{a,i} - z_i\right)$ can be integrated in the solution of the system (Ciaponi *et al.*, 2007). Generally, the actual nodal flow can be expressed as a fraction of the demand:

$$Q_{a,i} = \alpha_i Q_{d,i} \tag{28}$$

where α_i varies between zero and one, depending on actual nodal pressure. If we define $h_{min,i}$ as the minimum nodal pressure below which the correspondent nodal flow is zero, the following relations hold:

$$\alpha_i = 1 \qquad if\ h_{a,i} \geq h_{r,i} \tag{29}$$

$$\alpha_i = 0 \qquad if\ h_{a,i} \leq h_{min,i} \tag{30}$$

$$0 < \alpha_i \leq 1 \qquad if\ h_{min,i} \leq h_{a,i} \leq h_{r,i} \tag{31}$$

Several relations defining α_i proposed by different authors are available in the literature and the most popular is the one introduced by Wagner *et al.* (1988):

$$\alpha_i = \left(\frac{h_{a,i} - h_{min,i}}{h_{r,i} - h_{min,i}}\right)^{\frac{1}{2}} \qquad if\ h_{min,i} \leq h_{a,i} \leq h_{r,i} \tag{32}$$

Eq. (32) is differentiable in every point except for $h_{a,i} = h_{min,i}$ and $h_{a,i} = h_{r,i}$ and this could represent an issue in numerical calculation procedure where differentiability is needed. For this reason, other formulations were proposed, as the one provided by Tucciarelli *et al.* (1999):

$$\alpha_i = \left(\sin \frac{\pi^{(h_{a,i} - z_i)}}{2(h_{r,i} - z_i)} \right)^2 \tag{33}$$

Authors such as Fujiwara *et al.* (1998) proposed different formulations that, similarly to Eq. (33), are characterized by differentiability in every point, though the only one with a physical basis is represented by Wagner relation of Eq. (32).

The head driven approach, although more realistic, is known to cause convergence difficulties and this issue has been examined in studies like the one carried out by Creaco (2025), in which the development of a global algorithm, based on the inverse outflow-head relation and on Newton-Raphson linearization, is described. The algorithm is extended to the cubic order of convergence and is able to incorporate multiple nodal outflows. The results provided by the analyzed tests cases indicate that the developed algorithm ensures stable and reliable convergence, eliminating the need for numerical relaxation procedure in all the case studies analyzed and showing that algorithms based on the head driven model can reach convergence in a reduced number of iterations when the order of convergence is increased to cubic.

2.3.2.4. Leakage modeling approaches

The modeling of leakages is a crucial aspect of WDNs management, made necessary by the fact that the traditional demand driven simulation approach assumes that the flow rates delivered to the nodes are always equal to the requested flow rates, regardless of pressure. As already described in previous sections, this hypothesis is not realistic under critical operating conditions, where the pressure is not sufficient to meet the demand, making head driven analysis or pressure driven analysis (PDA) necessary.

The software EPANET (Rossman, 2000), or its modified versions specialized in PDA simulations, uses emitters to simulate both water losses and the dependence of delivered flows on nodal pressure. The output flow $Q_{l,i}$ provided by an emitter is related to the pressure h_i by the general relation:

$$Q_{l,i} = c(h_i - z_i)^{\gamma} \tag{34}$$

where c is the emitter discharge coefficient and γ is an exponent which, in the absence of specific indications, can be assumed to be 0.5.

In leakage modeling, a modified version of the software EPANET-2 uses two main types of emitters: normal emitters and PDD emitters (Pressure Driven Demand). Normal emitters are specifically used to model water leakages, as it is assumed that leakages increase "indefinitely" with pressure. Their flow rate function is defined as:

$$Q_{l,i} = c{h_i}^{\alpha} \tag{35}$$

Where α is an exponent related to the emitter; Eq. (35) is valid unless pressures are negative, in which case emitters provide zero nodal flow rate. If a linear relation between losses and pressures is assumed, c coefficients of the normal emitters are calculated as the ratio between the reference localized leakage $Q_{lref,i}$ and the reference pressure $h_{ref,i}$:

$$c = \frac{Q_{lref,i}}{h_{ref,i}} \tag{36}$$

PDD emitters, on the other hand, are used to model the actual water flow rates delivered to users, as they limit the delivered flow rate $Q_{a,i}$ to the required flow rate $Q_{r,i}$ when the actual pressure $h_{a,i}$ is greater than the necessary pressure $h_{r,i}$ to fully meet the demand. The flow rate-pressure relation, assumed by default (proposed by Wagner, 1988), is expressed by the following equations, where $h_{min,i}$ is the minimum pressure above which a non-zero flow occurs:

$$Q_{a,i} = Q_{r,i}\sqrt{\frac{h_{a,i} - h_{min,i}}{h_{r,i} - h_{min,i}}} \qquad if\ h_{min,i} < h_{a,i} < h_{r,i} \tag{37.1}$$

$$Q_{a,i} = Q_{r,i} \qquad if\ h_{a,i} \geq h_{min,i} \tag{37.2}$$

$$Q_{a,i} = 0 \qquad if\ h_{a,i} \leq h_{min,i} \tag{37.3}$$

The FAVAD (Fixed and Variable Area Discharge) concept (May, 1994) represents an advanced model useful to describe the relation between pressure and losses in water distribution networks, overcoming the limitations of the simple theoretical orifice-based model.

Generally, a leak in a pipeline is comparable to the flow through an orifice, whose discharge is described by Torricelli equation:

$$Q = C_d A\sqrt{2gh} \tag{38}$$

where Q is the flow rate, C_d is the discharge coefficient, A is the area of the orifice, g is the acceleration due to gravity, and h is the pressure head. However, the orifice equation does not always provide a satisfactory model for the system's pressure dispersion. For this reason, a more general exponential-type relationship is widely used:

$$Q = Ch^{N1} \tag{39}$$

where C is the loss coefficient and $N1$ is the leakage model exponent, whose values experimentally range between 0.5 and 2.79.

The linear increase of the leak area A with pressure head h, especially when the pipe material behaves elastically, can be expressed as:

$$A(h) = mh + A_0 \tag{40}$$

where A_0 is the initial leak opening area in the absence of pressure, and m is the slope of the pressure head-area relation.

Replacing Eq. (40) in Eq. (38) results in the FAVAD equation:

$$Q = C_d\sqrt{2g}(A_0h^{0.5} + mh^{1.5}) \tag{41}$$

The relation between the conventional equation (Eq. 39) and the FAVAD equation (Eq. 41) was analyzed by Van Zyl & Cassa (2014) introducing the Leakage Number L_N, a dimensionless quantity that represents the ratio between the variable portion and the fixed portion of the water leakage in the FAVAD equation:

$$L_N = \frac{mh}{A_0} \tag{42}$$

The FAVAD-based analysis can provide useful information on the behavior of entire pressure management zones (PMZs) as showed by authors such as Deyi *et al.* (2014), who applied FAVAD concept to analyze the area of KwaDabeka Township, in KwaZulu-Natal (South Africa): the related studies conducted on real networks have shown anomalies, in particular that systems with $N1$ exponents greater than 1.5 had negative system leak areas, a physically impossible result, suggesting potential measurement errors, plastic deformation, or leaking boundary valves.

2.3.2.4.1. Head Driven numerical resolution of water distribution networks

A head driven numerical resolution of WDNs can be mainly based on simplified methods or methods that solve the entire system of equations.

Simplified methods are divided into two calculation steps: in the first step, a conventional demand-driven hydraulic calculation is performed, assuming $Q_{a,i} = Q_{d,i}$ in each node of the network. The second correction step is carried out only for critical nodes presenting an insufficient nodal head (i.e. $h_{a,i} < h_{r,i}$): therefore, corrected nodal flows $Q_{a,i}$ are calculated based on the piezometric line calculated in the first step. Among the simplified methods, one of the most common is that proposed by Tanymboh *et al.* (2001) which is based on the head value in the source node of the network. This method assumes that the relation between nodal flow in any critical node and the nodal head in source node remains the same even in pressure deficiency scenarios. However, this hypothesis is correct only if the pipes' flow rates, considering all the pipes connected to the considered critical node, remain unvaried in the tested conditions. Nonetheless, due to the fact that the results provided by the nodal flow rate correction step impact other nodes, apart from the critical nodes, the hypothesis is not valid anymore and the higher the pressure deficit conditions the higher the errors in the computed nodal flows. Besides, this method can only be applied to single reservoir networks (Ciaponi *et al.*, 2007).

Other methods solve the entire system of equations, including the momentum equations in each pipe, the continuity equations in each node and the equations linking the nodal flow and the pressure.

The number of equations is equal to the number of unknowns and therefore the problem has only one physically meaningful solution. Todini (2003) adapted his global gradient method (Todini & Pilati, 1998), initially designed for demand driven conventional calculation, to the head driven approach.

System for the head driven analysis can be expressed as follows:

$$\begin{bmatrix} \boldsymbol{D} & \boldsymbol{A_N} \\ \boldsymbol{A_N}^T & \boldsymbol{A_{nn}} \end{bmatrix} \begin{bmatrix} \boldsymbol{q} \\ \boldsymbol{h} \end{bmatrix} = \begin{bmatrix} -\boldsymbol{A_S h_s} \\ \boldsymbol{0} \end{bmatrix} \qquad (43)$$

where the matrices and vectors are the same given by system (10) and the main difference with respect to the traditional demand driven approach is represented by $\boldsymbol{A_{nn}}$ matrix, representing the relation between nodal heads and nodal flows. This is a diagonal matrix whose elements can be calculated by the scalar product $-(\boldsymbol{Q_a} + \boldsymbol{Q_l})\boldsymbol{h^{-1}}$, where $\boldsymbol{Q_a}$ is the vector containing the actual nodal flows $Q_{a,i}$ and $\boldsymbol{Q_l}$ is the vector of the concentrated leakages in nodes, calculated on the basis of the corresponding leakages in pipes. The nodal leakages-nodal heads relations can be obtained assuming that leakages in any pipe l are uniformly distributed; according to Germanopoulos (1985) the following equations can be applied:

$$Q_{leak,l} = \beta_l l_l (p_{m,l})^{\alpha_l} \qquad if\ p_{m,l} > 0 \tag{44}$$

$$Q_{leak,l} = 0 \qquad if\ p_{m,l} \leq 0 \tag{45}$$

where $p_{m,l}$ is the mean pressure of pipe l, calculated as the mean between the pressure of the two nodes of pipe itself, and l_l is pipe's length; α_l and β_l need an appropriate preliminary evaluation.

Water leakages distributed along the pipes can be correlated to the nodes in several ways: the simplest solution consists in equally dividing (50% - 50%) the total leakage between the two nodes of the pipe. Otherwise, a realistic alternative can be to divide the leakage depending on the nodal heads of the two nodes of the considered pipe. Water leakage in node i can be obtained as sum of the pipes flow rates from the pipes converging at the node itself:

$$Q_{leak,i} = \frac{1}{2} \sum Q_{leak,l} \tag{46}$$

Finally, matrix $\boldsymbol{Q_l}$, related to pipes, can be obtained as follows:

$$\boldsymbol{Q_l} = \frac{1}{2} diag \left(\boldsymbol{A_N}^T \begin{bmatrix} Q_{leak,1} & 0 & 0 & 0 & 0 \\ 0 & \vdots & 0 & 0 & 0 \\ 0 & 0 & Q_{leak,l} & 0 & 0 \\ 0 & 0 & 0 & \vdots & 0 \\ 0 & 0 & 0 & 0 & Q_{leak,L} \end{bmatrix} \boldsymbol{A_N} \right) \tag{47}$$

where $diag$ indicates that only the elements along the diagonal are considered. Taking into account matrix $\boldsymbol{Q_l}$ is essential in rehabilitation planning for WDNs, as supplementary water is needed due to leakages which significantly influence the performance of the network.

2.3.3. Hydraulic modeling - extended period simulation

Extended period simulation (EPS) is a hydraulic modeling approach that allows to analyze a water distribution network hydraulic behavior over a specific range of time, unlike steady state models which only consider a single time instant. EPS is essential in simulating more realistic conditions, with respect to steady state approaches, as the effective conditions of a WDN often vary considerably even in short periods of time: usually, in fact, demands from consumers change over a single day, where hours with the low demands are followed by hours where the demand raises until reaching its peak which can become even double with respect to the mean demand. Moreover, seasons have an impact on the typical consumers' demand, and periods such as summer can be characterized by a water supply shortage.

Generally, EPS simulations simply consist of a succession of steady state simulations, where each simulation is characterized by a different multiplier coefficient for the demands, impacting the nodal demand of every node. The series of multiplier coefficients is usually referred to as demand pattern. Each steady state simulation is carried out separately but only after the previous one has ended, as in this way the new initial conditions can be set.

Extended period simulations take into account the reservoirs and tanks' water level variations, that clearly depend on the balance between the water volumes supplied to the network and those extracted by consumers, hour after hour. In this case, the water levels are assumed as constant during each single steady state simulation, updated at its end, and finally becoming known piezometric heads of the successive simulation.

The parameters needed to perform an EPS usually consist in the duration of each single time interval in which the simulation is divided (*time step*) and the total simulation duration, that has to be sufficiently extended to characterize the studied events. Several models adopt a simulation duration of 24 hours, assuming that the demand pattern will be identical every day after the first. Usually, *time step* is set to be 1 hour or 30 minutes depending also on the considered network and the computational time.

Issues may arise about reservoirs' water levels, especially for simulations considering more than two or three days and this is why a different simulation or a shorter total simulation time approach could be needed.

Observe that EPS is applicable only to slow transients because, in the given time interval, flow conditions are assumed to be constant and inertial effects are neglected. However, flow regime is actually variable in different time intervals and for this reason a more realistic approach would be needed, considering and analyzing the rapid transients occurring in a network. In this context, the water hammer theory can be used to simulate rapid pressure transients in WDNs, as it can describe situations characterized by sudden variations of flow velocity, due e.g. to rapid valve closure, and accounts for water compressibility as well as pipe wall elasticity.

EPS is useful also for dynamic nodal vulnerability assessments, giving the possibility to identify the hours in which the network is more hydraulically vulnerable. EPS is supported by software as EPANET and WaterGEMS, and its capabilities are also enhanced by toolkits that allow interfacing with programming environments such as MATLAB.

2.3.4. Hydraulic modeling - unsteady state modeling

Unsteady state modeling concerns the transient physical and dynamic phenomena that could occur inside a water distribution network. Unlike steady state or extended period simulations, which assume constant or gradually variating conditions, unsteady state modeling analyzes the rapid response of the system to sudden changes, as for water hammers that can normally happen in the daily functioning of the network, and whose prevention is usually realized by actuating the appropriate isolation valves.

Low pressures in a network can induce water not to fill the entire pipe through which it flows, causing open channel flow that can be studied more in depth using an unsteady state modeling, focusing on the transition between open channel and pressurized flow.

Moreover, this modeling approach is useful also to get a more realistic monitoring of water quality, especially in the events of pipe failure.

However, while being certainly more accurate and giving more detailed insights about the network's real operating conditions, unsteady state modeling is considerably more complex, both from a mathematical and a numerical point of view, compared to traditional steady state modeling and extended period simulation, which instead can provide adequately reliable results with much less numerical effort.

2.3.5. Software for hydraulic modeling

Hydraulic modeling software is an essential tool to numerically simulate the hydraulic behavior of a water distribution network in real time but also to predict its performances in future scenarios. These programs incorporate the mathematical equations of the WDN problem (i.e. continuity and momentum equations) and solve them numerically using one of the methodology presented before (Global Gradient Algorithm, Linear theory etc.), to finally calculate values such as flow rates in pipes, nodal heads, reservoirs levels and even the concentrations of chemical substances inside the network. The utilization of these models constitutes a fundamental and necessary step to take for planning, management, improvement and efficiency of WDNs.

2.3.5.1. EPANET

EPANET is a software package widely used in a variety of contexts, both professional and academic, to simulate WDN hydraulic behavior. It was developed by U.S. Environmental Protection Agency (EPA) and its first version dates back to 1993. EPANET currently represents the standard reference software for WDNs numerical modeling worldwide, thanks to its variety of features and its simple graphical interface. Its numerical solver is based on the Global Gradient Algorithm proposed by Todini and Pilati (1988) and requires as input information some data as the topology of the network (nodes-pipes connections and their respective IDs) as well as the real geometrical data about pipes (length, diameter) and their roughness coefficients; it is also able to simulate the effect of pumps located in the network, using the pump's functioning curve as input parameter, and valves located in specific points. Once the simulation has been run, nodal flow rates, nodal heads and pipes flow rate are calculated and can be easily shown by a gradually colored map which depicts nodes and pipes with a color depending on the value of the parameter analyzed; results can also be shown in simple tables where the selected columns can be activated or deactivated. EPANET is also able to perform Extended Period Simulations, showing in each *time step* the computed values, and also perform water quality analysis, if the correct input data are provided.

While EPANET was originally based on a demand driven approach, some applications were developed to adapt it to a head driven approach: one of the most common is represented by the utilization of elements called "emitters" that allows to modulate a head dependent demand for nodes. Emitters can be used both to model nodes demand and also leakages in nodes. Nodal demand is partially satisfied when minimum pressure is not attained and is not satisfied at all (zero flow rate) if it is not possible to attain a positive pressure in the respective node. A newly developed method consists in a non-iterative procedure based on inserting a sequence of devices (GPV valve, fictitious junction, check valve and reservoir) at each demand node to represent different flow-pressure relations.

Extensions were developed and integrated into other software such as the EPANET-MATLAB toolkit, which is an open-source software that allows to significantly decrease computational effort and at the same time to implement optimization and performance evaluation algorithms for WDNs; moreover, several python packages incorporate EPANET numerical solver and can be easily downloaded. The known open-source software QGIS, useful for spatial visualization and design of different kinds of maps and that can be used also to build a WDN model, gives the possibility to download plugins implementing EPANET numerical solver, to dispose of an integrated and simple visualization interface. Another extension is WaterNetGen, useful for the automatic network model building and pipes design.

EPANET also has a complete and free user manual, with detailed description of each feature as well as of the mathematical equations behind the model.

For all these reasons, EPANET is a cornerstone in the study of WDNs, enabling complex analyses and serving as the basis for the development of new simulation and optimization methodologies.

2.3.5.2. WaterCAD

WaterCAD is a commercial software developed by Bentley System and used for WDNs modeling and design. It contains its own graphical editor in a Windows-based interface and provides detailed network modeling capabilities, being able to simulate water flow and pressure in complex networks, considering also elements such as pumps and valves. WaterCAD is able to perform both steady state and extended period simulations and provides models for water quality analysis, as chlorine decay, allowing to assess the impact on the whole network; it also includes features for automatic analysis of fire-fighting risks, numerically simulating network's behavior during fire scenarios and incorporates tools for the management and evaluation of energetic costs of the WDNs and demand prediction.

One of the main features consists in its capability to be used as standalone software or integrated in MicroStation or AutoCAD, using CAD functionalities in a simple and user-friendly environment. The input and output data are provided using tables inside the modeling environment and can be connected to GIS programs using shapefiles for data import and export.

WaterCAD also includes tools for data management, reports creation and for evaluating different design alternatives, making it easy to compare the results also using contour plots to depict areas with high pressures or with the selected parameters of interest.

2.3.5.3. WaterGEMS

WaterGEMS is another software developed by Bentley System and it is commonly used for WDNs modeling and management and for decision-making support. The software is considered a "superset" of WaterCAD, meaning that it integrates all WaterCAD main characteristics with the new features of WaterGEMS.

The network can be modeled in the software by using planimetries or satellite images, providing the necessary input information. WaterGEMS allows also to validate parameters such as pipes' lengths and diameters but also nodal and pipes flows, using features like "*flex table*". One of the main peculiarities consists in its ability to identify critical areas, as nodes with excessive pressure that can induce leakages or pipe failures, or as pipes with low velocities that can lead to deposit accumulation and consequently water quality deterioration. WaterGEMS was also the first commercial software to introduce the segment-valve topology and representation, providing instruments for segments identification and criticality analysis of the WDN. It is also efficiently combined with GIS tools to improve design and management of networks and it is able to support the implementations of pressure regulating valves or pipe modifications in critical areas, to finally increase hydraulic performance. WaterGEMS is known as a complete instrument for complex networks management and the identification of adequate interventions.

2.3.5.4. Other software for hydraulic modeling

In addition to the already presented software, the landscape of hydraulic modeling of WDNs also includes other important tools: InfoWorks WS Pro, developed by Innovyze, is one of the most powerful commercial software available, providing the possibility to precisely model large urban networks, including nodal demand management, dynamic modeling of reservoirs and pumps, emergency scenarios analysis and real-time support. Its graphical interface, integrated with GIS, and the possibility to interact with SCADA systems makes it an optimal tool for extensive utilities. Another noteworthy tool is Mike Urban+ Water Distribution (WD), part of the MIKE suite developed by DHI. This software integrates hydraulic modeling with geospatial data and offers both hydraulic and water quality simulations, with a particular focus on transient dynamics (hydraulic transients). It is particularly appreciated for its ability to integrate network models with broader hydrological and urban models. At the academic and open-source level, WDNetXL represents an interesting alternative, developed by the hydraulic engineering research group at the University of Perugia. This tool, based entirely on Microsoft Excel and VBA, allows for static and dynamic analyses, pressure optimization, criticality analysis, and leak detection. Although its interface is simpler than that of commercial software, it offers great flexibility for research and teaching purposes. Finally, in the advanced research field, numerous groups use custom modeling platforms in MATLAB or Python environments, leveraging libraries such as WNTR (Water Network Tool for Resilience), developed by NIST. These tools enable resilience analysis, failure simulation, and integration with machine learning algorithms for predictive network management.

The variety of tools available on the market reflects the complexity and diversity of needs in designing, managing and rehabilitating WDNs, with each software program having specific strengths or usage preferences based on context and objectives.

2.3.6. Assessing performance and criticality of water distribution networks

Performance and reliability evaluation of water distribution networks is a fundamental process to ensure an adequate water supply to people, to contrast the ongoing deterioration process and to identify critical elements of the system. WDN management is increasingly becoming risk-based and for this reason system reliability indicators are crucial for developing robust intervention policies in the event of potential crises.

In order to assess hydraulic performance and reliability there are some key aspects to take into consideration. First of all, the lack of structural and reliable data about the networks easily becomes a significantly limiting factor when a rehabilitation planning has to be realized: indeed, several water managers do not have all the necessary information to use complex numerical models or commercial software for decision-making support. To face these issues, several tools have been developed in the past to optimize economic investments in WDNs simply starting by realistic conditions of missing available data.

It is also important to realize that different tools can be used in a WDN reliability or performance assessment and that each one has its own advantages, as the simplicity of its application in certain conditions and limitations, especially in terms of the data neglected or not considered in the calculation. It is clear therefore that the choice of the appropriate evaluation tool has to be considered from more than one point of view, and that often a broader evaluation using more than one single tool can give a more comprehensive idea about the functioning of the network.

Different benchmarking strategies were developed and, while not being fully developed for systems working intermittently, they represent convenient instruments for comparing the effective hydraulic performance of the system with the expected one. Three main categories of benchmarking approaches exist, respectively based on: physical models, data models and performance indicators (PI), and criticality indicators (CI) models. The last category includes intrinsically simple instruments that are widely applicable in multi-objective systems like WDNs.

2.3.6.1. Performance indicators

Performance indicators are metrics that aim to provide a comprehensive and global evaluation of network's state and its capability to efficiently operate. These metrics often derive from calculations involving several parameters of the network, possibly related both to topological features and hydraulic ones, to finally output a single aggregated value, condensing all the incorporated information, that offers a clear and synthetic outlook on the performance of a specific network's configuration.

2.3.6.1.1. Reliability

Among the several developed indicators, one of the best known is the resilience index RI, originally suggested by Todini (2000), that quantifies the reliability of a WDN based on the system's power, including input, dissipated and surplus power and can be expressed as follows:

$$RI = \frac{\gamma \sum_{i=1}^{N} Q_i \left(h_i - h_{r,i}\right)}{\gamma \sum_{r=1}^{R} Q_r \, h_r + \gamma \sum_{p=1}^{P} Q_p h_p - \gamma \sum_{i=1}^{N} Q_i h_{r,i}} \tag{48}$$

where N, R, P are respectively the number of nodes, reservoirs and pumps and Q_i, h_i refer to nodal flow and head at node i, Q_r and h_r to source flow and total head at reservoir r, Q_p and h_p to pumping flow and head at pump p; γ is the specific weight of water and $h_{r,i}$ is the required head at node i. This index, which varies between zero and one, can be considered as the fraction between the surplus power (excluding the minimum power required at the node) and the total power provided by the system. A higher value of RI expresses a better capability of the system to face sudden failures: in a looped network, the goal is to provide more than the necessary energy to each node, in order to have a surplus amount of energy ready in case of failures.

Other variations of the resilience index were proposed, as the Modified Resilience Indicator MRI, developed by Jayaram & Srinivasan (2008), which quantifies network's reliability considering only the requested power and the surplus power:

$$MRI = \frac{\gamma \sum_{i=1}^{N} Q_i \left(h_i - h_{r,i}\right)}{\gamma \sum_{i=1}^{N} Q_i h_{r,i}} \tag{49}$$

unlike Todini's index, MRI can assume values greater than one and is useful in comparing different network's configurations, especially for design and rehabilitation.

While RI and MRI consider only hydraulic features, other indices where formulated encompassing topological metrics of the network, such as the Network Resilience Index NRI, proposed by Prasad & Park (2004) which considers a network as reliable if the diameters of the pipes connected to the same node do not vary excessively:

$$NRI = \frac{\gamma \sum_{i=1}^{N} C_i Q_i \left(h_i - h_{r,i}\right)}{\gamma \sum_{r=1}^{R} Q_r \, h_r + \gamma \sum_{p=1}^{P} Q_p h_p - \gamma \sum_{i=1}^{N} Q_i h_{r,i}} \tag{50}$$

where C_i is the uniformity coefficient of node i, depending on the number of pipes connected to it and their diameters, and it is equal to 1 in the diameters of the pipes connected to the node considered are the same, otherwise it decreases.

Observe that formulation of Eq. (48) was developed considering only the demand driven approach, admitting the possible presence of pumps in the WDN but not considering leakages. For this reason, a different formulation was proposed by Creaco *et al.* (2016) in order to deal with pressure driven models and also to be able to include the effect of water leakages. Starting from the original definition of Eq. (48) and after some manipulations, the Generalized Resilience Index is expressed as:

$$GRI = \frac{\max\left(\boldsymbol{q}_{user}{}^{T}\boldsymbol{H} - \boldsymbol{d}^{T}\boldsymbol{H}_{des}, 0\right)}{\boldsymbol{Q}_{0}{}^{T}\boldsymbol{H}_{0} + \boldsymbol{Q}_{p}{}^{T}\boldsymbol{H}_{p} - \boldsymbol{d}^{T}\boldsymbol{H}_{des}} \tag{51}$$

Where $\boldsymbol{q}_{user}$ and $\boldsymbol{d}$ represent respectively the vectors of nodal discharges and demands, $\boldsymbol{H}$ the vector of nodal heads corresponding to $\boldsymbol{q}_{user}$, $\boldsymbol{H}_{des}$ the vector of threshold desired values of nodal heads necessary to meet the demand in each node, and finally $\boldsymbol{Q}_{0}$, $\boldsymbol{H}_{0}$ and $\boldsymbol{Q}_{p}$ $\boldsymbol{H}_{p}$ the flow rates and nodal heas respectively in fixed head nodes and pumps. This index is more suitable to describe the variations in the power delivered to the users through the ratio of leakage to whole network outflow changes.

2.3.6.1.2. Redundancy

Redundancy in a water distribution network can be defined as the existence of alternative supply paths between a source node and a target node, or as a water supply backup capacity provided by additional loops connecting two nodes. It can be measured (Jeong & Kang, 2020) considering the network's average surplus head Red_1 and minimum surplus head Red_2, evaluated under abnormal conditions (i.e. where regular functioning of the WDN is not possible, as in failure events):

$$Red_1 = \frac{\sum_{i=1}^{N}\left(h_i - h_{r,i}\right)}{N} \tag{52}$$

$$Red_2 = \min\left\{h_i - h_{r,i}\right\}, \qquad i = 1, 2, \ldots, N \tag{53}$$

where Red_1 is the total head calculated subtracting elevation and required head $h_{r,i}$. Higher values of both parameters Red_1 and Red_2 refer to higher redundancy of the network.

Redundancy can be defined also considering only topological metrics of the WDN through parameters such as the Meshed-ness coefficient (Buhl *et al*., 2006) that quantifies the actual number of independent loops $(L - N + 1)$ with respect to the maximum number of possible loops $(2N - 5)$ in a planar graph:

$$R_m = \frac{L - N + 1}{2N - 5} \tag{54}$$

where L and N are respectively the number of edges/pipes and nodes. Eq. (54) provides an estimation of network's redundancy by calculating the percentage of independent loops but does not distinguish between source node and demand node.

2.3.6.1.3. Robustness

Robustness is defined as the capability of a system to withstand a given level of stress without suffering degradation or loss of function (Bruneau *et al.*, 2003) in the event of elements' failures or abnormal functioning conditions. It can be evaluated by calculating network average pressure maintenance Rob_1 and minimum pressure maintenance Rob_2 under abnormal conditions (Jeong & Kang, 2020):

$$Rob_1 = \frac{1}{N}\sum_{i=1}^{N}\frac{h_{i,abnormal}}{h_i} \tag{55}$$

$$Rob_2 = \min\left\{\frac{h_{i,abnormal}}{h_i}\right\}, \qquad i = 1, 2, \dots, N \tag{56}$$

where $h_{i,abnormal}$ is the nodal head evaluated under abnormal functioning conditions and Rob_1 depends on the sum of the fractions between respectively nodal head in abnormal and nodal head h_i in normal functioning conditions. Consequently, higher values of Rob_1 and Rob_2 corresponds to a higher network robustness.

A topological assessment of robustness can be realized using the central point dominance C_B (Freeman, 1977) that evaluates the concentration of network's nodes around a central location:

$$C_B = \frac{1}{N-1}\sum_{i}(B_{max} - B_i) \tag{57}$$

B_{max} represent the centrality of the most central point in the graph and B_i the centrality of other nodes, where the centrality (or betweenness centrality) for a node i is defined as the number of shortest geodesic paths between two vertices that cross said node i

divided by the total number of geodesic paths between the two vertices. This parameter acts as a quantifier of the network's robustness in failure events that might occur around the central location and can assume values between zero and one.

2.3.6.1.4. Efficiency

Efficiency concept in water supply systems was developed (Latora & Marchiori, 2001) with the aim of quantifying the average efficiency of paths considering any two nodes in the network. The network efficiency indicator NE depends on the average distance between two generic nodes in the WDN as follows:

$$NE = \frac{1}{N(N-1)} \sum_{i=1}^{N} \sum_{j=1}^{N} \frac{1}{d_{ij}}, \qquad i \neq j \tag{58}$$

where d_{ij} is the length of the shortest path between nodes i and j.

Another methodology to estimate efficiency is the network diameter d_T which measures the maximum eccentricity of nodes in the network as the geodetic distance:

$$d_T = \max\{d_{ij}\} \qquad i,j = 1, 2, \dots, N \quad i \neq j \tag{59}$$

Although Eqs. (58-59) can provide a good estimation of the efficiency, both do not distinguish between supply and demand nodes, nor they incorporate hydraulic features of the WDN in the calculation.

2.3.6.1.5. Serviceability

An essential parameter to be evaluated in water supply systems is the users' satisfaction, which may depend on several factors including both water quality and a guaranteed service without interruptions. One of the most impacting factors is serviceability (Jeon & Kang, 2020), measured on the basis of the number of supplied nodes Ser_2 and the available demand ratio Ser_1 under abnormal conditions, which represents the ratio between actual nodal flow rate in regular conditions and nodal flow rate in abnormal conditions:

$$Ser_1 = \frac{\sum_{i=1}^{N} Q_{a,i}}{\sum_{i=1}^{N} Q_{d,i}} \tag{60}$$

$$Ser_2 = \sum_{i=1}^{N} A_i, \qquad A_i = \begin{cases} 1 & if\ Q_{a,i} = Q_{d,i} \\ 0 & otherwise \end{cases} \tag{61}$$

where A_i is the water availability indicator, $Q_{a,i}$ and $Q_{d,i}$ are respectively actual nodal flow and nodal demand at node i; better serviceability of the WDN is suggested by higher Ser_1 and Ser_2 values.

2.3.6.2. Criticality indicators

Criticality indicators are metrics used to identify and classify the importance of the single elements of the WDN (pipes, nodes, segments or valves) based on their global impact on the system functioning, both in regular functioning and in abnormal conditions. Unlike performances indicators, which aim to provide a single encompassing value to characterize a network's configuration and evaluate its functioning state, criticality indicators' calculation yields a value for each element, aiming instead at suggesting intervention actions and providing prioritized maintenance planning for the network.

2.3.6.2.1. Identification of critical pipes

Among the established approaches, the most common one consists in determining the value of the considered criticality indicator for each pipe in the WDN, given that pipes often represent vulnerable elements due to age degradation, failures and leakages. Social index or supply shortage SS_p (Marlim *et al.*, 2019) constitutes a method to evaluate the dissatisfaction level of customers depending on unmet nodal demand when a pipe p is isolated from the network for maintenance:

$$SS_p = \frac{\sum_{i=1}^{N}\left(1 - \frac{Q_{a,i}^*}{Q_{a,i}}\right)}{N} \tag{62}$$

where $Q_{a,i}$ is the actual flow rate in node i in regular conditions and $Q_{a,i}^*$ is the nodal flow rate when pipe p is removed from the network. Given that the isolation of one pipe entails an entire flow redistribution in the whole network, it is possible that some nodal demands will be at least partially unmet, thus SS_p quantifies the rate of unsatisfied demand considering every node of the network.

Reduced water supply also has a direct impact in economic balance for the water manager and for users themselves: domestic users may experience inconveniences in daily activities, and commercial or industrial users could face economic losses or production halt. To quantify economic losses the economic value loss EVL_p was developed, calculated in the event of pipe isolation as follows:

$$EVL_p = 1 - \frac{\sum_{i=1}^{N} Q_{a,i}^{*} Tr_p u_i}{\sum_{i=1}^{N} Q_{a,i} Tr_p u_i} \tag{63}$$

where Tr_p is the time needed to realize maintenance on pipe p and can be calculated on the basis of a function depending only on diameter, as proposed by Walski & Pelliccia (1982); u_i is a unit value of water at node i, depending on the kind of user sector considered (for municipal sector, it is equal to 0.1577 \$/m^3). EVL_p is the economic value loss due to isolation of pipe p.

Pressure reduction is another common issue caused by failure events and can be measured by calculating the pressure decline indicator PD_p, which compares the normal pressure with the fault reduced pressure, using nodal demand as a weight factor so that nodes characterized by higher demands have a higher impact on the indicator:

$$PD_p = \frac{\sum_{i=1}^{N} \left[\left(1 - \frac{h_{a,i}^{*}}{h_{a,i}} \right) Q_{a,i} \right]}{\sum_{i=1}^{N} Q_{a,i}} \tag{64}$$

PD_p is the pressure reduction occurring in the network as a consequence of pipe p isolation, $h_{a,i}$ and $h_{a,i}^{*}$ are respectively pressure in node *i* in the event of pipe p isolation (abnormal conditions) and in regular conditions.

Water quality issues are of utmost importance in a drinking water network and the difficulties to quantify them can be in part overcome by considering the water age and integrating it into the development of a water quality index. Water age is defined as the time necessary for water to travel from source node to a given node (Marlim *et al.*, 2019). Using the chemical option in EPANET and setting a chemical with zero decay at the reservoir, it is possible to record, for each node, the time at which the chemical substance is detected. This information is expressed by the water age degradation index WAD_p as follows:

$$WAD_p = \frac{\sum_{i=1}^{N} \left[\left(1 - \frac{T_{a,i}}{T_{a,i}^*} \right) Q_{a,i} \right]}{\sum_{i=1}^{N} Q_{a,i}} \tag{65}$$

where $T_{a,i}^*$, $T_{a,i}$ represent water age degradation in node *i* respectively during isolation of pipe p and when pipe p is regularly operating in the network.

Finally, the overall criticality can be estimated by combining the values of the four indicators (SS_p, EVL_p, PD_p, WAD_p). Generally, it is computed simply as a sum of the four indicators, to provide a more accurate and balanced assessment of pipes' criticality; clearly, pipes near reservoirs tend to have a higher total criticality.

2.3.6.2.2. Identification of critical nodes

Approaches were also developed focusing on the identification of critical nodes rather than pipes: mostly, this choice is often related to the use of nodal vulnerability metrics that derive from graph theory. One of the most complete methodologies is represented by the nodal vulnerability indicator obtained by an integrated Fuzzy AHP-TOPSIS approach (Tornyeviadzi *et al*., 2021): the foundation of the method lies on assigning a proper weight to each criterion incorporated in the calculation, eventually gaining an all-encompassing vision on the network and providing a criticality ranking for nodes. In this methodology the first considered metric is the so called OutCloseness Centrality $C_{c(i)}^{out}$ (Tornyeviadzi *et al*., 2021) which includes all geodetic distances from a certain node and in a directed graph is defined as follows:

$$C_{c(i)}^{out} = \frac{N-1}{\sum_{j \in \Re^{out}(i)} \delta_{ij}} \tag{66}$$

where $\Re^{out}(i)$ is the set of reachable nodes and δ_{ij} are the shortest path distances between i and j. A node i having high $C_{c(i)}^{out}$ value is influential in the network and thus its eventual failure would induce failures in all the other nodes supplied by node by i. The topological details provided by $C_{c(i)}^{out}$ are coupled with the nodal demand: thus, for each node the OutCloseness Centrality is weighted introducing a demand weighting factor $\omega_{j,i}$:

$$D_{ACC(i)} = \frac{N-1}{\sum_{k \in \Re^{out}(i)} \delta_{jk}} \omega_{j,i} \tag{67}$$

$$\omega_{j,i} = \frac{R_g}{\delta_{ji}} q_i \tag{68}$$

$$R_g = \sqrt{\frac{\sum_{j=1}^{N} \delta_{ji}^2}{N}} \tag{69}$$

$D_{ACC(i)}$ represents the demand adjusted closeness centrality of node i, $\omega_{j,i}$ is the demand weighting factor of each shortest path, q_i is the average daily nodal demand δ_{ji} is the shortest distance between a source node j and i and R_g is the radius of gyration. Eq. (68) ensures higher relevance to be given to nodes closer to the reservoir of the network, as they act as mediator between source nodes and downstream demand nodes. The last parameter introduced in the nodal vulnerability assessment is the water quality index which depends on two factors: Water Age and Residual Chlorine Concentration. This indicator constitutes a modified version of the Junction Vulnerability Index, defined as a linear combination of the two aforementioned factors and is expressed as:

$$WQI = \alpha WA + \beta RCC \tag{70}$$

Thus WQI is a linear combination of Water Age and Residual Chlorine Concentration and for the two coefficients α and β the relation $\alpha + \beta = 1$ holds. For a more in-depth description refer to Baoyu *et al*. (2009). Finally, the Fuzzy AHP-TOPSIS framework is used to aggregate vulnerability scores of each indicator in a single synthetic and comprehensive indicator, that is defined as relative closeness of the potential location of the alternative solution considered with respect to the ideal and non-ideal solutions:

$$C_i = \frac{S_i^-}{S_i^+ + S_i^-} \tag{71}$$

in which S_i^- is the separation distance of the alternative solution from the non-ideal solution and S_i^+ from the ideal solution, as defined in (Tornyeviadzi *et al*., 2021). Nodes characterized by higher vulnerability will have higher C_i values.

2.3.6.2.3. Segments vulnerability

A different methodology for identifying critical areas of the WDN consists in focusing on the segments forming the network, rather than on pipes or nodes, to prioritize the maintenance and strengthening of the crucial ones. This strategy aims to provide a better overall vision of the entire network, given that nodes and pipes do not “work” alone and, as already discussed at the beginning of chapter 2, cannot be isolated without impacting other areas of the WDN, which means directly or indirectly isolating other nodes (users) or pipes. Depending on the network considered, prioritizing the maintenance and protection of a certain segment, and therefore of all the elements inside of it, could be more rewarding than repairing a single pipe, given that each single element in a WDN acts as a part of a whole and the failures of some components could have a cascade impact on other ones.

For these reasons, several approaches were elaborated to identify the most vulnerable and critical segments in WDNs: Liu *et al*. (2017) and Mottaleb & Walski (2020) developed a graph theory-based method which evaluates the importance and criticality of segments, with the final goal of strategically allocating isolation valves. The procedure obviously starts from the identification of network segments, using software such as WaterGEMS, and follows by building a reachability matrix, which stores a score for each segment depending on the impact its isolation has on the other segments reachability to water sources. Reachability matrix distinguishes between stable water sources, as reservoirs, and tanks which are considered ephemeral water storage, assigning higher values to segments whose isolation results in the isolation from reservoirs of other segments. The matrix is used to calculate an importance index for each segment, obtained as the sum of all scores in the row corresponding to the isolated segment; then a vulnerability index is calculated as the sum of all the elements along the respective column. The authors show that the calculated indexes proved good correlations with the results provided by the hydraulic simulations in terms of unmet nodal demands.

3. Materials and methods

3.1. Air intrusion in water distribution networks

The methodology described in this section, as well as some of the figures and equations, are included in the paper "*Air intrusion in Water Distribution Network (WDN) modelling*" (Tucciarelli, T., Puleo, D., Nasello, C. & Sinagra, M., 2025), *Journal of Hydroinformatics* (https://doi.org/10.2166/hydro.2025.027).

Numerical steady state modeling of water distribution networks is built upon several fundamental approximations of the physical phenomena occurring inside the pipes. One of the most important underlying assumption regards the permeability of pipes to the exchange of fluids, such as water and air, between the inside of pipes and the external environment outside of them: indeed, most of the existing numerical steady state approaches (Demand Driven, DD and Head Driven, HD) assume and accepts only a positive permeability of pipes for water leakages, from the internal part of the pipes to the external area, and model these leakages as head driven outflow terms. In any case, the vast majority of WDNs numerical models suppose no external fluid intrusion in the pipes. This hypothesis lays the foundation for the entire hydraulic numerical modeling, and the computed results will clearly be highly dependent on it. However, several reasons cast doubt on the validity of this assumption: the first is that in urban water networks, the final distribution pipes directly linked to customers' delivery points often take water from a tank placed on the roof of apartments or in the underground (Fig. 9) and when relative pressure drops even a bit under zero value, the floating valve located in the tank lowers and the air enters the tank and then in the delivery pipe:

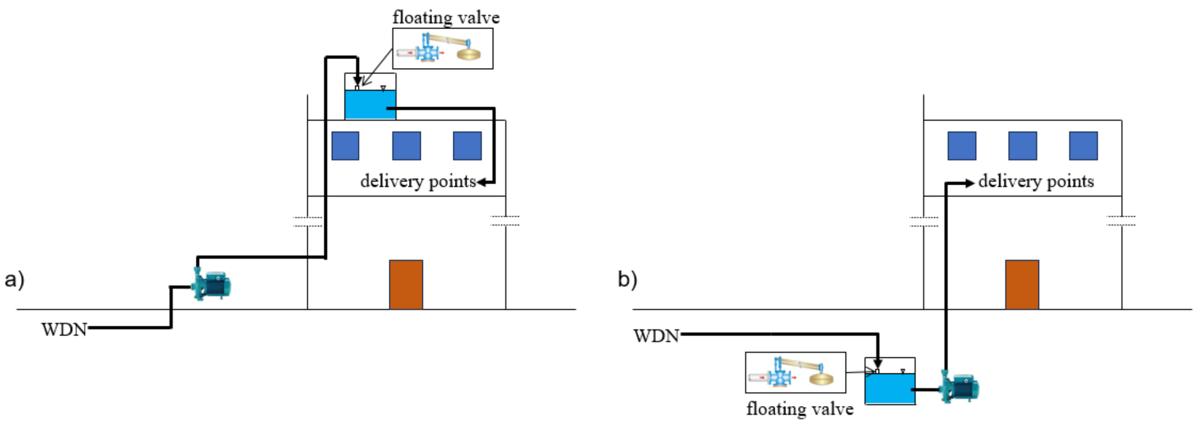

Figure 9. Typical distribution pipe connection to delivery points in apartments through (a) rooftop tank. (b) underground tank

Apart from this common event, even when water tanks are missing, a quite similar effect occurs in the flush boxes located in the apartments, where the lowering of the floating valve can lead to air intrusion. The second reason is that in water distribution networks there are different points, located along the pipes, which could become paths for the infiltration of air particles from outside: the vents, usually installed in the highest elevation nodes to free the pipes from air bubbles, allow air intrusion when water relative pressure attains zero value; moreover, small fractures in the pipes become pathways for air particles to enter, leading to a zero relative pressure. The potential water intrusion from the saturated or partially saturated soil inside of which the pipes could be installed has also a major impact on the quality of the service, because it would lead to contaminant transport inside the network, significantly deteriorating water quality in the WDN. However, accurately modeling this water intrusion would require the knowledge of several parameters (soil permeability, intrusion area dimension etc.) as well as a three phase 3D discretization, that are not realistic for a typical network under standard design conditions: this is why the new numerical model, described in this section and defined as Minimum Pressure (MP) model, assumes no water intrusion in the network. It will be shown that the model provides much more accurate and closer to reality results with respect to the traditional DD and HD models.

To summarize, the main hypotheses on which the MP model is built upon are the following ones:

- Steady state modeling
- Positive pressure in all parts of the saturated pipes
- Uniform free surface flow in all parts of the pipes with zero pressure
- No water intrusion from an external soil surrounding the pipes
- Known partition coefficients of the inlet flow in each node, among all the downstream linked pipes with zero pressure.

3.1.1. Minimum Pressure approach

3.1.1.1. Boundary conditions

Air intrusion has a significant impact on the pressure inside the network and transforms part of the pressurized pipes into free surface flow pipes, where flow is directed downstream until pressure suddenly becomes positive again and the pipe returns to be fully saturated. The existence of free surface flow pipes entails changing the mathematical representation of the problem: the system of continuity and momentum equations, when all the pipes are completely saturated, represents a so-called diffusive problem, instead so-called convective problem needs to be solved when free surface flow pipes exist in the network.

In the demand driven approach, as described in the previous chapter, usually nodal demand $Q_{d,i}$ is a problem input parameter while nodal head h_i is a problem unknown; at the opposite, if we want to set a minimum pressure, nodal head h_i could be considered an input parameter or internal boundary condition (IBC) and consequently the demand could be computed as an unknown quantity: in this case nodal head is set at its minimum value z_i and the actual nodal flow $Q_{a,i}$ will be different from the demand $Q_{d,i}$ and computed as follows:

$$Q_{a,i} = (\boldsymbol{AS}^T \cdot \boldsymbol{qs})_i \tag{72}$$

Where $\boldsymbol{AS}$ is a topological matrix whose elements AS_{ij} are equal to 1 if node j is the final node of pipe i, to -1 if node j is the initial node of pipe i and to 0 if node j does not belong to pipe i. Considering the HD approach, the following Wagner relation holds between actual nodal flow and nodal demand:

$$Q_{a,i} = 0 \qquad if\ h_i \leq z_i \tag{73a}$$

$$Q_{a,i} = Q_{d,i} \left(\frac{h_i - z_i}{amax} \right)^{0.5} \qquad if\ z_i \leq h_i \leq z_i + amax \tag{73b}$$

$$Q_{a,i} = Q_{d,i} \qquad if\ z_i + amax \leq h_i \tag{73c}$$

In which $amax$ is usually set equal to 10 m (corresponding to 1 bar). After allocating the internal boundary conditions at some nodes, with the aim of coupling the convective problem of the unsaturated pipes with the diffusive problem of the saturated pipes, the sets of internal nodes and pipes are divided into four subsets:

- **Pressure Nodes (PN)**: internal nodes where nodal demand $Q_{d,i}$ is set as IBC, with unknown heads h_i.
- **Dirichlet Nodes (DN)**: internal nodes where the condition $h_i = z_i$ is set, with unknown outlet flux F_i.
- **Saturated Pipes (SP)**: pipes with pressure always higher than zero, unless in the lower end node where pressure can attain zero.
- **Unsaturated Pipes (UP)**: pipes where strictly positive pressure can occur only in a certain part of their length. A UP pipe can connect two DN nodes or an upper DN node and a lower PN node.

If a DN node is an intermediate node between a saturated pipe SP and an unsaturated pipe UP, Eq. (72) changes in the following:

$$F_i = (\boldsymbol{AS}^T \cdot\ \boldsymbol{qs} + \boldsymbol{AH}^T \cdot\ \boldsymbol{qu})_i \tag{74}$$

Where $\boldsymbol{qs}$ and $\boldsymbol{qu}$ represent the flow rates vector respectively in saturated (SP) pipes and unsaturated (UP) pipes. $\boldsymbol{AS}$ matrix includes only the rows related to SP pipes, while $\boldsymbol{AH}$ matrix includes only the rows related to UP pipes where the elevation z_i of node i is smaller than the elevation of its second node. The following Fig. 10 shows all possible typologies of pipes-nodes connections according to the four subsets previously defined:

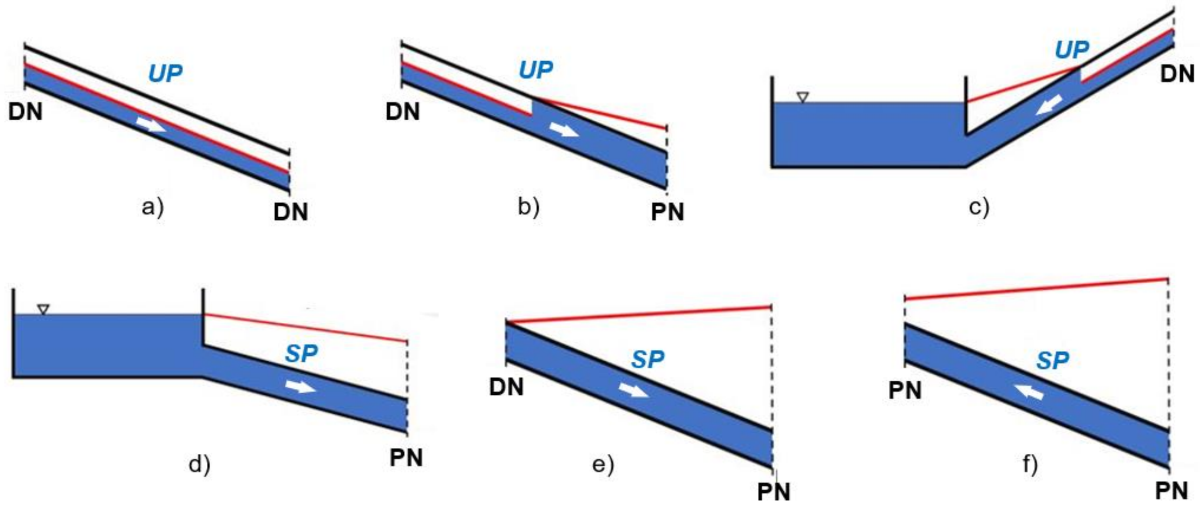

Figure 10. Nodes DN and PN, pipes UP and SP with red piezometric line. Arrows in each figure show flow direction

3.1.1.2. Problem equations

Kinematic approximation can be applied to the momentum equations of the unsaturated pipes (UP), assuming the water depths to be only a fraction of the respective pipe diameter and much smaller than the difference between the respective nodal heads in the pressurized PN nodes; furthermore, the friction slope is assumed to be equal to the pipe elevation slope. In steady state conditions, this implies a uniform water depth and a fraction of the total nodal flow rate leaving the respective DN node. A diagonal matrix $\boldsymbol{DS}$ is defined for the SP pipes as follows:

$$DS_{l,l} = r_l |qs_l|^{\alpha-1} \tag{75}$$

where r_l and α are the resistance law parameters for pipe l. The partition coefficient $F_{i,l}$ of the total outlet discharge flux $qout_i$ (entering node *i*), between all the UP pipes sharing the upper DN node, is assumed to be dependent only on the pipes' resistances and slopes:

$$F_{i,l} = \frac{\text{cost}_l}{\sum_m \text{cost}_m}, \quad \text{cost}_l = \left(\frac{|z_i - z_j|}{r_l}\right)^{\frac{1}{\alpha}} \tag{76}$$

Where *i* and *j* are the two nodes of pipe *l* and the sum is extended to all UP pipes linked to node *i* with $z_i < z_j$. A more detailed explanation of the reasons leading to the assumption of Eq. (76) is provided in Appendix A of the above mentioned paper, at https://doi.org/10.2166/hydro.2025.027.

The governing system of continuity and momentum equations for the minimum pressure model, assuming the demand driven approach for the internal nodal flows, is presented here:

$$\begin{pmatrix} \boldsymbol{DS} & \boldsymbol{AS} \\ \boldsymbol{AS}^T & 0 \end{pmatrix} \begin{pmatrix} \boldsymbol{qs} \\ \boldsymbol{h} \end{pmatrix} = \begin{pmatrix} -\boldsymbol{AS}_s \cdot \boldsymbol{h}_s - \boldsymbol{AD} \cdot \boldsymbol{zd} \\ \boldsymbol{Q}^n \end{pmatrix} \tag{77}$$

$$h_i = z_i \qquad if\ i \in DN \tag{78}$$

$$Q_i^n = Q_{d,i} + \boldsymbol{AU}_i^t \cdot \boldsymbol{qu} \qquad if\ i \in PN \tag{79}$$

$$Q_{a,i} = Q_{d,i} \qquad if\ i \in \text{PN} \tag{80}$$

$$Q_{a,i} = \min\left(Q_{d,i}, \boldsymbol{AS}_i^t \cdot \boldsymbol{qs} + \boldsymbol{AH}_i^T \cdot \boldsymbol{qu}\right) \qquad if\ i \in \text{DN} \tag{81}$$

$$qout_i = \boldsymbol{AS}_i^T \cdot \boldsymbol{qs} + \boldsymbol{AH}_i^T \cdot \boldsymbol{qu} - Q_i \qquad if\ i \in \mathrm{DN} \qquad (82)$$
$$qu_l = qout_i F_{i,l} \qquad if\ l \in \mathrm{UP} \qquad (83)$$

In which $\boldsymbol{AS}_s$ is the topological matrix related to pipes SP linked to external nodes (reservoirs), $\boldsymbol{AD}$ is related to pipes SP linked to DN nodes, $\boldsymbol{AU}$ is related to the connections between PN nodes and UP pipes. The system (77-83) forms a non-linear algebraic system where the unknows are the flow rates in SP pipes, the water levels in PN nodes and the sum of the upstream fluxes $qout_i$ in each DN node. Observe that momentum equations in UP pipes are missing because they are replaced by the partition Eqs. (76) and (83). Eqs. (77) constitute continuity and momentum equations in respectively PN nodes and SP pipes, expressed according to Todini (2003) and Q_i^n is obtained as the sum of the demand $Q_{d,i}$ in node *i* and the total flux, coming from all the UP pipes connected to node i, which is equal to $\boldsymbol{AU}_i^t \cdot \boldsymbol{qu}$ in Eq. (79). While in pressure nodes PN the actual flow rate $Q_{a,i}$ is equal to the demand (Eq. 80), in the DN nodes it is computed as the sum of the fluxes coming from all the SP pipes linked to node i and the fluxes related to the respective UP pipes, as provided by Eq. (81). However, if the total sum is less than the demand itself $Q_{d,i}$, then the actual flow is set equal to the demand (i.e. $Q_{a,i} = Q_{d,i}$): when this occurs, a zero flux is assumed to be available for all the nodes linked to node *i* by UP pipes in downstream direction.

As regards the traditional external boundary conditions (known nodal demands or reservoirs water levels) these can be applied if all the pipes linked to external nodes remain completely saturated. On the other hand, if the elevation of a node *j* linked to a reservoir is higher than the water level in the reservoir itself and *j* is a DN node, the flow rate in the corresponding pipe will depend only on the upstream shallow water flow and the water level in the reservoir will not impact flow rates and pressures in the network (case of Fig. 10c).

3.1.1.3. Diffusive problem solution

Solution of the diffusive problem, expressed by Eqs. (77-79) can be simply found by applying any algorithm available for WDNs steady state solution, as the global gradient algorithm (GGA) of Todini (2003), already presented in section 2.3.2.1.1.

Applying the GGA, iteration k of Newton-Raphson method provides the following nodal heads and pipes flows:

$$\boldsymbol{h}^{k+1} = -(\boldsymbol{AS}^T \cdot \boldsymbol{DS}^{-1} \cdot \boldsymbol{AS})\left[\boldsymbol{AS}^T \cdot \left(\boldsymbol{qs}^k + \boldsymbol{DS}^{-1} \cdot (\boldsymbol{AN}_S \cdot \boldsymbol{h}_S + \boldsymbol{AD} \cdot \boldsymbol{zd})\right) + \alpha(\boldsymbol{Q} - \boldsymbol{AS}^T \cdot \boldsymbol{qs}^k)\right] \quad (84)$$

$$\boldsymbol{qs}^{k+1} = \frac{\alpha - 1}{\alpha}\boldsymbol{qs}^k - \frac{1}{\alpha}\boldsymbol{DS}^{-1} \cdot (\boldsymbol{AS} \cdot \boldsymbol{h}^{k+1} + \boldsymbol{AS}_S \cdot \boldsymbol{h}_S + \boldsymbol{AD} \cdot \boldsymbol{zd}) \quad (85)$$

It is also possible to include the head driven source terms at the internal nodes in the original formulation of momentum equations, as proposed by Todini *et al.* (2022); more information can be found in the mentioned paper at https://doi.org/10.2166/hydro.2025.027.

Observe that the diffusive problem has a single solution only when the pipes in the network are fully connected and this could not occur because only SP pipes were included in the diffusive problem, while each UP pipe acts as a disconnection between its two nodes. Network separation can easily occur if several demand driven nodes are present. Adding a new head driven node is equivalent to add a fictitious DN node and a fictitious SP pipe and this implies that the real node remains always connected until water head is lower than $amax$.

3.1.1.4. Convective problem solution

Solution of the convective problem can be efficiently computed by applying the Marching in Space and Time (MAST) numerical procedure, proposed by Aricò &

Tucciarelli (2007). In order to apply this methodology, it is necessary to order the DN nodes depending on their elevations, from the node with highest elevation to the one with the lowest. Considering the highest elevation node $iord_1$, the pipes flow rates qu_l of the ln_I pipes with index l connected to node I as their upper node are updated by setting:

$$qout_I = \max\left(0, \boldsymbol{AS}_I^T \cdot \boldsymbol{qs} + aux_I - Q_{d,i}\right) \tag{86}$$

$$qu_l = qout_l F_{j,I}, \qquad j = 1, \dots, ln_I \tag{87}$$

where $F_{j,I}$ is the partition coefficient and $\boldsymbol{aux}$ is an auxiliar vector, with dimension N, initially set equal to zero. In the next step, the elements belonging to the auxiliary vector and related to the nodes connected, in the previous iteration, to node I, are correspondingly updated:

$$aux\left(ld_{j,I}\right) + qu_l \rightarrow aux\left(ld_{j,I}\right), \quad j = 1, \dots, ln_I \tag{88}$$

The procedure continues until the lowest elevation DN node has been considered. If ln_I in Eq. (87) is equal to zero, flux qu_l can be assumed to exit from the network if I is the index of an external boundary node, otherwise this implies an error in the sub-set partition.

3.1.1.5. Solution of the Minimum Pressure problem for known nodes and pipes partitions

Assuming a known partition for the sub-sets PN, DN, SP and UP, the entire system (77-83) can be solved by properly combining Newton-Raphson algorithm (NR) with Linear

Theory (LT) method. Flow rates $\boldsymbol{qs}$ and nodal heads $\boldsymbol{h}$ can be computed by applying NR algorithm and the computed flow rates in SP pipes allow to calculate the $\boldsymbol{quot}$ in Eqs. (81-82). System (77-83) can therefore be written as:

$$\boldsymbol{qout} = \boldsymbol{G}(\boldsymbol{qout}) \tag{89}$$

According to linear theory (Wood *et al.*, 1972), the system of Eq. (89) has a solution in the limit of the series:

$$\boldsymbol{qout}^{k+1} = \theta\boldsymbol{qout}^{k} + (1-\theta)\boldsymbol{G}(\boldsymbol{qout}^{k}) \tag{90}$$

In which θ is called relaxation coefficient and usually set equal to 0.5. If the sub-sets partition is known, the following procedure can be applied to solve the minimum pressure problem:

1) Solve the diffusive problem at iteration *k* as follows:

$$\begin{pmatrix} \boldsymbol{DS} & \boldsymbol{AS} \\ \boldsymbol{AS}^t & 0 \end{pmatrix}\begin{pmatrix} \boldsymbol{qs}^{k+1} \\ \boldsymbol{h}^{\boldsymbol{k+1}} \end{pmatrix} = \begin{pmatrix} -\boldsymbol{AS}_S \cdot \boldsymbol{h}_S - \boldsymbol{AD} \cdot \boldsymbol{zd}^{k+1} \\ \boldsymbol{Q}^{n,k} \end{pmatrix} \tag{91}$$

   where $\boldsymbol{zd}$ is a vector whose elements are the elevation of DN nodes (lower nodes of pipe *l*) and $\boldsymbol{Q}^{n,k}$ is computed depending on the $\boldsymbol{qu}^k$ flow rates in UP pipes calculated at iteration *k* such that:

$$h_i^{k+1} = z_i \qquad if\ i \in \text{DN} \tag{92}$$

$$Q_i^{n,k} = Q_{d,i} + \boldsymbol{AU}_i^T \cdot \boldsymbol{qu}^k \qquad if\ i \in \text{PN} \tag{93}$$

2) Solve the convective problem in all DN nodes:

$$qout_i^{k+1/2} = max\left(0, \boldsymbol{AS}_i^T \cdot \boldsymbol{qs}^{k+1} + \boldsymbol{AU}_i^T \cdot \boldsymbol{qu}^{k+1/2} - Q_{d,i}\right) \qquad for\ all\ i \in \text{DN} \quad (94)$$

$$qd_l^{k+\frac{1}{2}} = qout_i^{k+\frac{1}{2}} F_{i,l} \qquad for\ all\ l \in \text{UP} \quad (95)$$

3) Compute the Residual:

$$Res = \sum_l \left(qu_l^k - qu_l^{k+\frac{1}{2}}\right)^2 \qquad for\ all\ l \in UP \quad (96)$$

If Res is lower than the desired tolerance, stop the procedure. Otherwise set in all UP pipes:

$$qu_l^{k+1} = \frac{qu_l^k + qu_l^{k+1/2}}{2} \qquad for\ all\ l \in \text{U}P \quad (97)$$

And the actual nodal flows are computed accordingly:

$$Q_{a,i}^{k+1} = Q_{d,i} \qquad if\ i \in \text{PN} \quad (98)$$

$$Q_i^{k+1} = \min\left(Q_i^d, \boldsymbol{AS}_i^t \cdot \boldsymbol{qs}^{k+1} + \boldsymbol{AD}_i^t \cdot \boldsymbol{qu}^{k+1}\right) \qquad if\ i \in DN \quad (99)$$

After setting $k+1 \rightarrow k$, return back to step 1. It is also possible to calculate the length ξ_l of the pressurized part in each pipe l of the UP set, where the upper node is i and lower node is j as follows:

$$\xi_l = \frac{L_l(h_j - z_j)}{z_i - z_j - r_l|qu_l|^\alpha} \qquad for\ all\ l \in \text{U}P \quad (100)$$

Observe that due to the unknown sub-sets partition and to the non-linearity of system (77-83), the problem is quite complex, and the partition of pipes (UP, SP) and nodes (DN, PN) must be selected to avoid negative pressures in the internal nodes. Moreover, a rigorous mathematical solution of the mentioned problem is hard to find and would require complex mixed-integer programming.

3.1.1.6. Iterative procedure to find nodes and pipes partition

An iterative numerical procedure to determine the correct partition of nodes (DN or PN) and pipes (UP or SP) is here presented. The first step consists in solving a series of problems (77-83) each with a set s of small demands $\boldsymbol{Q}_d$ given by:

$$\boldsymbol{Q}_d = K(s)\boldsymbol{Q}_D \tag{101}$$

in which $K(s)$ is a positive function slowly increasing from a small quantity ΔK to 1, and $\boldsymbol{Q}_D$ is the vector containing the final real target demands. Observe that $K(s)$ can be simply expressed as the ratio between the actual number of iterations it and the control parameter it_p, which determines how many iterations are needed to reach the target demand (attained when $it = it_p$); see Fig. 11 at the end of the paragraph and the related flowchart description.

In the first iteration, UP and DN sets are empty and at the end of each iteration, a node i, initially belonging to the PN set, is moved into the DN set if it holds the following:

$$h_i < z_i \ and \left(\left(r_l\left|q_l^k\right|^{\alpha} < z_i - z_{ia} \ and \ h_{ia}^k < h_i^k\right) \ or \left(z_i - z_{ia} < 0 \ and \ z_{ia} < h_{ia}^k\right)\right) \tag{102}$$

where l is the index of any pipe linking node ia with node i. Observe that the first constraint of Eq. (102), given by the first couple of interior brackets, is necessary because if for a l pipe belonging to UP it holds $h_{ia}^k < h_i^k$, then the slope of the same pipe linking node i with a lower node ia is always higher than the slope of the energy line in the saturated part of the same pipe (see Fig. 10b): as a consequence, node ia will have negative pressure unless the first constraint is satisfied. The second constraint, inside the second couple of brackets in Eq. (102) is required because a DN node i can have an elevation smaller than the head of the corresponding second node ia only if $z_i - z_{ia} < 0$. A pipe initially belonging to the SP set is moved into the UP set if:

$$h_{iu}^k > h_{id}^k \quad and \quad iu \in DN^{k+1} \tag{103}$$

where iu and id represent respectively the upper and lower node of pipe *l*. It is assumed that, according to the applied variation of nodal flows $\boldsymbol{Q}_d$, the heads in PN nodes at iteration *k*+1 will always be lower than the corresponding heads at iteration *k*. This implies that the new UP^{k+1} and DN^{k+1} sets at iteration *k*+1 will include the UP^k and DN^k sets of iteration *k* and that all remaining nodes will maintain a positive pressure or equal to zero. If flow rates variation between two consecutive iteration is small enough, the residual converges to zero. In Fig. 11 a synthetic flowchart of the minimum pressure algorithm is proposed, along with the corresponding pseudo-code:

1) **Start**: Initialize it_p and it_{max}
2) Set $k = 0$, $it = 0$. Initially, all nodes are PN nodes and all pipes are SP pipes.
3) Increase it ($it = it + 1$)
4) Check if $it < it_p$:

   4.1) Yes: set all nodes demands $Q_d = \frac{it}{it_p} Q_D$

   4.2) No: set all nodes demands $Q_d = Q_D$
5) Solve the diffusive problem of Eqs. (77–79) with $\boldsymbol{qu} = \boldsymbol{qu}^k$ in the $\boldsymbol{h}$, $\boldsymbol{qs}$ unknown.
6) Solve the convective problem of Eqs. (80–83) in the $\boldsymbol{qu}^{k+1}$ unknown
7) Check if $\left|\boldsymbol{qu}^{k+1} - \boldsymbol{qu}^k\right| < \varepsilon$.

   7.1) Yes: go to 8)

   7.2) No: set k+1=k, and go back to 4)
8) Check if $it = it_{max}$:

8.1) Yes: update it_p and it_{max} and go to 2)

8.2) No: go to 9)

9) Check if there is any node with $h_i < z_i$ or $it < it_p$:

9.1) Yes: for nodes with $h_i < z_i$, set $h_i = z_i$; these nodes are now DN nodes. Accordingly update all sets DN, PN, UP, SP and go back to 3)

9.2) No: **End**

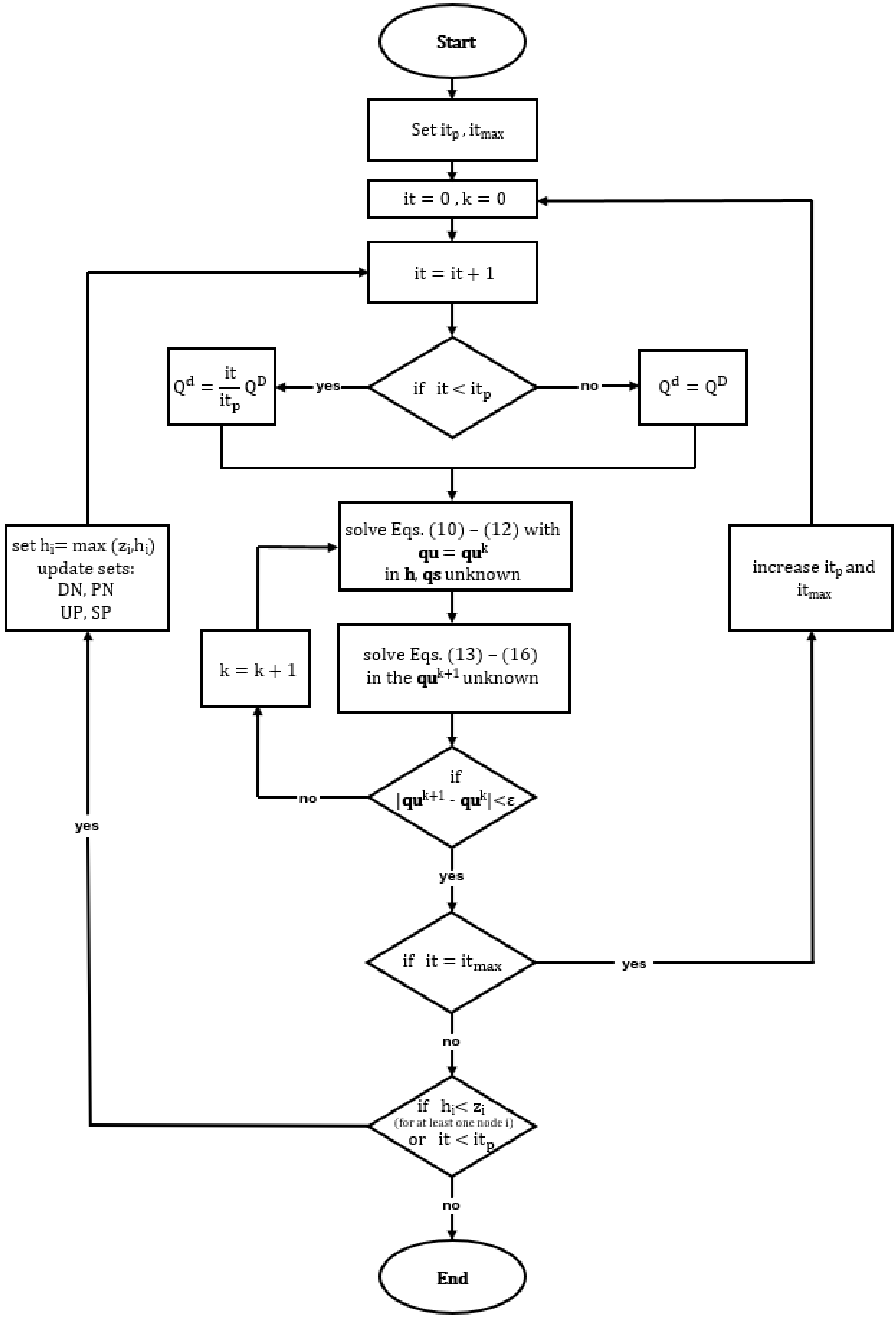

Figure 11. Flowchart of the minimum pressure algorithm

3.2. Integrated topological-hydraulic criticality indicator

The present thesis focuses on the development of a new criticality indicator, called Minimum Pressure Criticality Indicator (MPCI), incorporating both topological and hydraulic characteristics of the network while also being able to integrate the results provided by the Minimum Pressure (MP) approach. The proposed indicator properly merges the topological metrics provided by the structural hole theory with the hydraulic constraints and results provided by the steady state WDN solution, highlighting in particular the pipes where free surface flow could occur which, as shown by the MP approach, could lead to serious water quality issues. It will be shown that the developed indicator can provide a different perspective for prioritized maintenance of pipes in water distribution networks as well as a reliable estimation of critical pipes, also compared to criticality indicators available in the literature. This is true especially in water scarcity scenarios where the classical demand driven and head driven numerical approaches are not adequate to represent the real flow dynamics occurring in the network.

3.2.1. Structural hole theory

The new developed methodology lays its foundations on the structural hole theory, initially introduced by Burt (1992) in the context of social networks. If an undirected and unweighted network, represented by a graph G containing N nodes and M edges, is considered, then the adjacency matrix $A=[a_{ij}]_{NxN}$, where *i* and *j* are the indices of two nodes, can be defined as follows:

$$a_{ij} = \begin{cases} 1 & \text{if nodes } i \text{ and } j \text{ share a common edge} \\ 0 & \text{if nodes } i \text{ and } j \text{ do not share a common edge} \end{cases} \tag{104}$$

Two nodes *i* and *j* are defined to be directly connected if $a_{ij} = 1$. Structural hole theory was elaborated in order to obtain a simple but effective method to identify key nodes in a complex network: these nodes act as a bridge, broker the flow of information and are therefore essential for the network's functioning. When two nodes or two groups of nodes share neither a direct connection nor an indirect redundancy relationship (i.e. if no redundant relationships are found, then there is only a single indirect path to reach one node from the other one) then the hinders between them are known as structural hole, as it can be observed in Fig. 12:

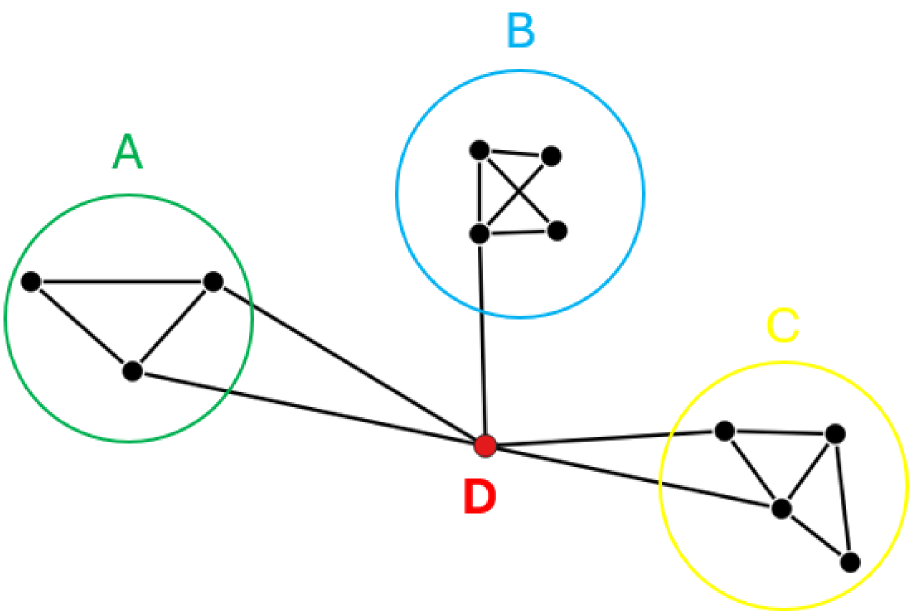

Figure 12. Clusters (A, B, C) of nodes sharing a structural hole

Node D in Fig. 12 is the only direct connection between the groups (or clusters) of nodes A-B, but also between A-C and B-C and thus it is critical in the transmission of the flow of information among them. As a way of measuring the structural holes in a network, several parameters can be defined: first, p_{ij} coefficient is computed as:

$$p_{ij} = \frac{a_{ij}}{\sum_{j \in \Gamma(i)} a_{ij}} \tag{105}$$

In which $\Gamma(i)$ is the adjacency list, or set of nodes connected to node i, and p_{ij} represent the fraction of the total effort node i has to make in order to maintain its connection with node j. Definition of “effort” was originally proposed by Burt (1992) in reference to social networks, where each node in the network represent one person and edges constitutes the connections or relationships between nodes/people: in this context, each node i has to make an effort to maintain each one of the relationships with the other connected nodes, which belong to the set $\Gamma(i)$. The total effort each node exerts to maintain all of its connections, irrespective of the number of connected nodes, is always equal to 1. This implies that, if only a single node j is connected to node i, the total effort node i exerts to maintain all its connections is completely directed towards j; otherwise, if node i is connected both to node j and node k, the total effort will be equally divided between j and k and will consequently be equal to 0.5. From Eqs. (104-105) derives also that p_{ij} is always equal to the inverse of the number of connections of node i. In Fig. 13 an easy calculation example of p_{ij} is shown:

$$\begin{cases} a_{12} = a_{13} = a_{14} = 1 \qquad \Gamma(1) = \{2,3,4\} \\ p_{12} = \dfrac{a_{12}}{\sum_{j\in\Gamma(1)} a_{1j}} = \dfrac{a_{12}}{a_{12} + a_{13} + a_{14}} = \dfrac{1}{3} \\ p_{13} = \dfrac{a_{13}}{\sum_{j\in\Gamma(1)} a_{1j}} = \dfrac{1}{3} \\ p_{14} = \dfrac{a_{14}}{\sum_{j\in\Gamma(1)} a_{1j}} = \dfrac{1}{3} \\ p_{12} + p_{13} + p_{14} = 1 \end{cases}$$

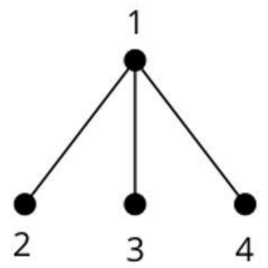

Figure 13. p_{ij} computed for a node and its neighboring nodes

Definition of p_{ij} allows to introduce the constraint coefficient C_i of node i, calculated as follows:

$$C_i = \sum_{j\in\Gamma(i)} \left(p_{ij} + \sum_k p_{ik} p_{ki}\right)^2, \qquad k \neq i, j \tag{106}$$

where k is a common neighboring node between nodes i and j. Usually, low values of constraint coefficients are related to nodes sharing structural holes: these nodes connect separated areas of the network, do not have a common link with other nodes and their influence on the spread of information in the network is critical. On the opposite, high constraint coefficient values characterize nodes that share more than one common neighbor with other nodes, and consequently they are part of a loop in the network: this means that there are more paths to reach a node in the loop, hence these nodes are not particularly critical in the spread of diffusion of information in the network.
The last parameter to consider, already presented in section 2.3.6.2.2, is the closeness centrality $C_c(i)$ which measures the influence of a node in the network:

$$C_c(i) = \frac{N-1}{\sum_{j=1}^{N-1} d_{ij}} \tag{107}$$

where d_{ij} is the length of the shortest path between nodes i and j. A high closeness centrality value for a node implies that its position in the network is crucial, whereas low values are related to peripheral nodes.

3.2.2. Structural hole influence matrix

Once Eqs. (105-107) have been described, it is possible to introduce the structural hole influence matrix, proposed first by Zhu *et al.* (2017) with the aim of identifying critical nodes in the network. By combining the adjacency matrix (Eq. 104) and the closeness centrality (Eq. 107) the node impact factor matrix can be defined as follows:

$$H_A = \begin{bmatrix} 1 & a_{12}C_c(2) & \cdots & a_{1N}C_c(N) \\ a_{21}C_c(1) & 1 & \cdots & a_{2N}C_c(N) \\ \vdots & \vdots & \vdots & \vdots \\ a_{N1}C_c(N) & a_{N2}C_c(2) & \cdots & 1 \end{bmatrix} \tag{108}$$

Each element $H_A(i,j) = a_{ij}C_c(j)$ represents the influence factor of node j on node i and depends on two main factors: the global influence factor (related to the location of j in the whole network, and expressed by $C_c(j)$) and the local influence factor (expressed by the respective term a_{ij} of the adjacency matrix. Along the matrix diagonal every value is equal to one, due to the impact of each node on itself being 100%.

By aggregating the information provided by the node impact factor matrix and the constraint coefficient C_i (Eq. 106) the structural hole influence matrix is obtained:

$$H_C = \begin{bmatrix} C_1^{-1} & a_{12}C_c(2)C_2^{-1} & \cdots & a_{1N}C_c(N)C_N^{-1} \\ a_{21}C_c(1)C_1^{-1} & C_2^{-1} & \cdots & a_{2N}C_c(N)C_N^{-1} \\ \vdots & \vdots & \vdots & \vdots \\ a_{N1}C_c(N)C_1^{-1} & a_{N2}C_c(2)C_2^{-1} & \cdots & 1 \end{bmatrix} \tag{109}$$

in which $H_C(i,j) = a_{ij}C_c(j)C_i^{-1}$ represents the fraction of influence node j exerts on node i, and C_i^{-1} is the inverse of the constraint coefficient. It is then clear that the higher the closeness centrality C_c of a node, the larger its impact on the network, while at the opposite, low values of constraint coefficient entail high values of $H_C(i,j)$.

Finally, given a node i, it is possible to evaluate its comprehensive influence in the network by averaging the $H_C$values, provided by the structural hole influence matrix, of the nodes connected to it with the inverse of its constraint coefficient:

$$M_i = \frac{1}{nd_i}\left(H_C(i,1) + H_C(i,2) + \cdots + H_C(i,nd_i)\right) = \frac{1}{nd_i}\sum_{j=1}^{nd_i} H_C(i,j) =$$

$$= \frac{1}{nd_i}\left(C_i^{-1} + \sum_{j=1.j\neq i}^{nd_i} a_{ij}C_c(j)C_j^{-1}\right) \tag{110}$$

where nd_i is the number of adjacent nodes to i. Eq. (110) constitutes an extensive approach to establish the influence of a node i by integrating both the global factor and the local influence factor, related to the adjacent nodes.

3.2.3. Criticality indicator derived from minimum pressure approach and structural hole theory

In the new methodology described in this thesis, the influence that each node in a WDN exerts on the adjacent nodes is computed by applying the structural hole influence matrix approach within the context of Minimum Pressure model: the structural hole theory provides the necessary information to identify critical nodes only on the basis of their topological relevance, whereas MP model integrate this information with the hydraulic features of the nodes and pipes, with a particular focus on pipes where free surface flow occurs, for the water quality reasons already described in section 1.

3.2.3.1. Pipe hydraulic weight definition

The first step necessary to integrate the topological features with the hydraulic ones consists in building a weighted adjacency matrix, conceptually similar to the one of Eq. (104). In this new matrix the connections of each pair of nodes are weighted and therefore depend on the hydraulic parameters resulting from the numerical simulations, as actual nodal flow $Q_{a,i}$ and mean velocities in all the connected pipes.

Before introducing the weighted adjacency matrix, it is necessary to develop a method to weight the pipes of the network: the consequent choice is to define a parameter that describes the criticality of each pipe in the network only on the basis of hydraulic data (because the topological data, provided by structural hole theory, will be integrated afterwards), in which higher values are assigned to more critical pipes (e.g. pipes carrying high flow rates or connected to nodes having high demand) and, conversely, lower values to less critical pipes. A final aspect also to be considered in the formulation of this parameter regards its suitability to be computed and used with both the traditional hydraulic models (DD and HD), and the new MP approach taking into account pressure limits and free surface flow pipes.

In the light of these observations and with the aim of finally proposing a dimensionless criticality indicator, the following hydraulic pipe weight W_p is introduced:

$$W_p = \left(\frac{Q_{d,i}}{Q_{net}} + \frac{Q_{d,i} - Q_{a,i}}{Q_{d,i}} + \frac{Q_{d,j}}{Q_{net}} + \frac{Q_{d,j} - Q_{a,j}}{Q_{d,j}} + \frac{q_p}{Q_{net}}\right)\left(\frac{v_{p,ff}}{v_{p,sf}} + 1\right) \qquad (111)$$

where, given a pipe p connecting nodes i and j, $v_{p,sf}$ represents the mean velocity in the pressurized part of pipe p and $v_{p,ff}$ is the uniform flow velocity along the part of the pipe with zero pressure, computed when free surface flow occurs, or otherwise equal to $v_{p,sf}$ when all the pipe is fully pressurized. $Q_{d,i}$ and $Q_{d,j}$ are the nodal demands in nodes i and j while $Q_{a,i}$, $Q_{a,j}$ represent the respective actual nodal flow rate in the two nodes, computed by the numerical simulation with the chosen hydraulic model. Eventually, Q_{net} is the total flow rate extracted from every node in the WDN, computed as sum of all actual nodal flows $Q_{a,i}$, and q_p is flow rate in pipe p.

Eq. (111) is formulated to give more relevance to pipes where nodal demands $Q_{d,i}$ and $Q_{d,j}$ are significant when compared to the total demand Q_{net}, but also to give importance to pipes in which at least one of the two nodal demands is not completely satisfied, which implies that $Q_{a,i} < Q_{d,i}$ and an increment of the difference $Q_{d,i} - Q_{a,i}$.

Observe that the difference $Q_{d,i} - Q_{a,i}$ (as well as the corresponding difference for flow rates in node j) is divided by the corresponding nodal demand $Q_{d,i}$ and not by the total demand Q_{net}, unlike all the other terms in the first couple of brackets in Eq. (101): this choice was made in order to always obtain, from the ratio $(Q_{d,i} - Q_{a,i})/Q_{d,i}$, values of the same order of magnitude of all the other ratios in Eq. (111). Indeed, if the ratio $(Q_{d,i} - Q_{a,i})/Q_{d,i}$ were replaced by $(Q_{d,i} - Q_{a,i})/Q_{net}$ then, when the total demand Q_{net} were much higher than the difference $Q_{d,i} - Q_{a,i}$ (which is the most common case in a real WDN with many nodes), the denominator Q_{net} would always be much higher than the numerator, independently from how much the nodal demand $Q_{d,i}$ diverges from the actual flow rate $Q_{a,i}$; consequently the entire fraction $(Q_{d,i} - Q_{a,i})/Q_{net}$ would always be equal to low values and this would mean losing all the information about a node which instead has to be considered quite critical, given that its nodal demand is not satisfied.

Therefore, choosing $(Q_{d,i} - Q_{a,i})/Q_{d,i}$ as the ratio to be computed, ensures that when the demand is completely satisfied, the fraction is equal to zero ($Q_{d,i} = Q_{a,i}$), while in the worst possible case (demand completely unsatisfied, $Q_{a,i}$=0) the fraction is equal to 1, increasing pipe weight W_p.

Clearly, pipes carrying a consistent portion of flow rate of the WDN have a great importance in the network, and similarly to what have been done for nodal demands $Q_{d,i}$ and $Q_{d,j}$, the fraction q_p/Q_{net} is computed. Observe that, while the nodal flows $Q_{a,i}$ and $Q_{a,j}$ are not independent from the flow q_p in the pipe, it is nevertheless important to compute q_p/Q_{net} in any case: in fact, even if the two nodes of pipe p have zero nodal demand, this does not necessarily imply a zero flow rate q_p in the corresponding pipe. The flow rate q_p instead could be relatively high, especially if pipe p is near one of the reservoirs of the WDN and even if its two nodes represent simply junction points in the WDN and not real consumers, with $Q_{d,i} = Q_{d,j} = 0$.

The last factor $v_{p,ff}/v_{p,sf} + 1$ is introduced in order to get low water quality for those pipes where the high velocities resulting from free surface flow could lead to detachment of material accumulated along the inner surface of the pipe. Also observe that, when free surface flow occurs in a pipe, the q_p flow rate computed by the MP approach is inferior to the one computed by the traditional HD approach and this would decrease the overall pipe weight W_p computed by the MP approach with respect to the one calculated with HD (assuming that all other parameters in Eq. (111) are the same in the two approaches).

Therefore, the factor $v_{p,ff}/v_{p,sf} + 1$ provides a sort of much higher compensation for this case, because when free surface flow occurs this factor increases when it is calculated with the MP approach (due to $v_{p,ff} > v_{p,sf}$), while according to the HD approach, which is unable to detect free surface flow pipes, $v_{p,ff}$ will always be equal to $v_{p,sf}$ and thus the entire $v_{p,ff}/v_{p,sf} + 1$ factor will be always equal to 2 (given that $v_{p,ff} = v_{p,sf}$) for every pipe in the network.

The additional unit term was introduced only to include the event in which $q_p = 0$ which implies that all velocities will be equal to zero: if the " $+ 1$" were not added, Eq. (101) would reduce to zero, meaning zero hydraulic weight for a pipe which instead is expected to be considered critical, given that, when $q_p = 0$ occurs, it often follows reduced or even zero actual nodal flows ($Q_{a,i}$ and $Q_{a,j}$) that instead should indicate an high criticality of the pipe, as explained above when discussing about the term $(Q_{d,i} - Q_{a,i})/Q_{d,i}$.

Finally observe that Eq. (111) can be computed with any desired numerical model (DD, HD or MP) and clearly the criticality values calculated will reflect the advantages and disadvantages of each model: according to DD model, demand will always be met (i.e. $Q_{d,i} = Q_{a,i}$) and this could largely and negatively impact results, especially in pressure reduction scenarios. HD model can estimate the differences between the nodal flows $Q_{d,i}$ and $Q_{a,i}$, but only the MP approach is able to take into account the impact on them of the reduction of the head gradient and of the corresponding pipe flow rate.

3.2.3.2. Weighted adjacency matrix calculation by means of pipe hydraulic weight

Before computing a weighted adjacency matrix, pipes hydraulic weight W_p must be normalized with respect to the maximum pipe weight $W_{p,max}$ among all the pipes in the network:

$$W_{p,n} = \frac{W_p}{W_{p,max}} \tag{112}$$

At this point a weighted adjacency matrix can be calculated by means of pipe hydraulic weights as follows:

$$a_{w,ij} = \begin{cases} W_{p,n} & if\ \ node\ i\ and\ j\ are\ connected \\ 0 & if\ node\ i\ and\ j\ are\ not\ connected \end{cases} \tag{113}$$

Some authors (Yang et. al. 2022, Marlim et. al. 2024) propose different hydraulic pipe weight W_p formulations for the weighted adjacency matrix. It was chosen to normalize W_p values, before defining the weighted adjacency matrix, because this process guarantees that the normalized $W_{p,n}$ values always belong to the range [0;1].

This choice was made bearing in mind that the final step of the proposed methodology, aimed to realize a pipes' criticality assessment, comprehends the implementation of the new pipe weight W_p into Eq. (110) to finally derive an integrated hydraulic-topological parameter to compute the criticality M_i of each node. For this reason, any modification in Eq. (110) must be done coherently with the original definition of M_i and with all the involved parameters. In particular, in the initial definition of Eq. (110), all values of the topological adjacency matrix (Eq. 104) belong to the range [0;1] and this condition has been preserved in the proposed approach: indeed, if we instead applied in Eq. (110) the W_p values without normalization, in place of the a_{ij} terms, this would lead to a variation of the lone term $\sum_{j=1.j\neq\mathrm{i}}^{nd_i} a_{ij} C_c(j) C_j^{-1}$, representing the influence of all adjacent nodes j, without a corresponding impact on the influence of node i itself (given by C_i^{-1}), which does not depend on the hydraulic pipe weight W_p. This possible variation, due only to a variation of the a_{ij} range, could lead in Eq. (110) to two completely different orders of magnitude respectively for the influence of node i (C_i^{-1}) and for the influence of connected nodes j ($\sum_{j=1.j\neq\mathrm{i}}^{nd_i} a_{ij} C_c(j) C_j^{-1}$), depending on the actual computed W_p values for the analyzed WDN. This implies that one of these two terms could be negligible with respect to the other one. On the opposite, normalization according to Eq. (112) ensures values within the range [0;1], regardless of the specific W_p formulation and the considered network.

It was also chosen to compute constraint coefficient C_i, for each node i, on the only basis of the surrounding topology, as provided by the a_{ij} values of the unweighted network (Eq. 104), and not by the $a_{w,ij}$ ones (Eq. 113), because all hydraulic characteristics are already taken into account by the $W_{p,n}$ formulation.

In the following Fig. 14 a simple calculation example of $W_{p,n}$ is shown for a network with one reservoir (node 16) and a total of 16 nodes. In each node a demand $Q_{d,i}$=2.5 l/s is set and all the pipes share the same geometry and material; a needle valve is located in pipe 7, so that the corresponding flow rate leaving the reservoir is equal to 31 l/s, and a water leakage affects node 6.

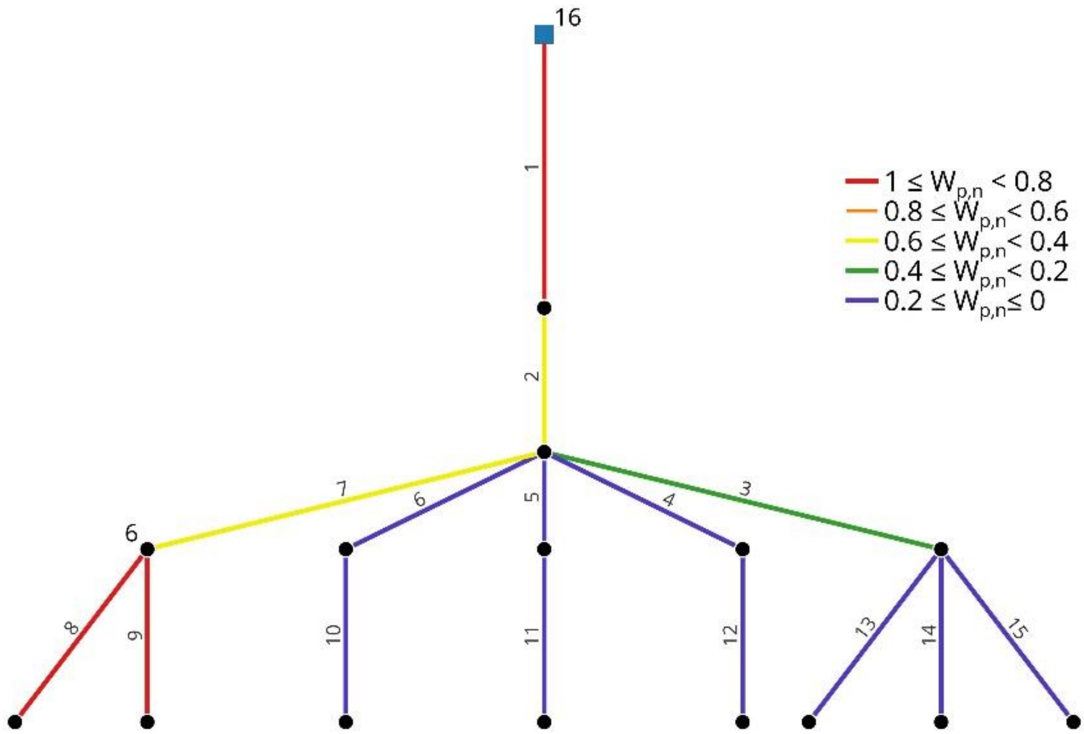

Figure 14. $W_{p,n}$ computed in a simple network. Pipes are colored depending on their $W_{p,n}$ value

In Fig. 14, pipes were classified in five criticality groups and depicted with a color depending on their computed $W_{p,n}$. As expected, the highest $W_{p,n}$ value is held by pipe 1, the nearest to the reservoir and the one carrying the total flow directed in all the downstream nodes. Pipes 8 and 9 occupy the 2nd and 3rd position in $W_{p,n}$ ranking, due to free surface flow occurring in almost all their length and nodal demands of their nodes being not completely satisfied: this is the combined effect of the needle valve located in pipe 7, significantly reducing water flow in this pipe, and the water leakage considered in node 6. Pipe 7, being directly connected both to pipes 8 and 9, presents a considerable $W_{p,n}$ and ranks in the third highest criticality group (depicted in yellow) as pipe 2.

From this test it is clear that the new formulation of Eq. (111) is able to correctly represent the physics of the analyzed problem, providing higher criticality values to pipes near the water sources or pipes connected to nodes with unmet demands but also to pipes characterized by free surface flow.

3.2.3.3. Modified closeness centrality

Once pipe hydraulic weights have been defined through Eqs. (111-112), it is possible to compute each node's criticality M_i using Eq. (110). However, the original formulation of Eq. (110) depends only on topological features and needs to be adjusted to incorporate the hydraulic parameters and the dynamics occurring in the network. In particular, nodal degree nd_i (which represents the number of nodes connected to i) is inversely proportional to the criticality M_i, because the more the connections shared by node i with other nodes, the more paths are available to reach node i and the lower is its criticality M_i. Nonetheless, in a directed network not every path can be crossed to reach a node j from a node i, given that each edge/pipe is characterized by a specific direction of the flow rate and for this reason, rather than simply considering in Eq. (110) the nodal degree nd_i, it is more appropriate to consider, among the nodes connected to i, only the number of nodes $nd_{WF(i)}$ that can reach node i (i.e., pipes connecting these nodes and node i are characterized by flow rate directed towards i). To summarize, each node i has a set of reachable nodes $n_{\Re(i)}$, that can be reached through an oriented path starting from node i, and a set of nodes $nd_{WF(i)}$ instead reaching node i.

A similar consideration can be made about the closeness centrality of Eq. (107), in which the total number of nodes N is considered: Eq. (107) evaluates in fact the importance of a node i based on its centrality in the network, calculating the length of the shortest paths between node i and every other node in the network, thus implying that every other node in the WDN can be reached starting from i. In a directed network this is no more true, as explained before, and a better and more appropriate version of the closeness centrality is the following one (Wasserman & Faust, 1994):

$$C_{WF(i)} = \frac{n_{\Re(i)} - 1}{N - 1} \frac{n_{\Re(i)} - 1}{\sum_{j=1}^{n_{\Re(i)}-1} (d_{Ri} + d_{ij})} \tag{114}$$

where the modified closeness centrality $C_{WF(i)}$ depends both on the shortest path d_{ij} (between node i and a node j belonging to the set of reachable nodes $n_{\Re(i)}$) and on the shortest path d_{Ri} (between the closest reservoir R and node i), assuming that source nodes in the WDN are all reservoirs. Consequently, the nodes closest to the reservoirs will be characterized by higher values of $n_{\Re(i)}$ and $C_{WF(i)}$. In the following Fig. 15 calculation of $C_{WF(i)}$ for node 6 is explained:

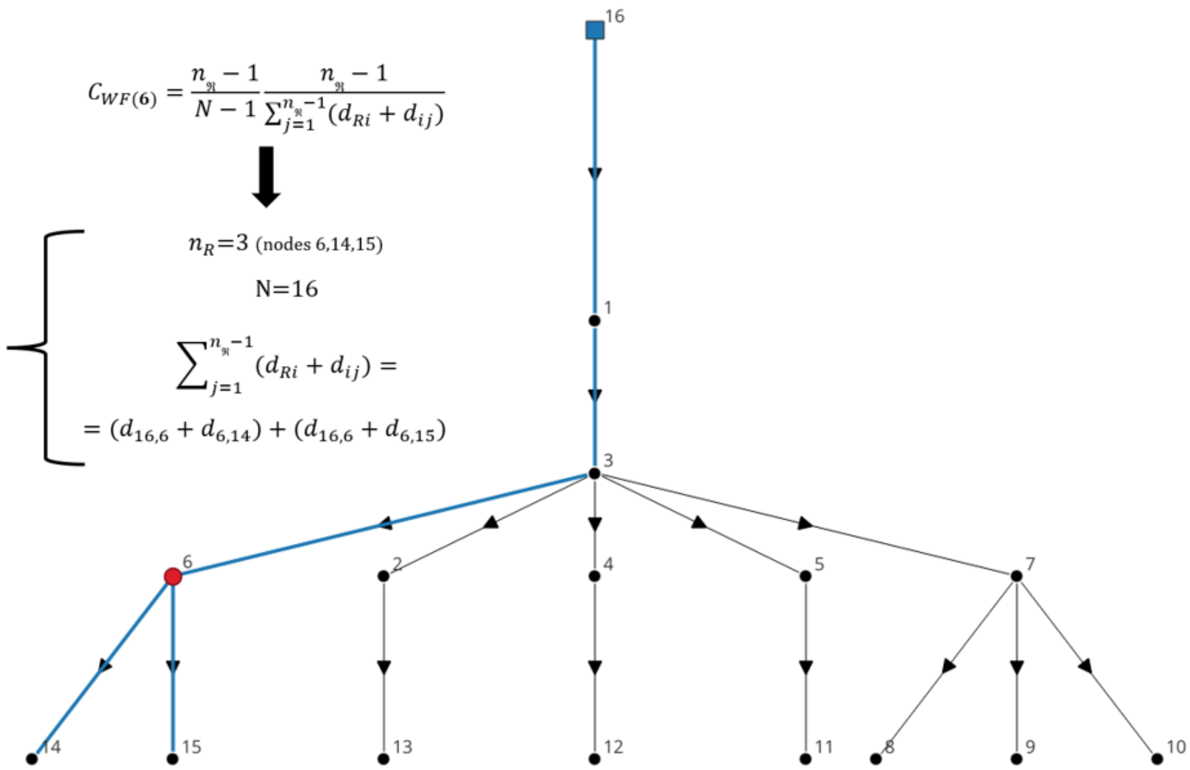

Figure 15. $C_{WF(i)}$ calculation for node 6 of Fig. 2. Arrows in pipes show flow direction; the shortest paths crossing node 6 between source node (16) and target nodes (14,15) are highlighted in blue

3.2.3.4. Minimum Pressure Criticality Indicator

On the basis of all the considerations carried out in the previous chapter, the following Minimum Pressure Criticality Indicator ($MPCI$) is proposed:

$$MPCI_i = \frac{1}{(nd_{WF(i)} + 1)} \left(C_{(i)}^{-1} C_{WF(i)} + \sum_{j=1, j \neq i}^{nd_i} W_{p,n(i,j)} C_{WF(j)} C_{(j)}^{-1} \right) \tag{115}$$

The proposed criticality indicator integrates the topological features of the network, provided by structural hole theory, with the hydraulic results provided by the hydraulic numerical simulation and it also able to incorporate the additional information provided the MP approach. This formulation was proposed on the basis of the definition of M_i in Eq. (110) and including the new defined parameters to finally evaluate, in a holistic approach that takes into account the whole network's hydraulic dynamics, the criticality of each node *i* considering both its relationships with adjacent nodes and also its role in the entire WDN.

Observe that the modified closeness centrality C_{WF} influences also node i through the term $C_{(i)}^{-1} C_{WF(i)}$, in addition to influencing adjacent nodes j as Eq. (110) already provided: this is crucial because otherwise, if the influence of node i were given only by the inverse of the constraint coefficient $C_{(i)}^{-1}$ (which depend only on topological parameters), this term would always be much higher than the influence of the adjacent nodes, provided by $\sum_{j=1, j \neq i}^{nd_i} W_{p,n(i,j)} C_{WF(j)} C_{(j)}^{-1}$, due mainly to the lower order of magnitude of $C_{WF(j)}$. This would be the consequence of summing two terms where the first one ($C_{(i)}^{-1}$) embeds only topological metrics, while the second ($\sum_{j=1, j \neq i}^{nd_i} W_{p,n(i,j)} C_{WF(j)} C_{(j)}^{-1}$) embeds both topological and hydraulic ones.

The term $(nd_{WF(i)} + 1)$ was introduced to be able to compute Eq. (115) even for reservoirs, given that the number of nodes $nd_{WF(i)}$ that can reach a reservoir is always zero (assuming that there are no fluxes entering reservoirs).

The normalized version can be expressed as:

$$MPCI_{i,n} = \frac{MPCI_i}{MPCI_{i,max}} \tag{116}$$

Finally, considering a pipe p connecting nodes i and j, its criticality indicator $MPCI_p$ can be computed as mean value of the $MPCI_i$ for the two nodes:

$$MPCI_p = \frac{MPCI_{i,n} + MPCI_{j,n}}{2} \tag{117}$$

In the following Fig. 16 a synthetic flowchart of the proposed $MPCI_p$ is presented:

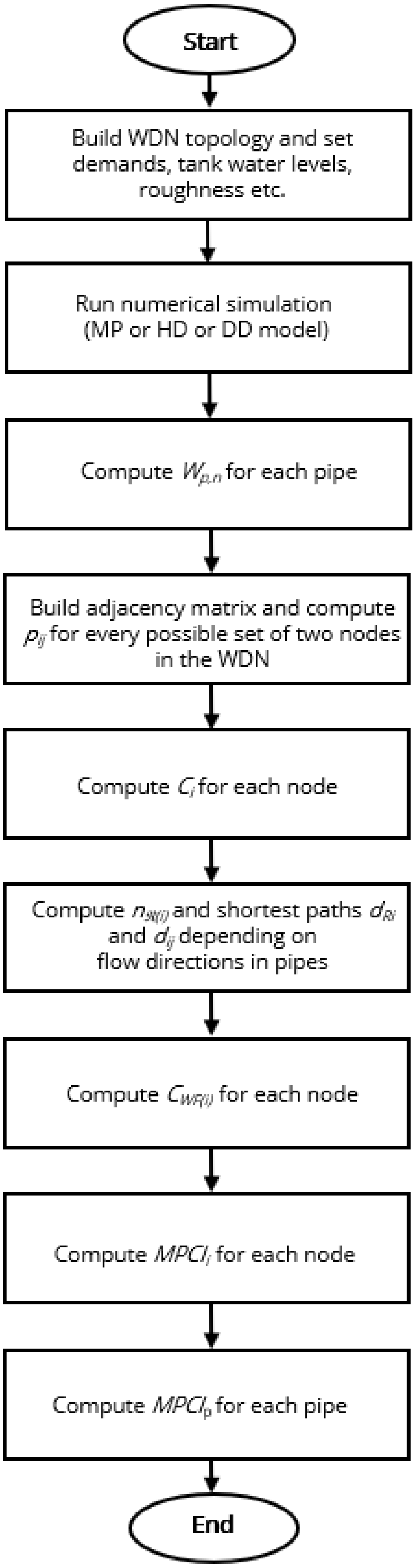

Figure 16. Flowchart of $MPCI$ algorithm

It is crucial to underline that the assumption of pipes' permeability to air is central to the MP numerical model but not to the proposed indicator: $MPCI$ equations were formulated in order to be able to integrate also the results provided by MP approach, especially in water scarcity scenarios where free surface flow could occur, but its formulations can be nonetheless used with traditional demand driven (DD) and head driven numerical (HD) models, as well as with commercial software (EPANET) relying on these models. In the following chapter 4 both results obtained using MP and traditional head driven approach are shown, demonstrating how $MPCI$ is able to provide accurate and physically based results, compared to other criticality indicators, even when only head driven approach is used. It will also be shown that, when $MPCI$ is used to compute results in water scarcity scenarios, differences between the results of MP and of more traditional numerical models become more remarkable and can lead to very different points of view for a prioritized maintenance of pipes.

3.3. WEC-Network

All hydraulic simulations presented in this thesis were performed using WEC-Network, a new hydraulic modeling software developed by the hydraulic research group of the University of Palermo. The software allows to perform steady state hydraulic numerical simulations using the minimum pressure approach or the head driven approach and it was built to read and manage shapefiles (.shp) as input data of the simulation, providing an output .txt file and optionally a different set of shapefiles, to be easily imported and visualized in the open source software QGIS, useful for spatial data representation. The interconnection between WEC-Network and QGIS allows a simple and straightforward network creation process in which, once nodes and pipes shapefiles are imported in QGIS, their parameters can be easily set and displayed using the several options provided by QGIS layers management.

A short description of the entire simulation process, from input shapefiles creation to output results visualization, is provided here:

1) **Input shapefiles creation**: the first step, after the creating a new WEC-Network project (.wnet), consists in the creation of input shapefiles, directly from WEC-Network. The necessary .shp files for the numerical simulation are the ones related respectively to nodes and pipes of the WDN, called here for simplicity “nodes.shp” and “pipes.shp”. Two other shapefiles can optionally be created but are not necessary to run the simulation: “valves.shp” contains the isolation valves of the network and it is meant to be used for segments identification of the network, and lastly “profiles.shp” can be used for piezometric profiles visualization directly in WEC-Network. Alternatively, after creating new empty shapefiles, it is possible to import directly into WEC-Network an EPANET input file (.inp): in this case, the information contained in the .inp file, if compatible, will be automatically written into the corresponding .shp files. In the following Fig. 17 the default interface of a new project in WEC-Network is shown:

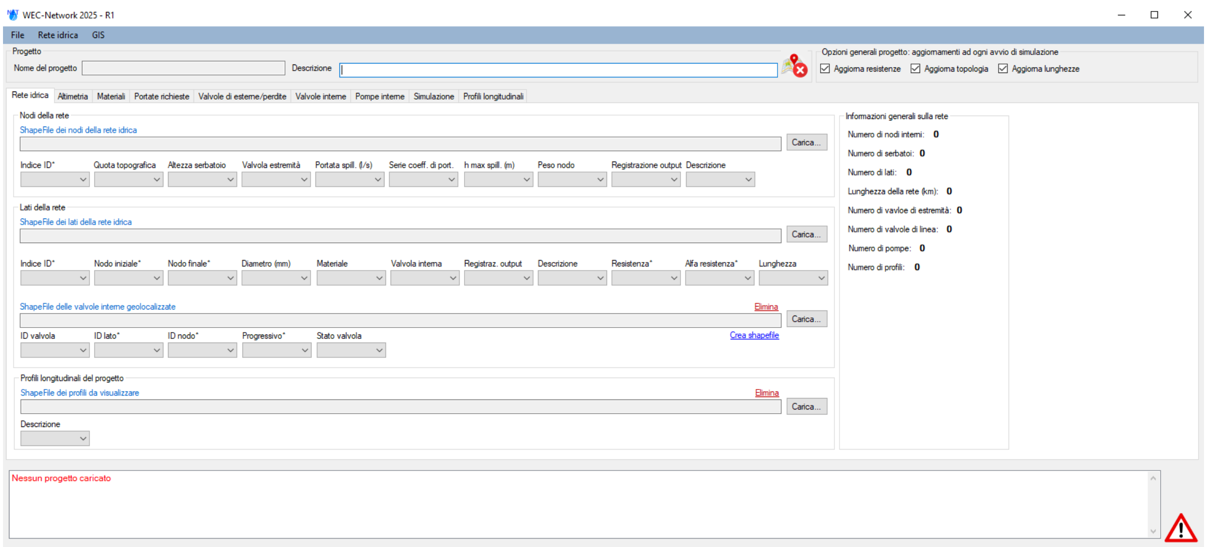

Figure 17. New project graphical interface in WEC-Network

2) **Setting of hydraulic and topological parameters**: after importing into QGIS nodes.shp and pipes.shp, all the necessary input parameters must be set. The network is manually created by first defining nodes, modifying the layer associated to nodes.shp (which by default is a Points shapefile) and adding every

node/junction of the WDN as well as reservoirs and tanks. All nodes are geo-referenced according to the chosen reference system selected in QGIS: this implies that their coordinates will be used to calculate the length of each pipe connecting two nodes. Nodes.shp contains ten fields in the corresponding attribute table: the essential fields that must be filled are the ones related to the topographic elevation and the nodal demand (l/s) of each node, as well as the reservoirs/tanks water levels where necessary. It is also possible to set a water leakage at an internal node, by simply selecting the appropriate curve of an external valve, located at the node itself, which “simulates” the effect of the leakage.

After creating all the nodes, pipes.shp (which by default is a Line-String shapefile) is modified by adding each pipe and its connections with the two corresponding nodes. For each pipe, the necessary information is the diameter (mm) and the ID of the chosen material, whose roughness will be defined afterwards; as specified before, lengths of the pipes are calculated automatically depending on node coordinates but otherwise they can be manually set in each pipe, after deactivating the related setting that allows the automatic calculation. All information about nodes, pipes and also valve IDs are set by the software once shapefiles modification is completed. In Fig. 18 an example of shapefiles modification in QGIS for a test network is shown:

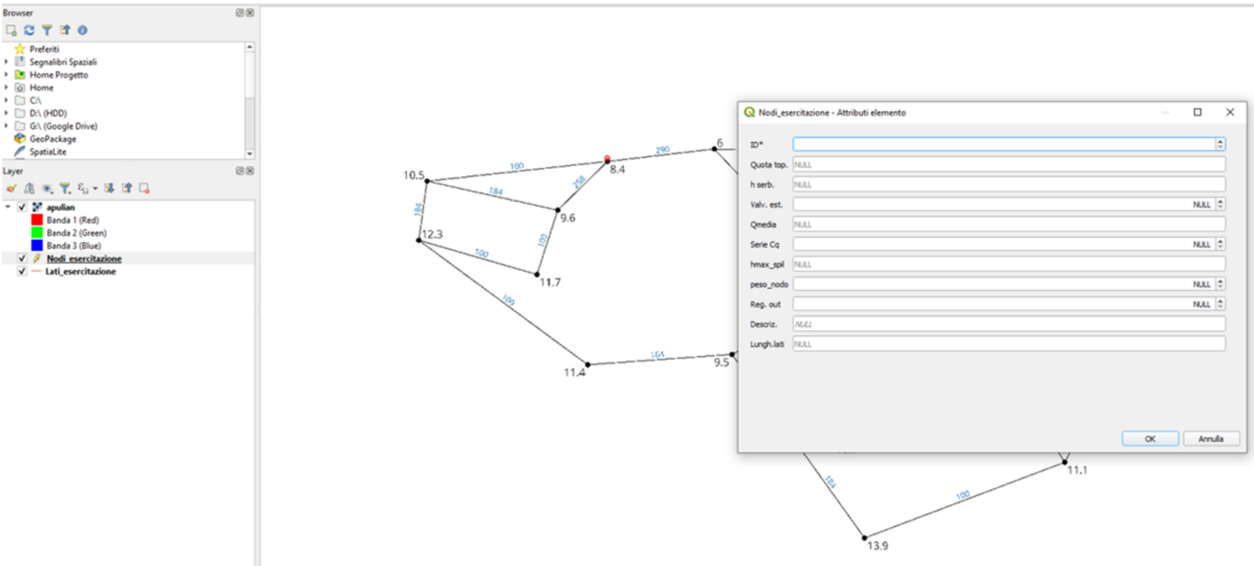

Figure 18. Definition of network properties in QGIS

3) **Materials definition**: for each material ID defined in pipes.shp, it is necessary to select the preferred resistance law and the corresponding roughness. The two available resistance laws, used to calculate pressure drop ΔH along each pipe, are Hazen-Williams and Chezy Bazin laws, respectively provided here:

$$\Delta H = \frac{10{,}675\, q_p^{1{,}852}\, L_p}{C^{1{,}852} D_p^{4{,}8704}} \tag{118}$$

$$\Delta H = 0{,}000857 \left(1 + \frac{2\gamma}{\sqrt{D_p}}\right)^2 \frac{q_p^2\, L_p}{D_p^5} \tag{119}$$

where D_p, L_p, q_p represent diameter, length and flow rate of pipe p, while C and γ are the roughness of the pipe according to the two resistance laws above.

4) **Internal / external valves and pumps definition**: if the network contains internal or external valves or pumps, already defined by simply indicating their IDs during shapefiles' modification, it is necessary to select the appropriate

curve for each valve or pump. WEC-Network already includes several curves for the most common typologies of valves (butterfly valves, gate valves etc.) and each curve contains a set of points correlating a valve opening degree with the corresponding k_v coefficient. For external valves, defined in nodes.shp, the following resistance law is adopted:

$$Q_{l,i} = k_v \Delta h^{1/\alpha} \tag{120}$$

in which Δh is pressure drop in meters of water column, $Q_{l,i}$ is the computed leakage in node i, expressed in m^3/s; α is usually set equal to 2.

The adopted resistance law in the internal valves, defined in pipes.shp, is the following one:

$$\Delta H = \frac{1}{K_v^{\alpha}} q_p^{\alpha} \tag{121}$$

where K_v depends on the valve opening degree.

Finally, to define pumps, it is required to provide the corresponding set of points (H, Q); once given, the software performs an interpolation to find the best approximation of pump's characteristic curve.

5) **Simulation run**: at this point, if the software does not show errors related to missing or wrong parameters setting, and after selecting the desired number of iterations, the simulation can be run. By default, the software runs both the simulation using the MP model and the HD model, creating two corresponding output .txt files with the computed flow rates and pressures. It is also possible to compute $W_{p,n}$ (Eq. 112) and $MPCI_p$ (Eq. 117) values for pipes: the related source code was converted into .exe extension and implemented into WEC-Network to

allow easy calculation. In Fig. 18 the output interface after running the simulation and computing criticality indicator is shown:

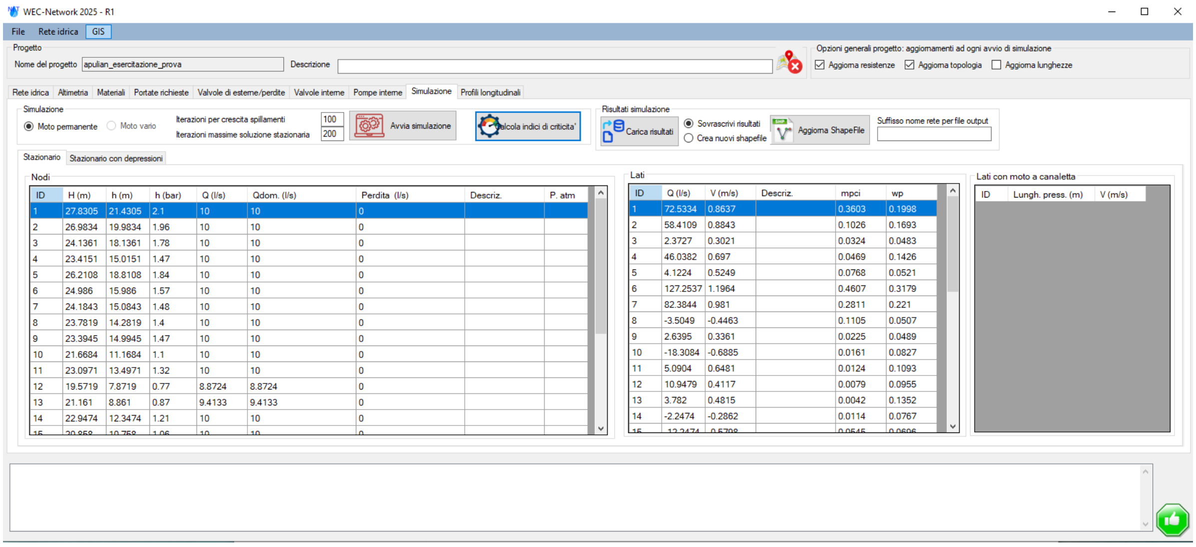

Figure 19. Output results shown by WEC-Network

All results can be written into output shapefiles to afterwards import them into QGIS. In Fig. 20a and Fig. 20b an example of visualization respectively for pressures in nodes and $MPCI$ of pipes can be observed:

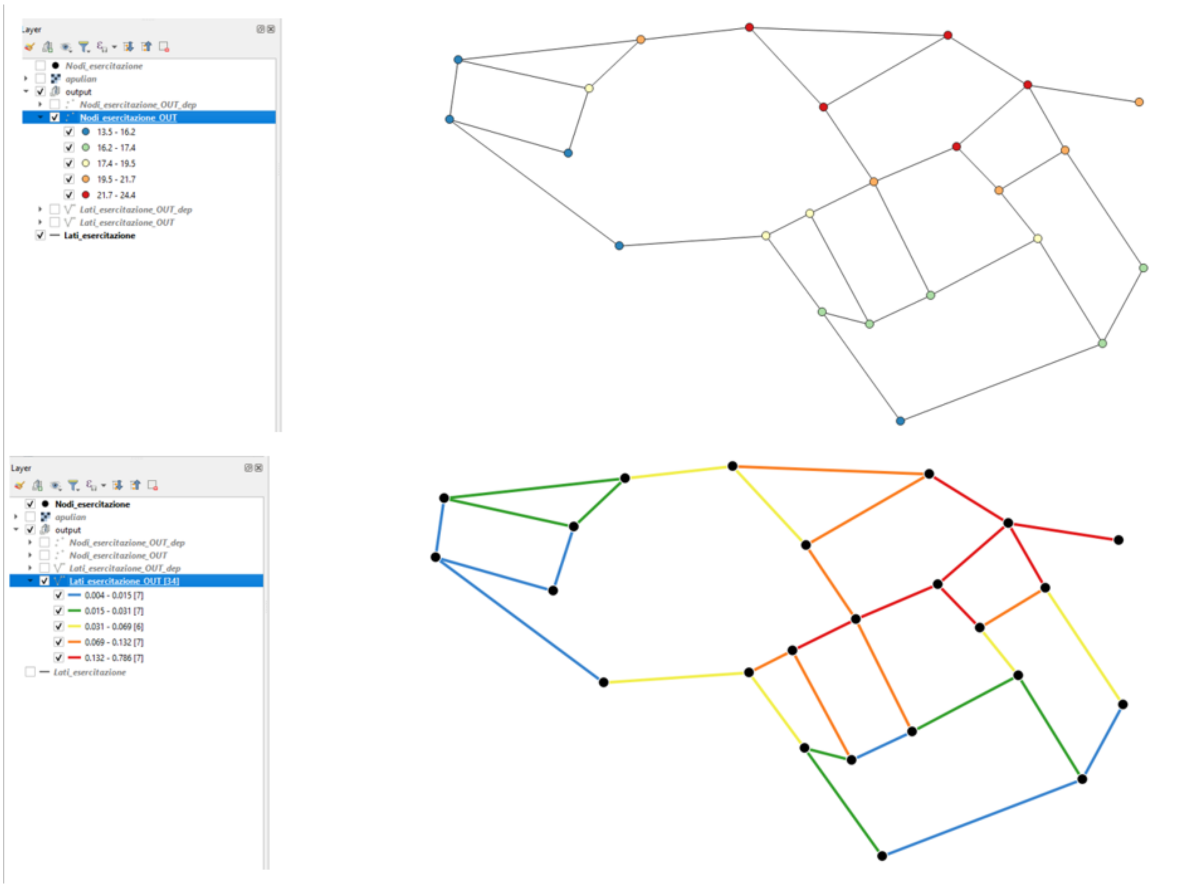

a)

b)

Figure 20. Visualization of pressures a) and b) MPCI results in QGIS

3.4.MPCI algorithm

$MPCI$ source code was written in Python 3.12.1, mainly to use open source libraries for complex networks management, like *networkx*, but also libraries to read and write shapefiles as *geopandas*; other common libraries for data management (*numpy*, *pandas*) and data visualization (*matplotlib*) were employed, while others were developed specifically for WDNs data representation, as well as for network topology metrics and hydraulic parameters calculation. A description of $MPCI$ algorithm follows here:

1) **Read input file**: after the hydraulic simulation has been run and completed, the $MPCI$ algorithm can be launched. The algorithm initially reads only one .txt input file, which is the same input file previously read by the MP hydraulic model (contained in another .exe file) and used to run the simulation. The input file contains only the working directory of the simulation files and, after being read, the corresponding .shp files, used to create the network in QGIS, are read using *geopandas* library. All network's topology and hydraulic data are properly stored into *geodataframes* and converted also into *numpy* arrays for easy manipulation.

2) **Calculate topology**: the code now rearranges the data read from the shapefiles and starts to compute several topology matrices such as the adjacency matrix for nodes (Eq. 104) and a similar adjacency matrix for pipes; nodal degree nd_i is then computed. The code contains also an optional algorithm to perform segments identification for the network, following the procedure described in Jun & Loganathan (2007) and Shin *et al.*, (2023). The methodology involves the calculation of a node-arc matrix (which constitutes a nodes-pipes adjacency matrix), a valve location matrix and a valve deficiency matrix. Even if optional and not necessary for $MPCI$ computing, segments identification can be used to create new input files for a network after a segment's shutdown, to eventually

run a separate numerical simulation for the part of the network still connected to water sources. Another optional algorithm was written in order to print .png files of the network, highlighting the identified segments. Moreover, it is also possible to print every matrix and array computed into .csv format for simple visualization.

3) **Read simulation results**: a separate library is called, written specifically to read the two output .txt files (related respectively to results provided by MP and HD approaches) created by the hydraulic model at the end of the numerical simulation. The read information include the computed nodal flows and pressures, nodes leakages, pipes flow rates as well as velocities in the saturated and unsaturated parts of each pipe and the length of pressurized part in each pipe, in case of free surface flow.

4) **Calculate $\boldsymbol{W_{p,n}}$**: two separate functions are called to compute $W_{p,n}$ (Eqs. (111-112)) respectively for MP and HD approach.

Observe that, according to Eq. (111), the term $v_{p,ff}/v_{p,sf}+1$ would be indeterminate in the event of a pipe with zero flow rate ($q_p = 0$), given that obviously this would correspond to zero velocities ($v_{p,ff} = v_{p,sf} = 0$): in this event the code skips the calculation of the fraction $v_{p,ff}/v_{p,sf}$, to avoid singularities, and directly set the $v_{p,ff}/v_{p,sf} + 1 = 1$.

While the corrective term $v_{p,ff}/v_{p,sf} + 1$ is meant to raise the criticality of pipes in which free surface flow occurs, setting it equal to 1 (which implies a lower criticality compared to a normal pressurized pipe, where $v_{p,ff}/v_{p,sf} + 1 = 2$) is consistent, because no accumulated material detachment is possible when there is no water flow in the pipe.

On the other hand, a pipe with zero flow rate is usually characterized by zero actual flow rate in both nodes (i.e. $Q_{a,i} = Q_{a,j} = 0$) and this will directly result in the maximum value (equal to 1) for the terms $(Q_{d,i} - Q_{a,i})/Q_{d,i}$ and $(Q_{d,j} -$

$Q_{a,j})/Q_{d,j}$. Therefore, the expected increase in criticality is anyway taken into account by Eq. (111) in the event of zero flow rate in pipe.

A similar calculation is performed in the case of pipes characterized by zero nodal demand in one of their nodes: in this event ($Q_{d,i} = 0$) the code sets the entire term $(Q_{d,i} - Q_{a,i})/Q_{d,i}$ equal to 0 and this is coherent because a zero nodal demand has to lower the overall criticality.

5) **Compute $\boldsymbol{p_{ij}}$**: according to Eq. (105), p_{ij} values can be calculated. Note that the computed values depend only on topological parameters and therefore are the same between MP and HD models.

6) **Compute $\boldsymbol{C_i}$**: according to Eq. (106), C_i values can be calculated. Same considerations provided in point 5 about p_{ij} computing hold.

7) **Compute $\boldsymbol{n_{\Re(i)}}$ and $\boldsymbol{d_{Ri} + d_{ij}}$**: for each node *i*, first compute the number of reachable nodes $n_{\Re(i)}$ and then, for each node *j* belonging to the set of reachable nodes, compute the length of the shortest path d_{ij} (between i and *j*) and of the shortest path d_{Ri} (between *i* and the closest reservoir *R*).

To compute all these values, a modified version of Dijkstra algorithm was written: the code creates a temporary copy of the oriented network, where paths are determined according to the direction of flow rate in each pipe, and using the function *networkx.shortest_path_length* it is possible to calculate $n_{\Re(i)}$. After that, a function was built to determine the specific path (given by a series of pipes) crossed, between each pair of nodes *i* and j, and its length.

The function computes also the number of nodes $nd_{WF(i)}$ that can reach node *i*, to be used afterwards in $MPCI$ calculation.

Observe that this is the most computationally expensive step of the entire algorithm and usually it requires about half of the total computation time.

8) **Compute the modified closeness centrality $C_{WF(i)}$**: this parameter can now be computed according to Eq. (114).

9) **Compute $MPCI_i$ (Eqs. (115-116)) for each node.**

10) **Calculate $MPCI_p$ (Eq. (117)) for each pipe**: all results can be also printed in .csv files or .png images for easy check.

Finally, the code is not parallelized as computation time is relatively short (about 5 seconds for mid-sized network with 100 nodes).

4. Results and discussion

This chapter presents several applications on real WDNs of the Minimum Pressure approach, carried out by first comparing the obtained results with those provided by HD approach. Comparison was realized first using regular functioning scenarios, where all nodal demands are met, and then under water scarcity scenarios characterized by demand shortfall and pressures reduction. In the second place, Minimum Pressure Criticality Indicator has been computed on the previously analyzed networks as well as on others, to define a prioritized maintenance planning. The contrast between the results provided by MPCI and by other criticality indicators will be shown and discussed, focusing on how the new MP model and MPCI provides a different and more detailed perspective for pipes rehabilitation planning, especially in water shortage scenarios. Finally, observe that in the figures depicted in the following sections only relevant node and pipe numbers are shown, in order to focus exclusively on the most crucial elements of the analyzed networks; more details about test cases can be found in the two related publications cited in section 1.4.1.

4.1. Applications of Minimum Pressure approach

4.1.1. Apulian Network

The first test to assess the validity of the proposed MP approach concerned the Apulian water distribution network, located in Puglia (Italy) and originally presented in Giustolisi *et al.* (2008). The network is characterized by 24 nodes, 1 reservoir and 34 pipes; all input hydraulic and geometric parameters, as nodal demands, pipe lengths, roughness etc., can be found at https://doi.org/10.2166/hydro.2025.027; pressure drops were calculated using Chezy-Bazin law (Eq. 119). In Fig. 21 Apulian Network is shown:

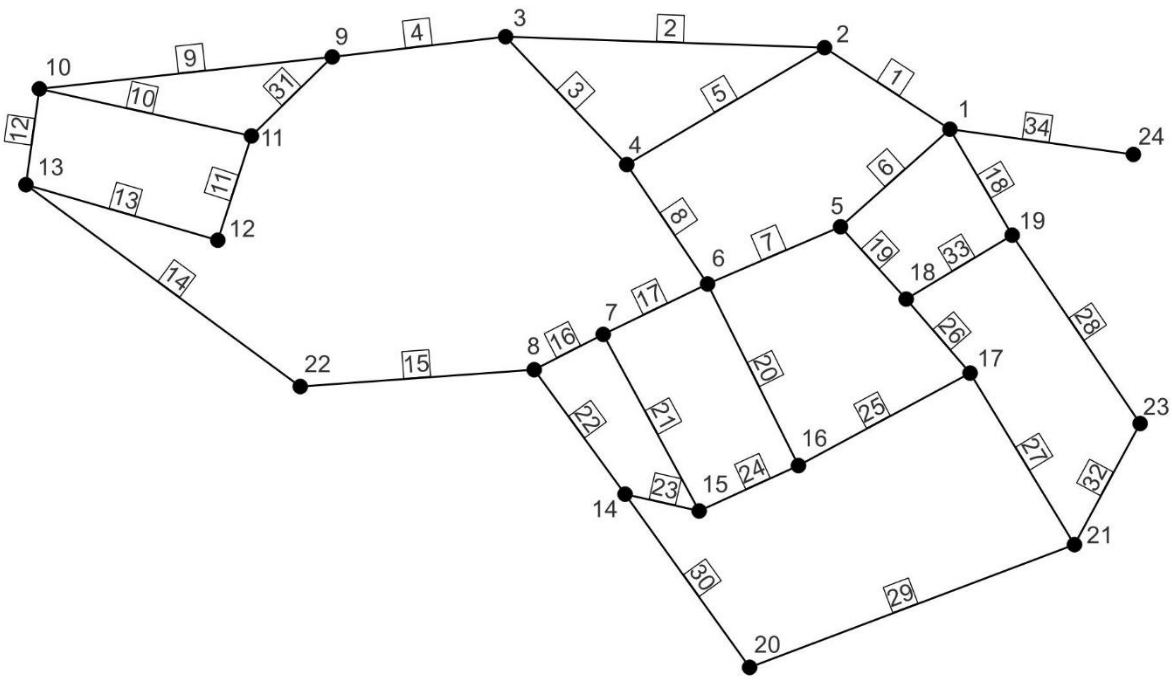

Figure 21. Apulian network layout

In an initial test a regular functioning scenario was considered, in which the flow rate leaving the reservoir (node 24) corresponds to the design one, all nodal demands are satisfied, and pressures remain positive in all nodes. In this case, the output values provided by the MP model are almost identical to those provided by HD model. This is due to the strictly positive pressures occurring in all nodes of the WDN.

A different scenario, characterized by the isolation for maintenance of only pipe 1 (connecting nodes 1 and 2), was then analyzed: in this instance significant differences between the outcomes of the two used numerical models (MP and HD) were evident, as it can be seen in Fig. 22:

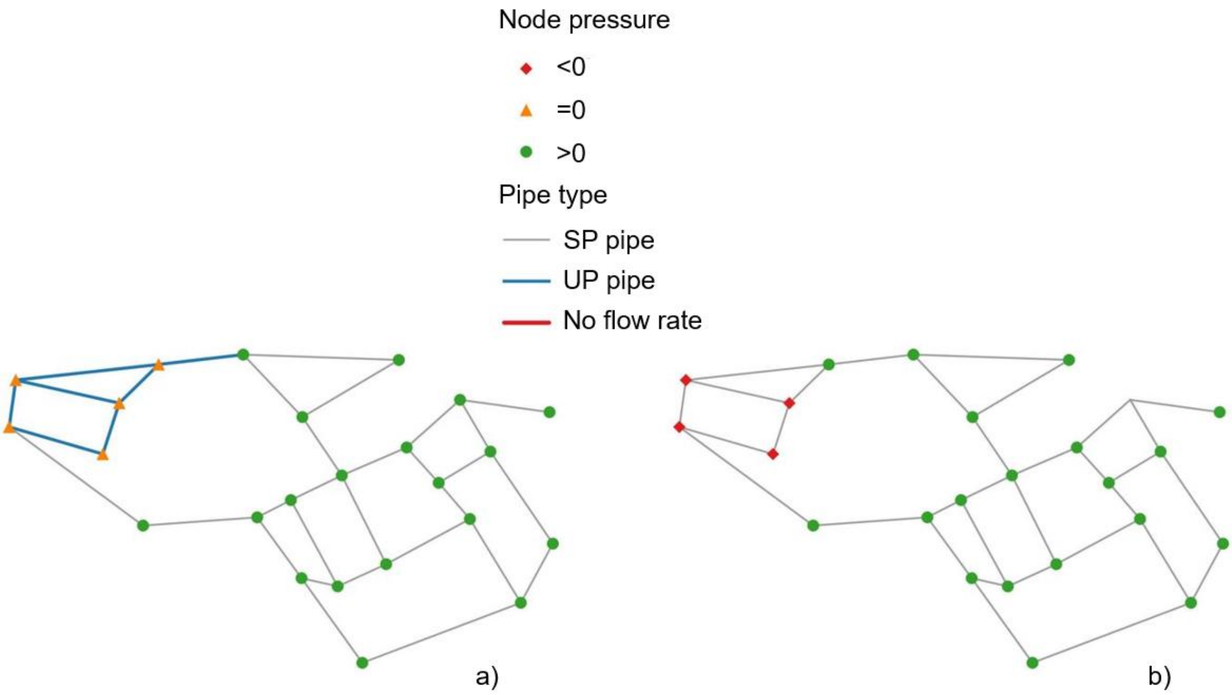

Figure 22. Pressures and nodal flow rates for Apulian WDN computed by a) MP approach and b) HD approach

In Fig. 22 it is clear how the removal of pipe 1 leads to a water flow redistribution in the whole WDN, impacting nodal pressures and finally resulting in a water crisis in the left area of the network (Fig. 22a): in fact, the MP model shows 5 nodes (9, 10, 11, 12, 13) with pressures equal to zero and consequently in 7 pipes free surface flow occurs. Differently, according to HD model (Fig. 22b), unrealistic negative pressure values characterize 4 nodes and there are no free surface flow pipes (UP pipes).

In the following Table 1 nodal flows computed by the two numerical models can be viewed:

Table 1. Computed pressures and flow rates for Apulian WDN

Node ID	Pressure with MP approach (m)	Pressure with HD approach (m)	Nodal flow rate with MP approach (l/s)	Nodal flow rate with HD approach (l/s)
1	28,5	28,5	10,9	10,9
2	1,3	1,4	6,2	6,4
3	2,4	2,4	7,2	7,3
4	1,7	1,7	5,9	5,9

5	24,8	24,8	10,1	10,1
6	21,0	20,9	15,4	15,4
7	19,7	19,6	9,1	9,1
8	18,6	18,5	10,5	10,5
9	0,0	0,0	0,0	0,5
10	0,0	-1,9	0,0	0,0
11	0,0	-1,2	0,0	0,0
12	0,0	-3,1	0,0	0,0
13	0,0	-3,6	0,0	0,0
14	16,2	16,1	13,6	13,6
15	14,9	14,8	9,2	9,2
16	15,3	15,2	11,2	11,2
17	16,5	16,4	11,5	11,5
18	20,1	20,1	10,8	10,8
19	20,7	20,7	14,7	14,7
20	10,8	10,8	13,3	13,3
21	12,6	12,5	14,6	14,6
22	13,7	13,4	12,0	12,0
23	11,6	11,6	10,3	10,3
24	21,4	21,4	-196,5	-197,3

Observe that, even though the overall discrepancies in the computed flow rates between the two models are negligible, node 9 instead has zero actual flow rate according to MP approach while the value computed by HD approach is 0,5 l/s: this proves that MP approach is able to better identify nodes where demand cannot be satisfied. Besides, in reservoir 24 the total flow rate computed by HD model is higher than the corresponding flow rate calculated by MP solution.

In Fig. 23 the residual *Res*, previously defined in Eq. (96), is shown. A total number of 100 iterations was used for the transition between the initial reduced nodal demand to the final desired demand in each node. It can be observed that residual remains close to zero after each iteration until the computed flow rates are low enough to maintain the whole piezometric line above nodes' elevations. The two peaks calculated at iterations 41 and 62 are correlated to two new groups of ID nodes, finally equal to five. Residual rapidly converges to zero after the effective nodal demands are reached at iteration 100.

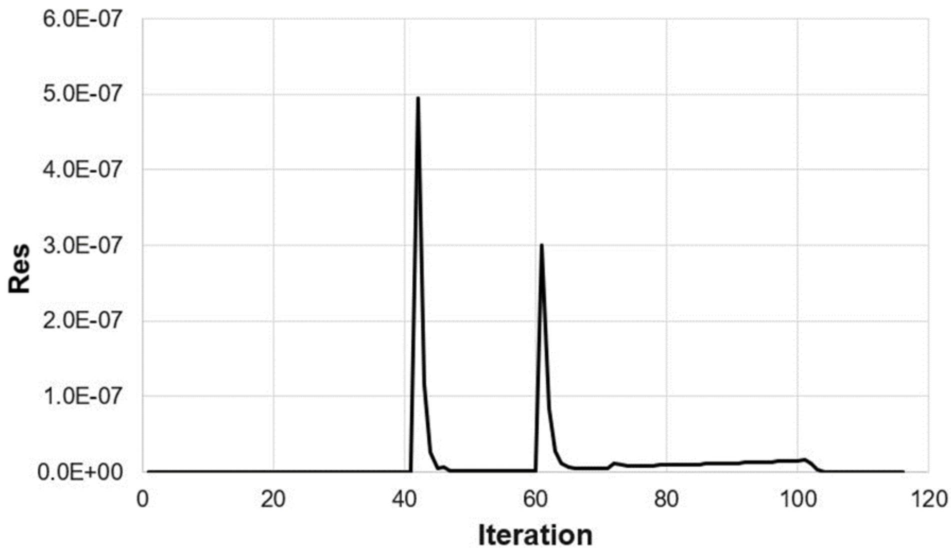

Figure 23. Residual Res computed for Apulian Network

Finally observe that the hypothesis of isolation for maintenance of the lone pipe 1, without impacting any other near pipe, actually implies that two isolation valves are located near the two nodes (nodes 1 and 2) of pipe 1, and that by closing both valves it is possible to perform the mentioned isolation.

4.1.2. Campofelice di Roccella Network

MP algorithm was applied also for the simulation of a new WDN for the residential area of Campofelice di Roccella, in Sicily, depicted in Fig. 24. The network has 129 nodes, 1 reservoir and 177 pipes and its total length L_{net} is equal to 9,82 km. Nodes elevations vary from 43 m in the upper region to 89 m in the lower region of the network, while the reservoir is located at 112 m of total elevation. A needle valve is positioned in pipe 129, downstream of the reservoir.

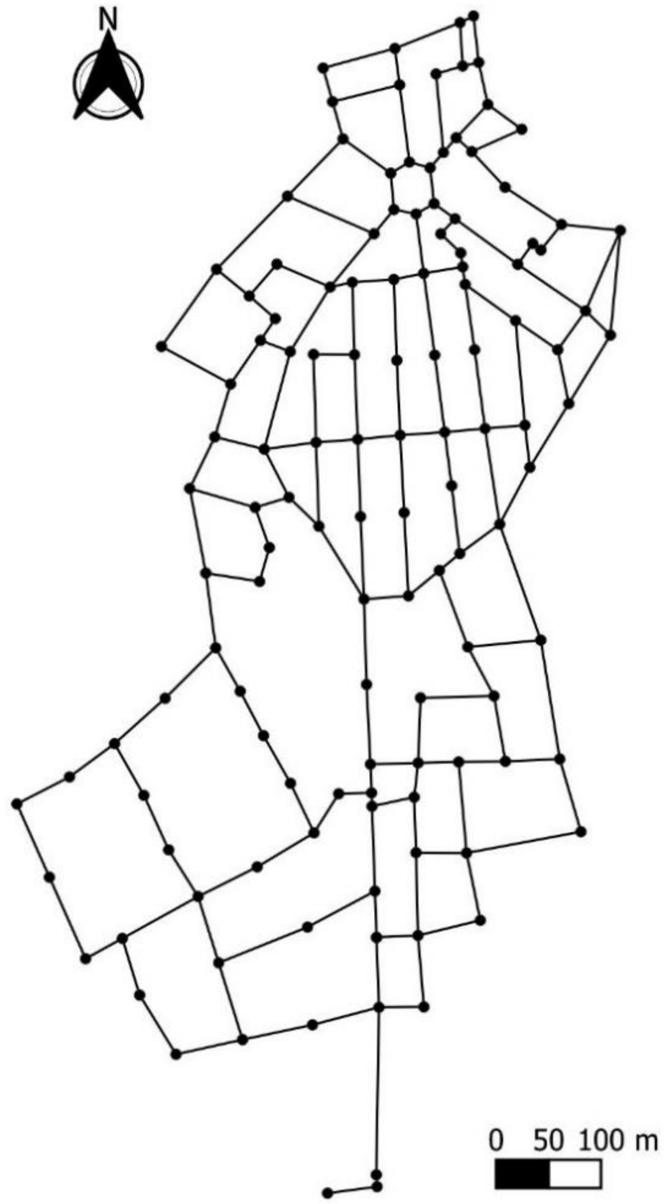

Figure 24. Campofelice di Roccella WDN layout

The WDN was designed to supply about 330 l/capita/day, corresponding to a water supply Q_{supply}, leaving the reservoir and equal to 30,6 l/s. In the design scenario, each nodal demand is assumed to follow Wagner law (Eqs. (73)), with $amax = 10\ m$. Moreover, the maximum nodal demand Q_i^{d0} is assumed to depend, in each node, on the sum of the lengths L_{ij} of all connected pipes, as follows:

$$Q_i^{d0} = \frac{\sum \frac{L_{ij}}{2}}{L_{net}} Q_{supply} \tag{122}$$

A water leakage Q_i^l is also assumed to occur, in each internal node, according to:

$$Q_i^l = \sum \frac{L_{ij}}{2} \cdot K_l \sqrt{h_i - z_i} \tag{123}$$

where K_l represents a constant, common to every node, calibrated to obtain a total leakage of 18% of the total water demand in the design scenario; pressure drops were calculated using Hazen-Williams law (Eq. 118). In the initial design scenario, the needle valve is fully opened and this led to a total demand Q_{net} = 25,2 l/s and a total leakage $Q_{leakage}$= 5,4 l/s. As expected, in this first simulation both MP and HD model provided the same results due to positive pressures occurring in every node.

However, in the event of water scarcity, it is necessary to reduce the actual nodal flows and this is usually realized by decreasing the opening degree of the needle valve downstream the reservoir. A new scenario was therefore considered in which the reduced water supply is 135 l/capita/day (about a half of the design water supply) and this was realized by setting the needle valve opening degree to 4,9%.

In this new configuration, the MP model leads to a reduced water flow rate of 15,3 l/s leaving the reservoir, with 42 nodes characterized by zero pressure and free surface flow occurring in 19 pipes, as it can be observed in Fig. 25a:

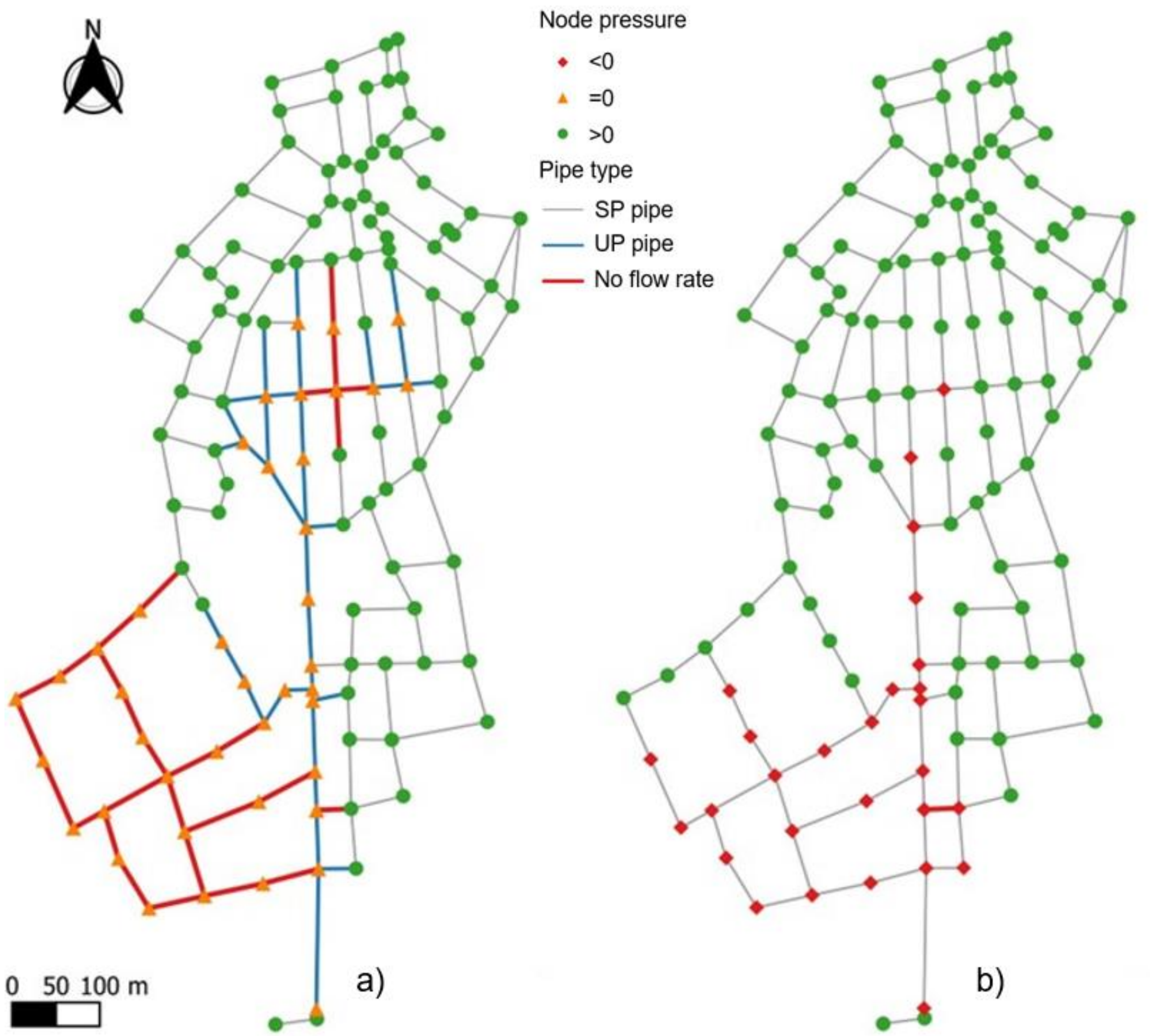

Figure 25. Pressures and nodal flow rates for Campofelice di Roccella WDN with same valve opening degree computed by a) MP approach and b) HD approach

Observe that in this configuration the resulting total leakage, considering all internal nodes, is $Q_{leakage}$= 1,8 l/s. Results provided by HD model (Fig. 25b) are significantly different: indeed, according to HD model there are 29 nodes characterized by negative pressures, with values reaching -10,3 m of water column; moreover, the total water flow leaving the reservoir is 18,1 l/s, higher than the corresponding one calculated by MP model.

A final test to compare the two numerical models was carried out by assuming two different valve opening degrees for each model, in order to get in both cases the same reservoir flow rate, equal to 15,5 l/s. In this scenario, presented in Fig. 26, opening degree was set equal to 3,97% in the HD model: the output results (Fig. 26b) show 43 nodes with negative pressure and values reaching up to -13,9 m of water column. Besides, according to HD model, there is only one pipe with zero flow rate, while according to MP there are even 28 pipes with zero flow rate. It is clear then that pressure results provided by HD model, along with the corresponding actual nodal flow rates, are physically inadmissible and consequently lead to substantial errors in the computed flow rates.

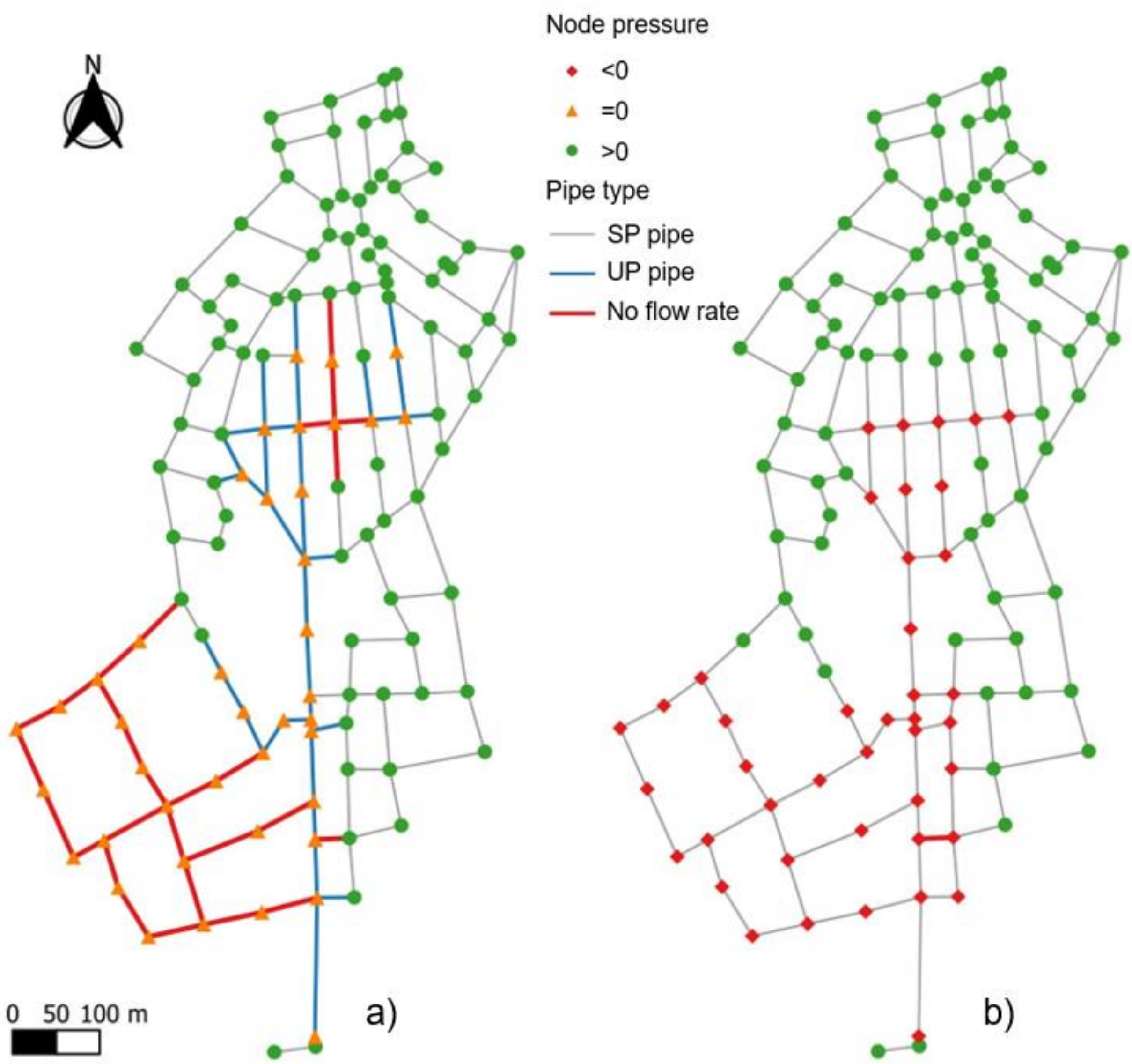

Figure 26. Pressures and nodal flow rates for Campofelice di Roccella WDN with same reservoir flow rate computed by a) MP approach and b) HD approach

The previous two tests showed how the new MP model is able to correctly describe the regular functioning scenario of a common water distribution network, as shown in the Apulian network test, providing results very close to the ones given by the traditional HD model. Instead, during maintenance of pipes or in water scarcity scenarios, the pressures and flow rates computed by HD model can be unrealistic and have a considerable impact on all the hydraulic parameters computed in other parts of the WDN, while MP model always guarantees at least a realistic minimum value of zero pressure in nodes and accordingly computes more realistic actual nodal flows.

Observe that the numerical problem solved by the minimum pressure approach could lead to non-unique solutions in pressure deficiency conditions where several nodes are characterized by zero flow rate: in water scarcity scenarios, such as drought, we expect the network to gradually shift from a regular operating condition, characterized by positive pressures and where every demand is satisfied, to a scarcity condition in which some nodes are characterized by progressively decreasing flow rates, finally leading to zero flow rate in specific parts of the WDN. The MP model tries to represent the above described process, which is likely to occur in drought scenarios, assuming a very slow transition from one partition of the elements (nodes and pipes) to the next one, according to the methodology explained in section 3.1.1.6.

4.2. Applications of MPCI

In this section the proposed formulations of $W_{p,n}$ and $MPCI$ will be applied to realize a criticality assessment of pipes on real water networks, comparing the results of the proposed indicators with the ones obtained by applying other criticality indicators available in the literature, to show how $MPCI$ is able to give a detailed and physically-based perspective on the hydraulic dynamics occurring in the networks. The new formulations will also be employed to evaluate and compare the results provided by the MP approach and HD approach, to highlight how the new numerical model can identify free surface flow pipes and zero flow rate pipes, finally yielding a significantly different outlook on WDN criticality assessment.

4.2.1. North Marin WDN

A first test was conducted on the EPANET Network3, based on the real North Marin water network (Clark *et al.*, 1995), which represents a well-known benchmark used in the literature for comparisons. All network data are available at the online database https://uknowledge.uky.edu/wdsrd/. The network presents 95 nodes, 4 reservoirs (nodes 92, 93, 94, 95), 115 pipes and 1 pump; the network configuration at 12.00 A.M. was considered, as shown in the following Fig. 27:

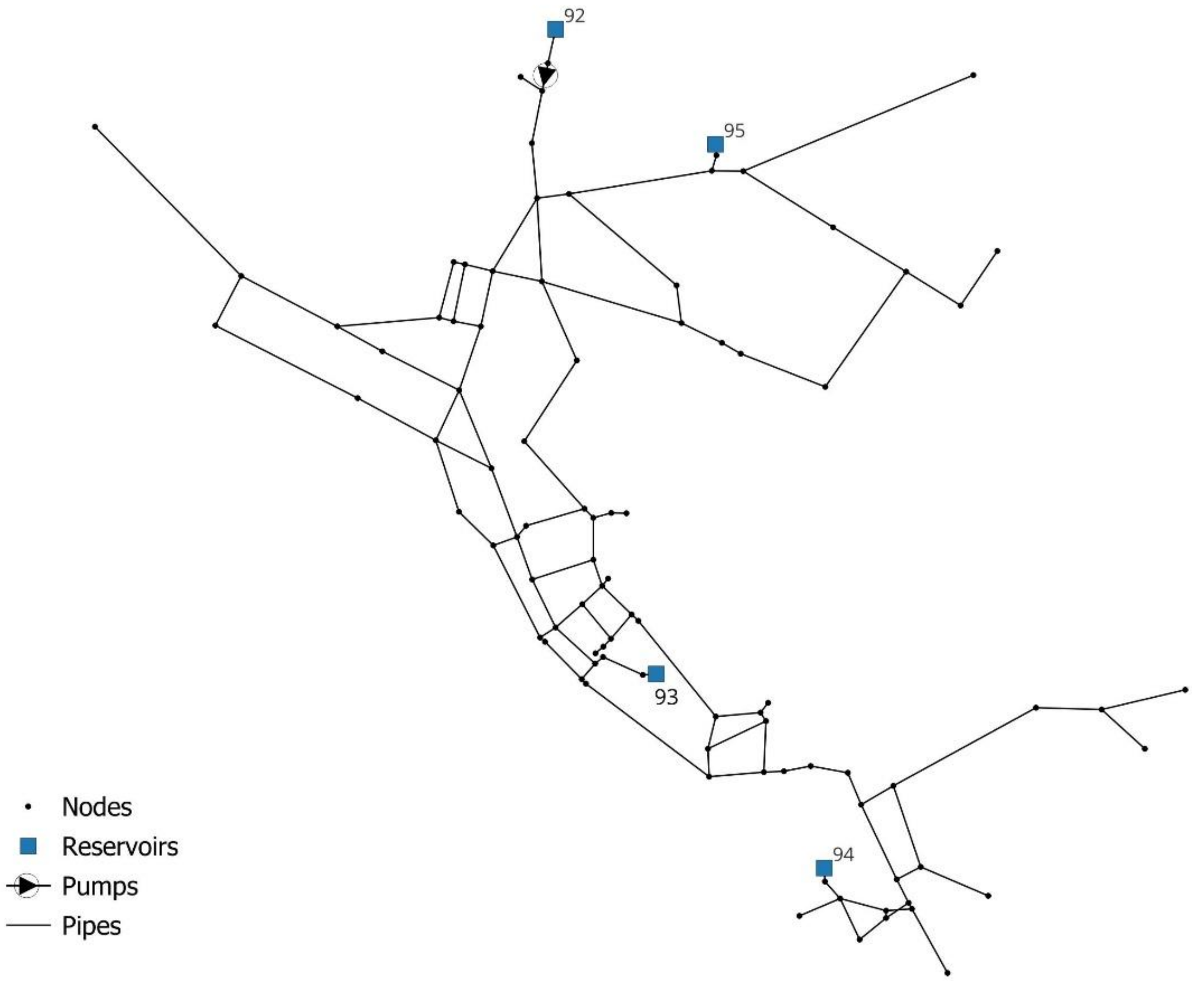

Figure 27. North Marin WDN layout

A water scarcity scenario was considered, removing three reservoirs (93, 94, 95) and installing a needle valve with 94,3% opening degree downstream reservoir 92. Numerical simulation was run using only the head driven approach, to compare the results obtained by applying the new $W_{p,n}$ and $MPCI$ respectively with the W_p and HCC formulations, proposed by Marlim & Kang (2024) and here reported for clarity:

$$W_p = \left(\frac{Q_{a,i}}{nd_i} + \frac{Q_{a,j}}{nd_j}\right)\frac{q_p}{Q_{net}} \tag{124}$$

$$HCC_{(i)} = \frac{1}{nd_i}\left(C_{(i)}^{-1} + \sum_{j=1, j\neq i}^{nd_i} W_{p(i,j)} C_{WF(j)} C_{(j)}^{-1}\right) \tag{125}$$

where all symbols were previously defined, and $C_{(i)}$ is computed according to Eq. (96) but all p_{ij} terms are computed as follows:

$$p_{(i,j)} = \frac{W_{p(i,j)}}{\sum_{j\in\Gamma(i)} W_{p(i,j)}} \tag{126}$$

In the following Fig. 28, after running hydraulic simulation with HD approach, results obtained with the new hydraulic weight formulation $W_{p,n}$ of Eq. (112) are compared with those provided by the W_p (Eq. 124) proposed by Marlim & Kang (2024). Pipes were classified in six criticality groups, depending on the computed values, and colored accordingly.

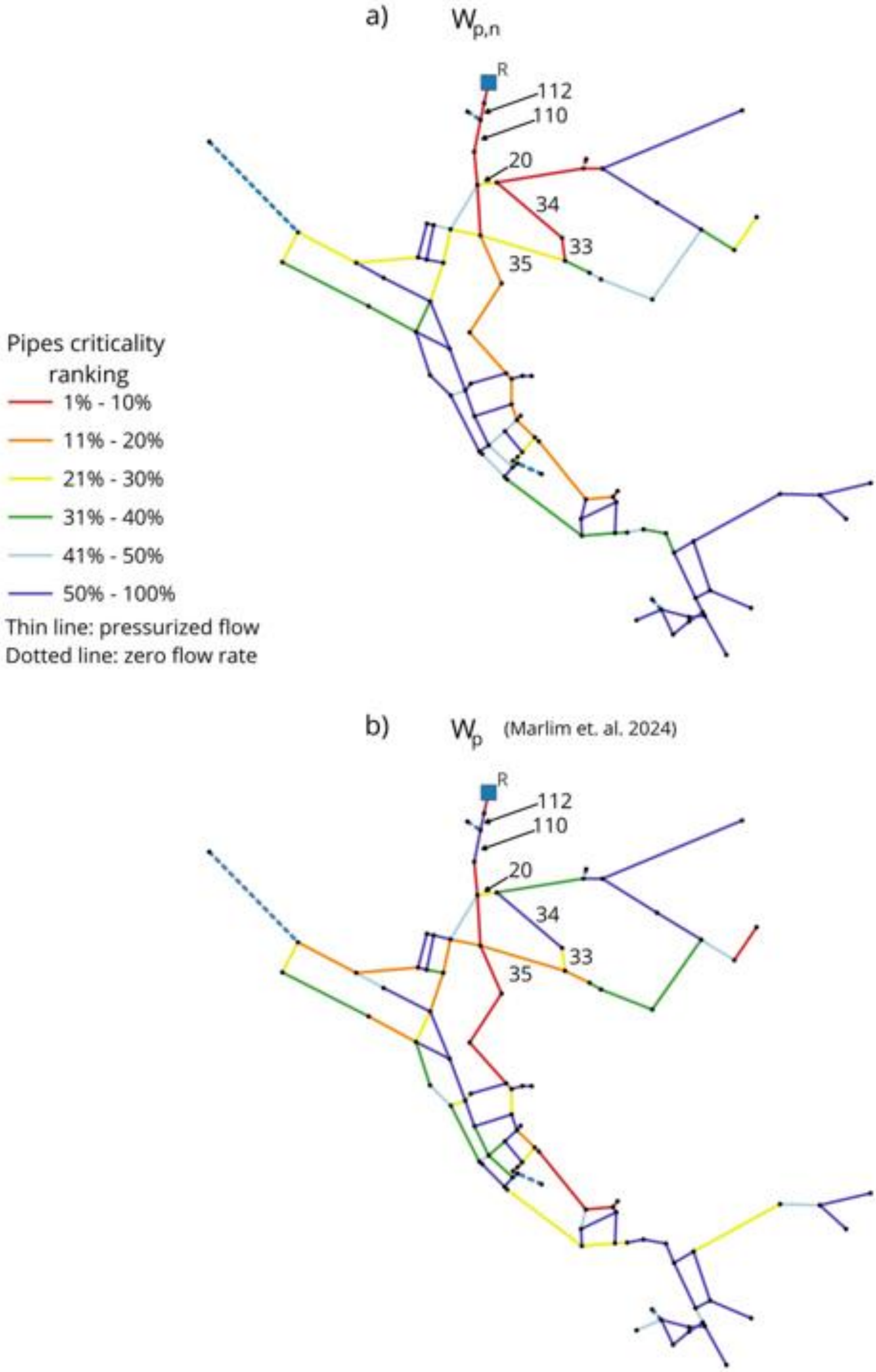

Figure 28. North Marin WDN pipes ranked in six criticality groups: e.g. considering the WDN with 112 pipes, "1% - 10%" refers to the first 11 (about 10%) pipes with the highest values of the computed indicator. IDs of relevant pipes are depicted in black; head driven (HD) approach was used. Ranking according to:
a) $W_{p,n}$ and b) W_p (Marlim & Kang (2024))

In Fig. 28a it can be seen that pipes characterized by the highest values of $W_{p,n}$ (between the top 1% and top 10% in $W_{p,n}$ criticality ranking, depicted in red) are those carrying large volumes of water, and are mainly located near the reservoir and in the central branch of the network, delivering water to all the other parts of the WDN. Instead, pipes located in peripheral areas generally occupy lower positions in the same criticality ranking, as they are not critical from only a hydraulic perspective.

Instead in Fig. 28b it can be observed that pipes 112 and 110, though being the two closest ones to the only reservoir, according to Eq. (124) rank in the last criticality group: in fact, even if they both carry the total flow rate delivered in the network, due to the fact that all their nodes have zero nodal demand, W_p computed according to Eq. (124) reduces to zero and it is unable to catch the real criticality of these pipes. Conversely, the new formulation of $W_{p,n}$ (Eq. 111) is still able to correctly represent the real hydraulic dynamics of the network, given that pipes 112 and 110 are surely the most important in the WDN, as the entire network would be isolated from the water source if even one of them were affected by failure or disconnected from the network. Another consistent difference to highlight between Fig. 28a and 28b concerns pipes 33 and 34: for both these pipes, one of their two nodes suffers a water deficiency due to nodal demand not being completely satisfied ($Q_{a,i} < Q_{d,i}$). Despite these nodal demands are quite small and the pipe flow q_p is low as well, $W_{p,n}$ in Fig. 28a takes into account this aspect and rises pipes 33 and 34 criticality, ranking them in the first criticality group, thanks to the increase of the terms $(Q_{d,i} - Q_{a,i})/Q_{d,i}$ and $(Q_{d,j} - Q_{a,j})/Q_{d,j}$. On the contrary, in Fig. 28b these pipes rank in the third and last criticality group.

In the following Fig. 29 criticality ranking obtained by computing $MPCI_p$ (Eq. 117) is compared to the ranking suggested by the HCC formulation of Eq. (125):

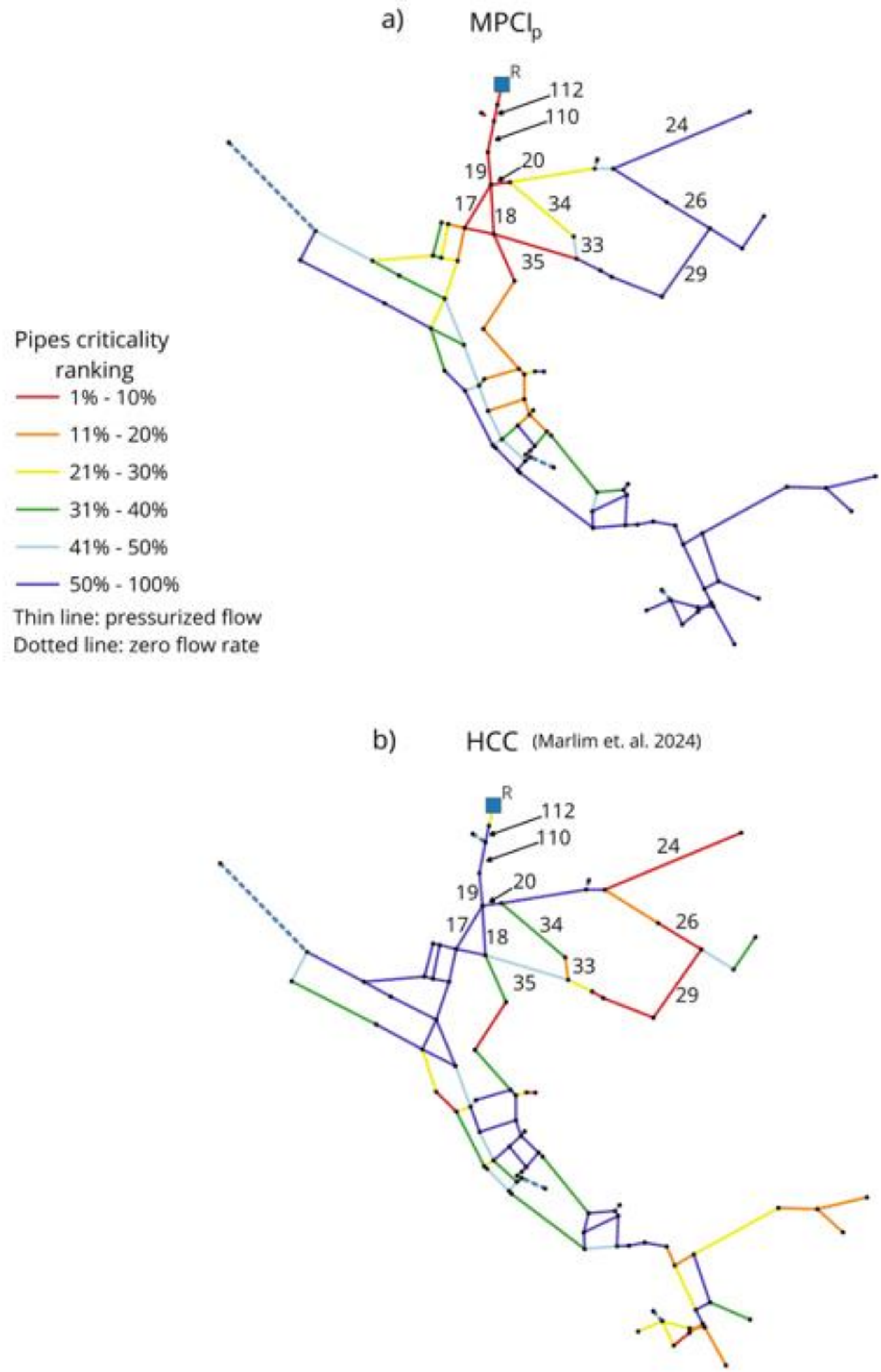

Figure 29. North Marin WDN pipes ranked in six criticality groups: e.g. considering the WDN with 112 pipes, "1% - 10%" refers to the first 11 (about 10%) pipes with the highest values of the computed indicator. IDs of relevant pipes are depicted in black; head driven (HD) approach was used. Ranking according to:
a) $MPCI_p$ and b) HCC (Marlim & Kang (2024))

It can be observed how pipes 33 and 34 are characterized by moderately high values of criticality according to $MPCI_p$ in Fig. 29a, although being located near more critical pipes: this is due mostly to the low fraction of the total water flow carried by these pipes to the upper region of the WDN. The highest fraction of water flow is instead carried by pipes 20 and 25, the only two pipes connected both to the central branch of the network and to the upper right region: this topological aspect is the main reason why they are placed in the first criticality group, unlike $W_{p,n}$ which, considering only hydraulic parameters, ranks them in the third criticality group (between top 21% and top 30%).

It is clear how $MPCI_p$ and HCC criticality rankings differ even more than the hydraulic weights compared in the previous Fig. 28, as both indicators integrate topological parameters, and this is reflected by the criticality ranking shown in Fig. 29b: pipes 112 and 110 are still placed in the least critical group but this time, differently from what shown by W_p in Fig. 28b, this criticality affects their downstream connected pipes as well (pipes 19, 17, 18), causing them to be placed in the sixth criticality group. Again, this is the consequence of zero nodal demands that affect both nodes of pipes 112 and 110, causing their W_p (Eq. 124) to drop to zero and losing all the information expressed by the highest values of q_p held by these pipes; this finally propagates into the HCC rankings of the connected pipes. On the other hand, $MPCI_p$ (Fig. 29a) correctly ranks pipes 112 and 110 among the most crucial pipes, as they transport a large part of the entire flow rate extracted from the WDN, coherently with the topology of the network.

Significant differences can also be observed in pipes 24, 26 and 29 located in the top right region of the network: according to HCC (Fig. 29b) they all rank in the first criticality group both because of their considerable distance from the water source, but especially due to the term $1/nd_i$ in Eq. (125) which drastically raises the whole HCC for pipes characterized by few connections (small nd_i). Differently, $MPCI_p$ ranking for the same pipes is the lowest (Fig. 29a) because $MPCI_p$ assigns higher criticality to the upstream pipes (as the already described pipes 112, 110 etc.) necessary to maintain pipes located in external regions connected to reservoirs.

Finally, in order to quantify the differences in criticality ranking of the proposed indicators, Spearman correlation coefficient r_s was calculated and results are shown in the following Table 2:

Table 2. Spearman's correlation coefficient r_s for North Marin WDN

$W_{p,n}$ - W_p (Figs. 27a-27b)	$W_{p,n}$ - $MPCI_p$ (Figs. 27a-28a)	W_p - HCC (Figs. 27b-28b)	$MPCI_p$ - HCC (Figs. 28a-28b)
0.536	0.477	0.386	-0.446

A good correlation (r_s=0.536) was found between $W_{p,n}$ and W_p (Marlim & Kang (2024)), mainly because of the influence of pipe flows q_p; a similar positive trend (r_s=0.477) exists between $W_{p,n}$ and $MPCI_p$ and this is consistent with the fact that $MPCI_p$ gives relevance to hydraulic parameters, even when topological parameters are integrated in criticality ranking. Differently, $MPCI_p$ and HCC show considerably different tendencies (r_s=-0.446), as confirmed in Figs. 28a-28b, and this depends on the different way of managing zero demand nodes by their respective formulations.

With the aim of providing a more accurate idea of how the computed results could give a different perspective on water quality issues arising in the WDN, a realistic 24h demand pattern was considered for Network3 and hydraulic simulations were performed accordingly:

Table 3. Demand pattern for North Marin WDN

Hour	Nodal demand multiplier coefficient
1	1.34
2	1.94
3	1.46
4	1.44
5	0.79
6	0.92
7	0.85
8	1.07
9	0.96
10	1.1
11	1.08
12	1.19
13	1.16
14	1.08
15	0.96
16	0.83
17	0.79
18	0.74
19	0.64
20	0.64
21	0.85
22	0.96
23	1.24
24	1.67

Results computed by the 24 simulations show that pipes velocities in 106 of the 112 pipes are subject to an increase up to 203%. Following Braga *et al.* (2020), these significant variations could lead to systematic detachment of the material accumulated along pipes' inner surfaces, especially due to the increase of shear stress. This effect is more remarkable in extended water scarcity scenarios, when several pipes with no flow rates do exist: when the network returns to normal operating conditions, the restored water flow in those pipes could cause the detachment of accumulated material over the water deficiency period.

4.2.2. Campofelice di Roccella WDN

The second case study to evaluate $MPCI$ performance is the Campofelice di Roccella WDN, already presented in section 4.1.2. In this second test the reservoir water flow in the design scenario is Q_{supply}=39,2 l/s. A different water scarcity scenario was considered, with a reduced water flow Q_{supply}=30,4 l/s (about 75% of the design water flow), obtained by placing a needle valve downstream the reservoir and setting a water leakage in each internal node, with a total $Q_{leakage}$=5,2 l/s. Before comparing the results provided by criticality indicators, in the following Fig. 30 the results obtained by using MP and HD approaches in the proposed scenario are shown:

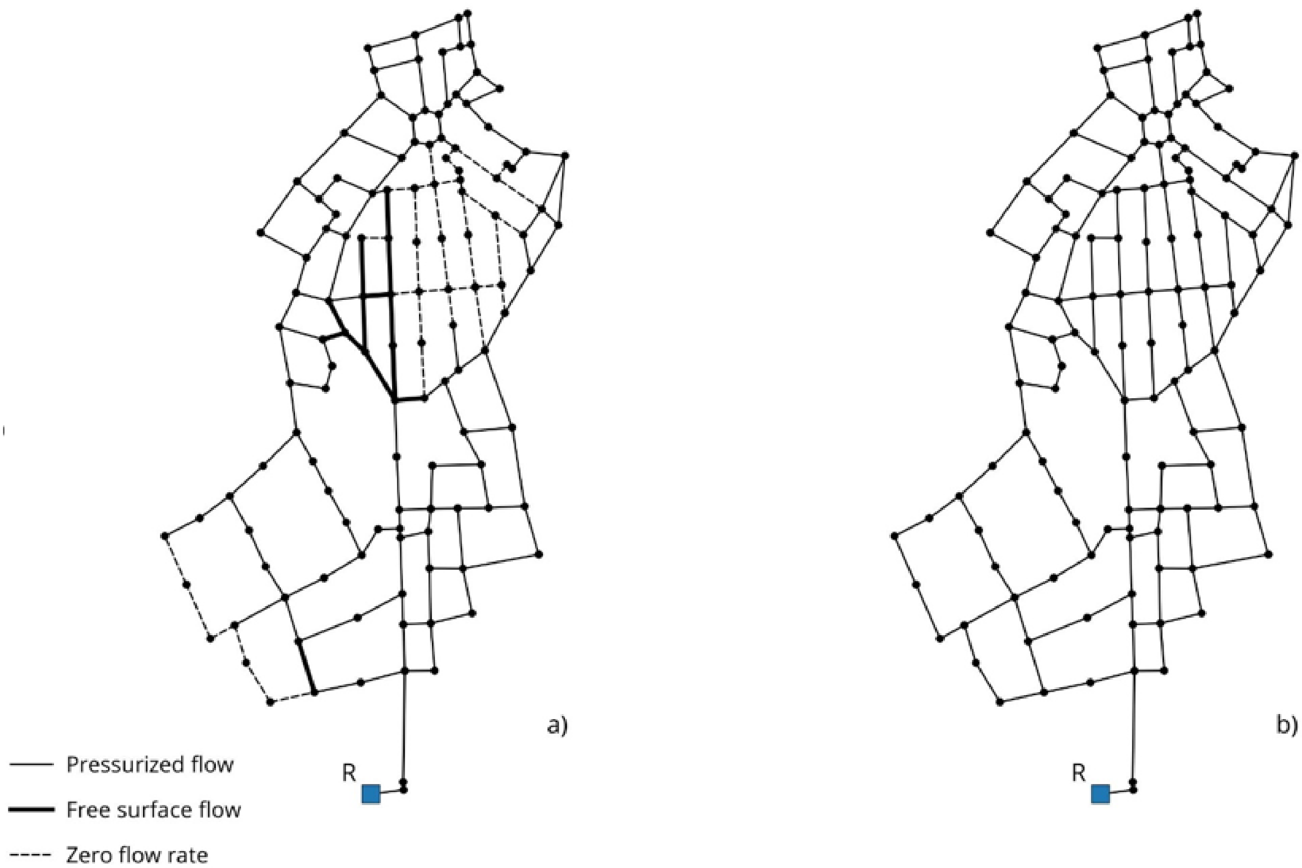

Figure 30. Flow rates in the water scarcity scenario computed by a) MP approach and b) HD approach

As it can be observed, in the considered water scarcity scenario considered HD model (Fig. 30b) does not identify pipes with zero flow rates, as well as free surface flow pipes as expected. On the contrary, MP model shows 13 pipes characterized by free surface flow and 36 pipes with zero flow rates, representing about 20% of the total number of pipes in the WDN. Clearly, these remarkable differences will be reflected by the computed values of hydraulic weight $W_{p,n}$ and criticality indicator $MPCI$, as depicted in Fig. 31:

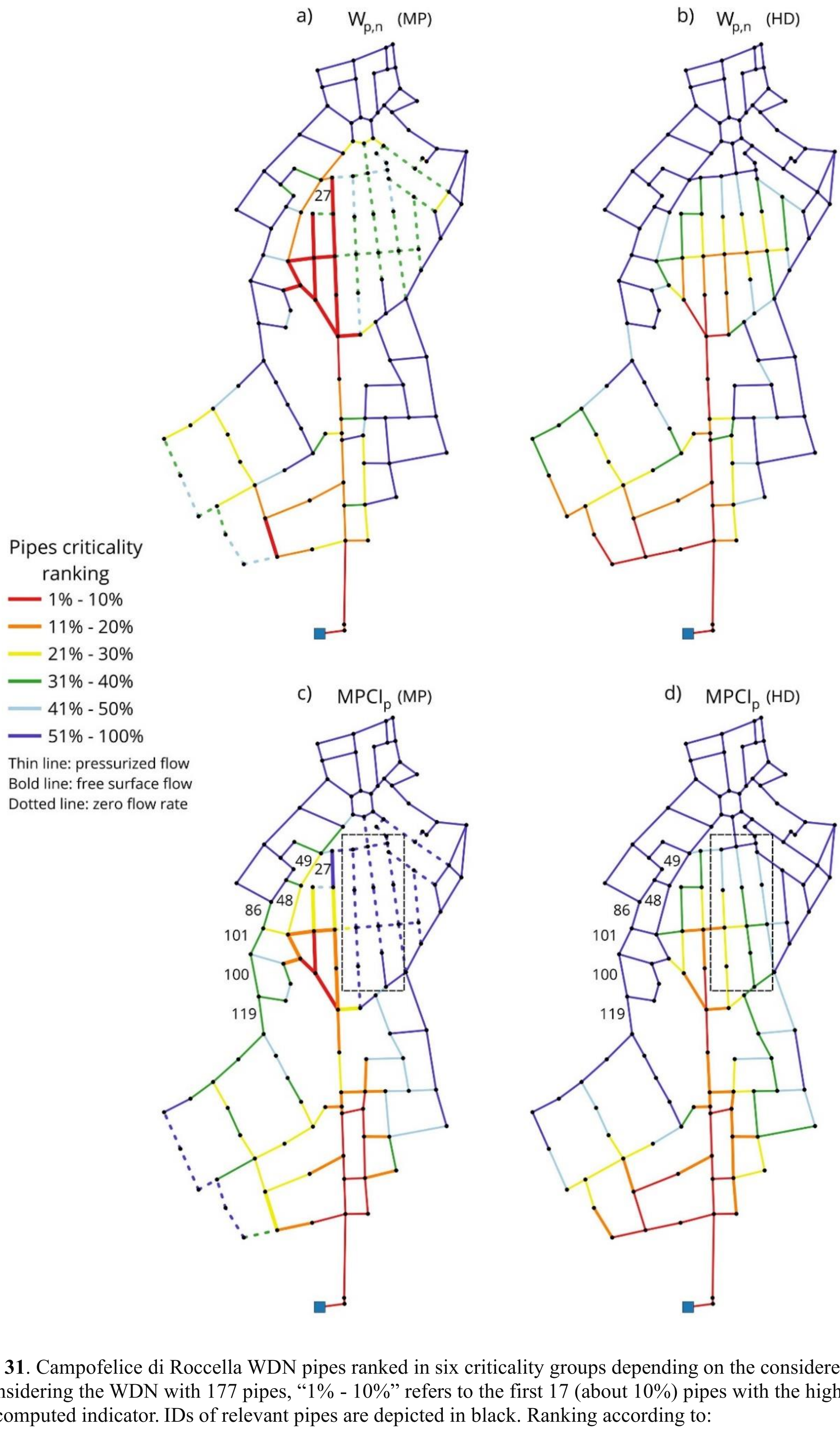

Figure 31. Campofelice di Roccella WDN pipes ranked in six criticality groups depending on the considered indicator: e.g. considering the WDN with 177 pipes, "1% - 10%" refers to the first 17 (about 10%) pipes with the highest values of the computed indicator. IDs of relevant pipes are depicted in black. Ranking according to:
a) $W_{p,n}$ (MP approach) ; b) $W_{p,n}$ (HD approach) ; c) $MPCI_p$ (MP approach) ; d) $MPCI_p$ (HD approach)

According to both results computed by $W_{p,n}$ and $MPCI_p$, the most critical pipes are those located near the reservoir in the bottom area of the WDN, followed by the adjacent pipes and the ones located in the central region.

As it can be observed, $W_{p,n}$ criticality rankings between MP and HD models (Figs. 31a-31b) do not differ particularly in key regions of the network. This is due to the high number of pipes characterized by unmet nodal demands in at least one of their nodes. This proves that Eq. (111) is correctly able to identify critical pipes from a hydraulic perspective and it is not overly affected by the hydraulic model chosen for the numerical simulation, though obviously free surface flow pipes computed by MP model tend to occupy higher positions, in criticality ranking, with respect to the same ranking provided by HD model.

Moreover, because of water leakages in nodes, the flow rates q_p will increase in some pipes, leading to a rise in the corresponding $W_{p,n}$ and this is coherent as the criticality of these pipes has to account for the consequences of leakages. Note that, for this reason, $Q_{a,i}$ and $Q_{a,j}$ values in Eq. (111) were computed considering only the actual nodal flow delivered to nodes, excluding leakages.

Criticality rankings suggested by $MPCI_p$ values offer a different view on the network: in fact, according to the $MPCI_p$ criticality classification obtained using the HD approach (Fig. 31d), there exists an entire group of pipes, located in the central region of the WDN (inside the dotted box in Fig 31d), that rank between the third and fifth criticality group. This is the consequence of HD model being unable to estimate the zero flow rate pipes in this area of the network, which instead is correctly identified by the MP model (Fig. 31c). Therefore, according to HD approach, all the pipes situated in this central region share considerable relevance, given that they carry the majority of water flow to the upper part of the network. For this reason, pipes located in the external regions of the WDN (49, 48, 86, 101, 100, 119 on the left side of Fig 30d) rank in the last critical group (between top 51% and top 100%).

On the opposite, MP model is able to identify free surface flow pipes as well as pipes with zero flow rate, and this leads to substantially different outcomes. A significant variation in criticality ranking affects almost all the pipes in the central region (inside dotted box in Fig. 31c) that rank in the least critical group, even though, from just a hydraulic point of view, they are quite critical (as confirmed by $W_{p,n}$ ranking in Fig. 31a that instead place the majority of these pipes in the highest criticality group). According to MP model, these pipes are not essential anymore for network's functioning in the considered water scarcity scenario, because a large part of water flow is now redirected towards different parts of the network, specifically to pipes on the left side (49, 48 ,86, 101, 100, 119): all these pipes have now a higher criticality as they are crucial for the water supply to the upper region that, following MP model, cannot be supplied by the pipes in the central area, as instead suggested by HD model.

This notable difference in $MPCI_p$ rankings provided by the two numerical models mainly derives from several pipes connected to nodes with zero nodal flow: when this happens, said nodes will have a low $C_{WF(i)}$ value (Eq. 114) due to their number of reachable nodes $n_{\Re(i)}$ reducing to zero, finally causing $MPCI_p$ to drastically decrease or even attain zero.

This fact proves that the introduction of the term $C_{WF(i)}$ in Eq. (115) is necessary because otherwise, if the influence of a node i were given only by $C_{(i)}^{-1}$ (and not by $C_{(i)}^{-1}C_{WF(i)}$) than, in the final criticality calculation, node i will always have much higher influence then all the other connected nodes (whose influence is given by $\sum_{j=1,j\neq i}^{nd_i} W_{p,n(i,j)}C_{WF(j)}C_{(j)}^{-1}$) due to the higher order of magnitude of $C_{(i)}^{-1}$, as discussed when Eq. (115) was introduced.

A final consideration regards pipes 27 which, despite being ranked in the first criticality group according to the hydraulic weight $W_{p,n}$ (Fig. 31a), according to $MPCI_p$ (Fig. 31d) is placed in the last criticality group. This difference is the effect of low or even zero flow rate in all pipes connected to pipe 27. This aspect is correctly accounted for by $MPCI_p$ formulation and suggests that pipe 27 role is not fundamental anymore for the entire WDN.

In the following Table 4 Spearman coefficient's results are shown:

Table 4. Spearman's correlation coefficient r_s for Campofelice di Roccella WDN

$W_{p,n}$ (MP) - $W_{p,n}$ (HD) (Figs. 30a-30b)	$W_{p,n}$ (MP) - $MPCI_p$ (MP) (Figs. 30a-30c)	$W_{p,n}$ (HD) - $MPCI_p$ (HD) (Figs. 30b-30d)	$MPCI_p$ (MP) - $MPCI_p$ (HD) (Figs. 30c-30d)
0.703	0.478	0.903	0.651

Results confirmed what it is depicted in Fig 31. In particular, a strong correlation (r_s=0,903) is observed between the hydraulic weight $W_{p,n}$ and the criticality indicator $MPCI_p$ when HD approach is used. The main reason for this is HD approach not being able to detect free surface flow pipes, differently from MP approach which accordingly leads to a lower correlation (r_s=0,478) between $W_{p,n}$ and $MPCI_p$, finally suggesting that the topological information encompassed by $MPCI_p$ are useful for the final ranking.

4.2.3. Marchi Rural WDN

The third case study is the Marchi Rural water distribution network in Australia, which is based on a real irrigation system and can be classified as a transmission dense-loop network, differently from Network3 and Campofelice di Roccella WDN. The network has 2 reservoirs, 380 nodes and 477 pipes. In the following test only a regular functioning scenario was analyzed, where all nodal demands are satisfied, considering only HD approach to show how the proposed hydraulic weight and criticality indicator differ from those available in the literature.

In Fig. 32a the comparison between the hydraulic weight computed according to Marlim & Kang (2024) and the new formulation of Eq. (111) is presented:

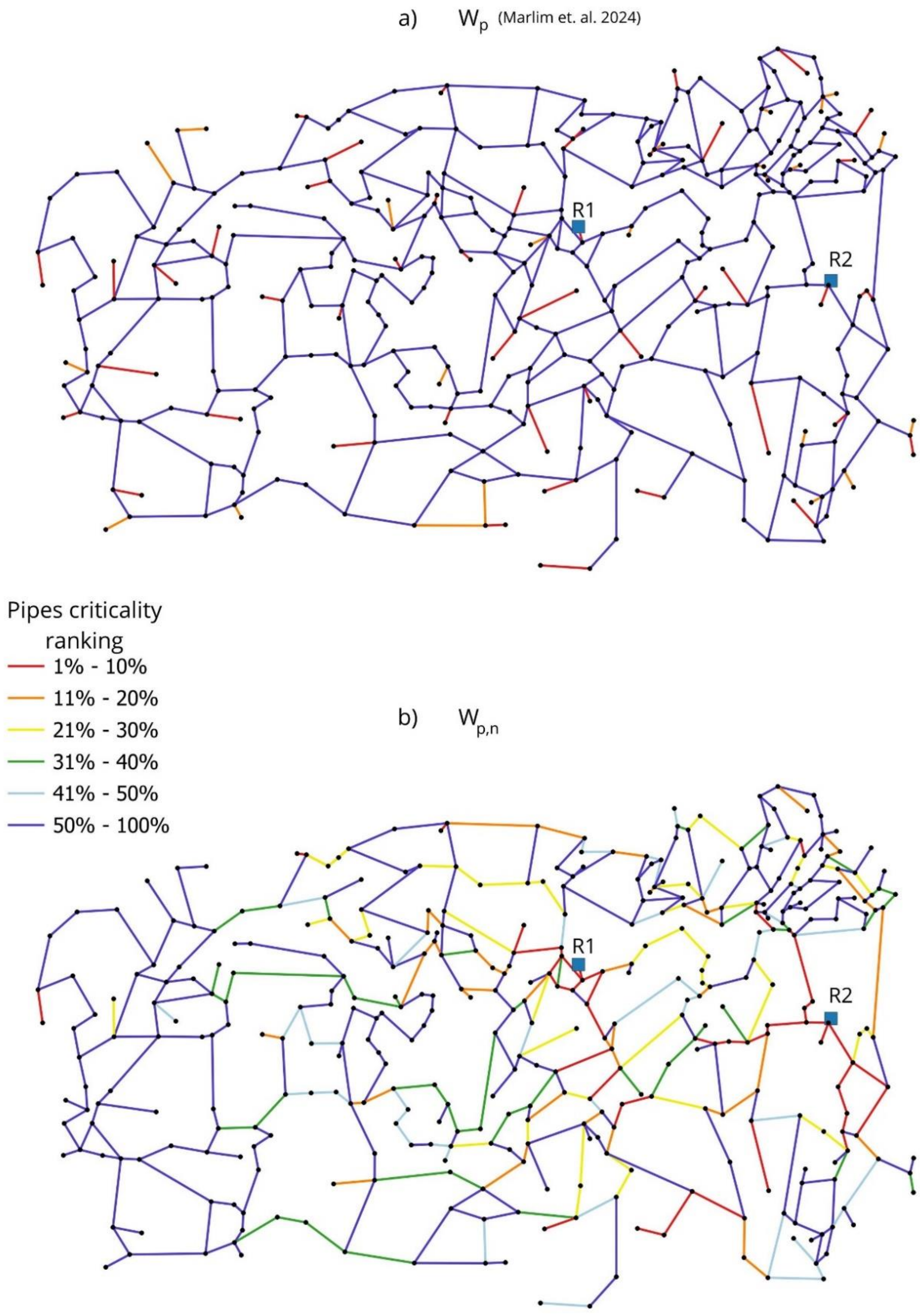

Figure 32. Marchi Rural WDN pipes ranked in six criticality groups depending on the considered indicator: e.g. considering the WDN with 477 pipes, “1% - 10%” refers to the first 47 (about 10%) pipes with the highest values of the computed indicator.. IDs of relevant pipes are depicted in black; head driven (HD) approach was used. Ranking according to:
a) W_p (Marlim & Kang (2024)) ; b) $W_{p,n}$

Large divergences emerge between Fig. 32a and Fig. 32b, mostly because of the high number of nodes characterized by zero demands: in fact, according to W_p proposed by Marlim & Kang (2024), when both nodes of a pipe have zero nodal demand, the corresponding W_p of said pipe will consequently be equal to zero, irrespective of pipe flow q_p that instead could be considerably high, especially in the areas near the two reservoirs R1 and R2 and in the area connecting separated regions of the network. For this reason, in Fig. 32a the real hydraulic dynamics occurring in the network cannot be observed, and the most critical pipes (depicted in red) are always those located in the peripheral areas of the WDN, independently from every other topological or hydraulic parameter.

Conversely, the proposed formulation of Eq. (111) correctly captures the real hydraulic dynamics and, as expected, the most critical pipes are located near the reservoirs, while a moderate criticality (between top 21% - top 40% $W_{p,n}$) is assigned to pipes that act as bridge between different sections of the WDN.

This test shows clearly that the proposed hydraulic weight is adequate even in network scenarios characterized by only few nodes having demands slightly higher than zero. Furthermore, even though only HD approach was applied, results are coherent with the expected hydraulic dynamics, and this again proves that the hydraulic weight of Eq. (111) does not need to rely on the MP approach, while obviously MP model is able to provide additional and useful information in the pressure reduction scenarios, as described in the previous section. The computed Spearman correlation coefficient is r_s=0,323, confirming the large divergence observed between Fig. 32a and Fig. 32b.

Finally, in Fig. 33 the criticality rankings obtained by HCC (Marlim & Kang (2024)) and $MPCI_p$ are shown:

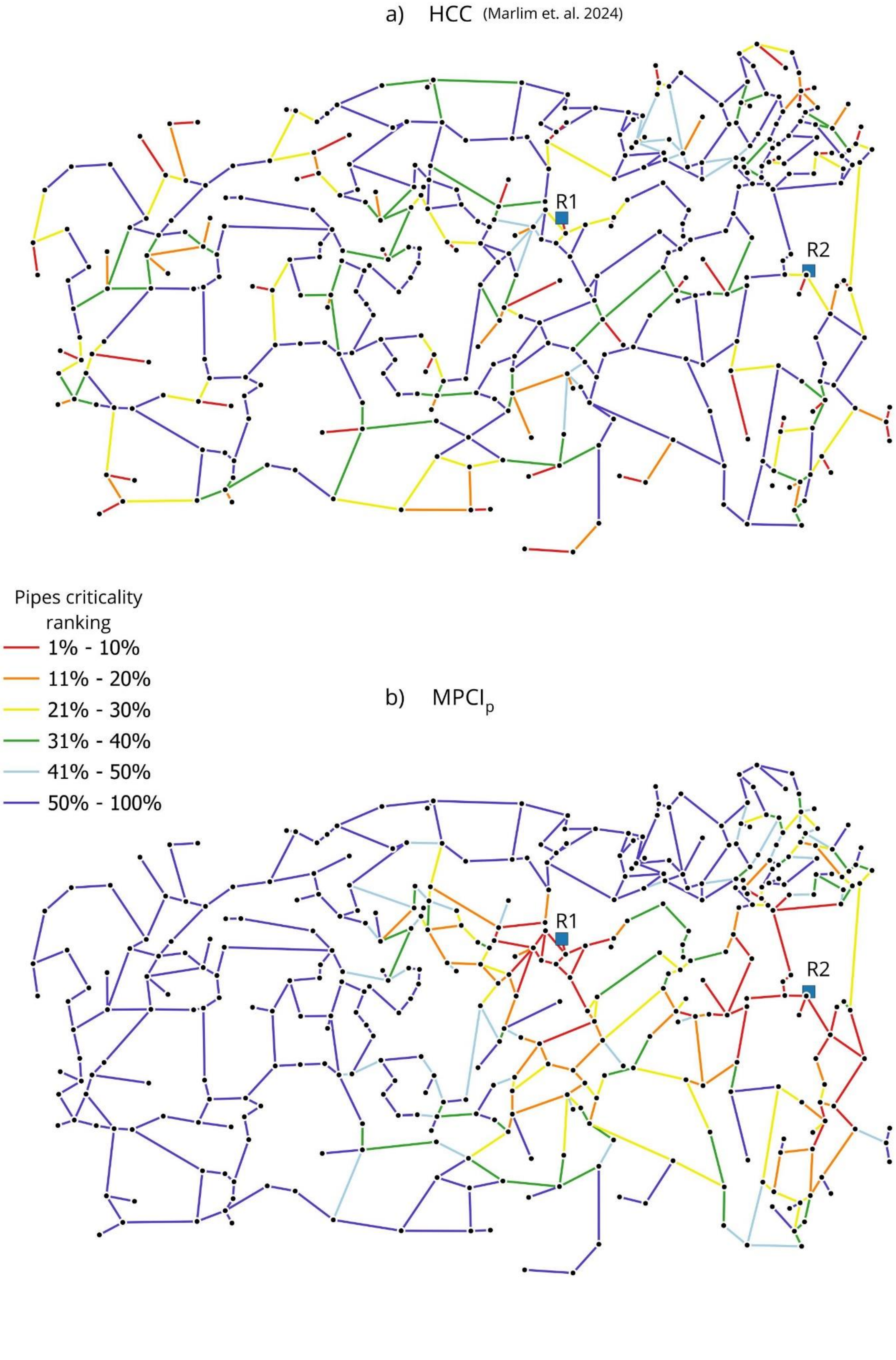

Figure 33. Marchi Rural WDN pipes ranked in six criticality groups depending on the considered indicator: e.g. considering the WDN with 477 pipes, "1% - 10%" refers to the first 47 (about 10%) pipes with the highest values of the computed indicator. IDs of relevant pipes are depicted in black; head driven (HD) approach was used. Ranking according to:
a) HCC (Marlim & Kang (2024)) ; b) $MPCI_p$

In this case it is extremely clear how the actual hydraulic dynamics of the network is almost completely lost when rankings are computed according to HCC (Fig. 33a): as expected, the errors arising from the W_p values of Fig. 32a were propagated and had a huge impact on HCC rankings, leading to an unclear criticality map where the external pipes of the network (characterized by one of their nodes with only a single connections) are always the most critical, regardless of every other parameter; moreover, some of the pipes that are quite close to reservoirs were ranked in the least critical group, while the opposite was expected, considering that they carry large water flows.

$MPCI_p$ ranking shown in Fig. 33b instead correctly represents the criticality expected, given that higher criticalities are assigned to pipes near reservoirs and medium criticality to pipes connecting different regions of the WDN; on the opposite, most pipes in marginal regions are depicted in blue.

5. Conclusions

The present thesis focused on the development of a new methodology for pipes criticality assessment in water distribution networks (WDNs). The proposed procedure is based on the new minimum pressure (MP) approach for hydraulic modeling of WDNs and the minimum pressure criticality indicator (MPCI).

The minimum pressure model for WDNs steady state modeling is built on the assumption that air entrainment could occur in the water network, due to even small leakages or due to vents in the pipes when water pressure attains zero relative value. It has been shown how air intrusion changes the original completely diffusive problem into a mixed convective-diffusive numerical problem, due to free surface flow occurring in some of the pipes. Numerical tests carried out on two real case studies highlighted the differences in computed nodal and pipe flow rates, as well as on nodal pressures, between minimum pressure approach and the traditional head driven (HD) model. As described in chapter 4, when only regular functioning scenarios are analyzed, results provided by MP approach almost completely coincide with those provided by HD model. However, in more critical scenarios, such as pipes' isolation for maintenance or water supply reduction, differences could become significant, leading to considerably diverse outcomes compared to traditional approaches, which are unable to identify free surface flow pipes and could lead to unrealistic negative pressures in nodes, consequently impacting the flow regime and pressures in the entire network. This shows that the hypothesis of network permeability to air leads to more realistic and physically based results compared to DD and HD approaches.

The new proposed criticality indicator ($MPCI$) was developed integrating both topological features of the network, provided by structural hole theory, and hydraulic parameters depending on the chosen model for numerical simulation, being also able to incorporate the information given by the MP approach about free surface flow occurring in some pipes due to zero relative pressure. $MPCI$ encompasses the new defined hydraulic weight W_p, which is aimed at providing a criticality ranking based only on hydraulic characteristics of pipes, taking into account several parameters such as actual nodal and pipes flow rates, unmet nodal demand and velocities in free surface flow part of each pipe. W_p is particularly useful to identify pipes experiencing hydraulic stress, especially those characterized by free surface flow that induce high velocities. Moreover, when WDNs are subject to intermittent supply, pipes velocities could be considerably low or even zero during water scarcity period, to subsequently return to a normal range in regular functioning conditions: these continuous variations between low and high velocities in pipes could pose a serious risk for water quality in the network. Thus W_p is valuable in detecting those pipes majorly exposed to these risks, offering to the water manager a simple but effective instrument for prioritized pipes maintenance. When the criticality ranking showed by the hydraulic weight W_p is properly integrated with the information provided by the structural hole influence matrix, $MPCI$ is obtained. Following the analyzed test cases, $MPCI$ proved to be able to give a reliable estimation of the most critical pipes in the considered network, even when the traditional HD approach is used. Nonetheless, considering water supply reduction, the use of MP numerical model to classify pipes according to $MPCI$ leads to substantially different criticality rankings compared to the ranking obtained using HD or even DD approaches. Test cases were performed to compare $MPCI$ with criticality indicator available in the literature as HCC: while in networks where almost all nodes have a demand higher than zero the results offered by $MPCI$ are similar to the one provided by HCC, in networks where several nodes are characterized by zero demands the criticality rankings differ remarkably; furthermore, in the case of pressure reduction or water supply deficiency results could completely diverge.

Finally, the adoption of MP model and $MPCI$ proved to be a useful tool for the modeling and management of WDNs, offering a more realistic representation of the hydraulic behavior of the network, especially in critical conditions characterized by air intrusion and free surface flow. $MPCI$ capability to integrate topological aspects with hydraulic ones, together with its sensitivity to the physical dynamics captured by MP model, makes it a helpful instrument to identify critical pipes.

Future improvements of the proposed methodology could include new tests in more complex and diverse networks with more reservoirs, pumps or isolation valves, to analyze the impact that valves' isolation has on the hydraulic dynamics on the network. $MPCI$ might be implemented in water quality studies to more accurately establish the relationship between pipes' velocities and water quality, especially in segments' isolation events that could lead to unexpected changes in flow directions in pipes. In addition, $MPCI$ could become an objective function for new networks planning, with the aim to optimize its layout and improve overall resilience.

In conclusion, this thesis showed that, although well designed WDN usually do not experience negative pressures, in the events of failure of one or more components of the network or in water scarcity periods the traditional HD and DD hydraulic models, as well as available criticality indicators, could fail to correctly represent pipes' criticality. The proposed MP numerical model along with $MPCI$ offer a new and more accurate perspective to help water manager in a prioritized planning for pipes maintenance.

References

Abbott, M.L. Optimization of Redundancy in Branched Water Distribution Systems, 2012.

Abdel-Mottaleb, N.; Walski, T. Identifying Vulnerable and Critical Water Distribution Segments. *World Environmental and Water Resources Congress 2011* **2020**, doi:10.1061/9780784482971.032.

Aricò, C.; Tucciarelli, T. MAST Solution of Advection Problems in Irrotational Flow Fields. *Advances in Water Resources* **2006**, *30*, 665–685, doi:10.1016/j.advwatres.2006.03.007.

Baoyu, Z.; Xinhua, Z.; Yuan, Z. *Vulnerability Assessment of Regional Water Distribution Systems*; 2009; pp. 473–477.

Boxall, J.B.; Saul, A.J. Modeling Discoloration in Potable Water Distribution Systems. *Journal of Environmental Engineering* **2005**, *131*, 716–725, doi:10.1061/(asce)0733-9372(2005)131:5(716.

Braga, A.S.; Saulnier, R.; Filion, Y.; Cushing, A. Dynamics of Material Detachment from Drinking Water Pipes under Flushing Conditions in a Full-Scale Drinking Water Laboratory System. *Urban Water Journal* **2020**, *17*, 745–753, doi:10.1080/1573062x.2020.1800759.

Bruneau, M.; Chang, S.E.; Eguchi, R.T.; Lee, G.C.; O'Rourke, T.D.; Reinhorn, A.M.; Shinozuka, M.; Tierney, K.; Wallace, W.A.; Von Winterfeldt, D. A Framework to Quantitatively Assess and Enhance the Seismic Resilience of Communities. *Earthquake Spectra* **2003**, *19*, 733–752, doi:10.1193/1.1623497.

Buhl, C.; Gautrais, J.; Reeves, N.; Solé, R.V.; Valverde, S.; Kuntz, P.; Theraulaz, G. Topological Patterns in Street Networks of Self-Organized Urban Settlements. *The European Physical Journal B* **2006**, *49*, 513–522, doi:10.1140/epjb/e2006-00085-1.

Burt, R.S. Structural Holes: The Social Structure of Competition. *SSRN Electronic Journal* **1992**.

Ciaponi, C. La valutazione delle prestazioni dei sistemi acquedottistici, Atti, Acqua e città – II Convegno Nazionale di Idraulica Urbana, Chia (CA), 25-28 settembre 2007.

Clark, R.M.; Rossman, L.A.; Wymer, L.J. Modeling Distribution System Water Quality: Regulatory Implications. *Journal of Water Resources Planning and Management* **1995**, *121*, 423–428, doi:10.1061/(asce)0733-9496(1995)121:6(423).

Creaco, E. Global Algorithm Based on Inverse Outflow/Head Relationship for Solving Water Distribution Networks with Multiple Nodal Outflows and Improved Convergence. *Journal of Water Resources Planning and Management* **2025**, 151, doi:10.1061/jwrmd5.wreng-6681.

Creaco, E.; Franchini, M.; Todini, E. Generalized Resilience and Failure Indices for Use with Pressure-Driven Modeling and Leakage. *Journal of Water Resources Planning and Management* **2016**, *142*, doi:10.1061/(asce)wr.1943-5452.0000656.

Cross, H. Analysis of Flow in Networks of Conduits or Conductors. *Bulletin No. 286, Engineering Experiment Station, Univ. of Illinois, Urbana, IL.* **1936**

Deyi, M.; Van Zyl, J.; Shepherd, M. Applying the FAVAD Concept and Leakage Number to Real Networks: A Case Study in Kwadabeka, South Africa. *Procedia Engineering* **2014**, *89*, 1537–1544, doi:10.1016/j.proeng.2014.11.450.

Eggimann, S.; Mutzner, L.; Wani, O.; Schneider, M.Y.; Spuhler, D.; De Vitry, M.M.; Beutler, P.; Maurer, M. The potential of knowing more: A review of data-driven urban water management. *Environ. Sci. Technol.* **2017**, 51, 2538–2553.

Fontanazza, C.; Freni, G.; Loggia, G.; Notaro, V.; Puleo, V. Evaluation of the Water Scarcity Energy Cost for Users. *Energies* **2013**, *6*, 220–234, doi:10.3390/en6010220.

Fortunato, A. Scelta degli interventi di riabilitazione delle reti idriche con una base informativa limitata, 2012.

Freeman, L.C. A Set of Measures of Centrality Based on Betweenness. *Sociometry* **1977**, *40*, 35, doi:10.2307/3033543.

Fujiwara, O.; Khang, D.B. A Two-phase Decomposition Method for Optimal Design of Looped Water Distribution Networks. *Water Resources Research* **1990**, *26*, 539–549, doi:10.1029/wr026i004p00539.

Fujiwara, O.; Li, J. Reliability Analysis of Water Distribution Networks in Consideration of Equity, Redistribution, and Pressure-dependent Demand. *Water Resources Research* **1998**, *34*, 1843–1850, doi:10.1029/98wr00908.

Germanopoulos, G. A Technical Note on the Inclusion of Pressure Dependent Demand and Leakage Terms in Water Supply Network Models. *Civil Engineering Systems* **1985**, *2*, 171–179, doi:10.1080/02630258508970401.

Giustolisi, O.; Savic, D.; Kapelan, Z. Pressure-Driven Demand and Leakage Simulation for Water Distribution Networks. *Journal of Hydraulic Engineering* **2008**, *134*, 626–635, doi:10.1061/(asce)0733-9429(2008)134:5(626.

Hommes, L.; Boelens, R. Urbanizing Rural Waters: Rural-Urban Water Transfers and the Reconfiguration of Hydrosocial Territories in Lima. *Political Geography* **2016**, *57*, 71–80, doi:10.1016/j.polgeo.2016.12.002.

Husband, S.; Boxall, J. Understanding and Managing Discolouration Risk in Trunk Mains. *Water Research* **2016**, *107*, 127–140, doi:10.1016/j.watres.2016.10.049.

Jayaram, N.; Srinivasan, K. Performance-based Optimal Design and Rehabilitation of Water Distribution Networks Using Life Cycle Costing. *Water Resources Research* **2008**, *44*, doi:10.1029/2006wr005316.

Jeong, G.; Kang, D. Comparative Analysis of Reliability Indices and Hydraulic Measures for Water Distribution Network Performance Evaluation. *Water* **2020**, *12*, 2399, doi:10.3390/w12092399.

Jun, H.; Loganathan, G.V. Valve-Controlled Segments in Water Distribution Systems. *Journal of Water Resources Planning and Management* **2007**, *133*, 145–155, doi:10.1061/(asce)0733-9496(2007)133:2(145.

Khadr, W.M.H.; Hamed, M.M.; Nashwan, M.S. Pressure Driven Analysis of Water Distribution Systems for Preventing Siphonic Flow. *Journal of Hydro-environment Research* **2022**, *44*, 102–109, doi:10.1016/j.jher.2022.09.001.

Latora, V.; Marchiori, M. Efficient Behavior of Small-World Networks. *Physical Review Letters* **2001**, *87*, doi:10.1103/physrevlett.87.198701.

Marlim, M.S.; Jeong, G.; Kang, D. Identification of Critical Pipes Using a Criticality Index in Water Distribution Networks. *Applied Sciences* **2019**, *9*, 4052, doi:10.3390/app9194052.

Marlim, M.S.; Kang, D. Hydraulic Connectiveness Metric for the Analysis of Criticality in Water Distribution Networks. *Water* **2024**, *16*, 1498, doi:10.3390/w16111498.

May, J. Leakage, pressure and control. *BICS International Conf. on Leakage Control* **1994** London.

Mays, L.W. *Water Distribution System Handbook*; 2000.

Mekonnen, M.M.; Hoekstra, A.Y. Four Billion People Facing Severe Water Scarcity. *Science Advances* **2016**, *2*, doi:10.1126/sciadv.1500323.

Pabi, S.; Amarnath, A.; Goldstein, R.; Reekie, L. Electricity use and management in the municipal water supply and wastewater industries. Palo Alto: Electric Power Research Institute; 2013. p. 194.

Pacchin, E.; Alvisi, S.; Franchini, M. A New Non-Iterative Method for Pressure-Driven Snapshot Simulations with EPANET. *Procedia Engineering* **2017**, *186*, 135–142, doi:10.1016/j.proeng.2017.03.219.

Prasad, T.D.; Park, N.-S. Multiobjective Genetic Algorithms for Design of Water Distribution Networks. *Journal of Water Resources Planning and Management* **2003**, *130*, 73–82, doi:10.1061/(asce)0733-9496(2004)130:1(73.

Rossman, L. A. EPANET 2 users manual. *Water Supply and Water Resources Division* **2000**, National Risk Management Research Laboratory, Rep. No. EPA/600/ R-00/057 Cincinnati.

Shin, G.; Kwon, S.H.; Lee, S. Designing Isolation Valve System to Prevent Unexpected Water Quality Incident. *Sustainability* **2023**, *16*, 153, doi:10.3390/su16010153.

Tanyimboh, T.T.; Tabesh, M.; Burrows, R. Appraisal of Source Head Methods for Calculating Reliability of Water Distribution Networks. *Journal of Water Resources Planning and Management* **2001**, *127*, 206–213, doi:10.1061/(asce)0733-9496(2001)127:4(206.

Todini, E. A More Realistic Approach to the "Extended Period Simulation" of Water Distribution Networks. In *Taylor & Francis eBooks*; 2003.

Todini, E. Looped Water Distribution Networks Design Using a Resilience Index Based Heuristic Approach. *Urban Water* **2000**, *2*, 115–122, doi:10.1016/s1462-0758(00)00049-2.

Todini, E. Un metodo del gradiente per la verifica delle reti idrauliche, Bollettino degli Ingegneri della Toscana n.11, Bologna, 1979, pp.11-14.

Todini, E.; Pilati, S. A Gradient Algorithm for the Analysis of Pipe Networks; 1988; pp. 1–20.

Todini, E.; Pilati, S. A gradient method for the solution of looped pipe networks", *Computer Applications in Water Supply* **1987**, Volume 1 (System analysis and simulation), John Wiley & Sons.

Todini, E.; Rossman, L.A. Unified Framework for Deriving Simultaneous Equation Algorithms for Water Distribution Networks. *Journal of Hydraulic Engineering* **2012**, *139*, 511–526, doi:10.1061/(asce)hy.1943-7900.0000703.

Todini, E.; Farina, A.; Gabriele, A.; Gargano, R.; Rossman, L.A. Comparing Alternative PDA Solvers with EPANET. *Journal of Hydroinformatics* **2022**, *24*, 697–710, doi:10.2166/hydro.2022.005.

Tornyeviadzi, H.M.; Neba, F.A.; Mohammed, H.; Seidu, R. Nodal Vulnerability Assessment of Water Distribution Networks: An Integrated Fuzzy AHP-TOPSIS Approach. *International Journal of Critical Infrastructure Protection* **2021**, *34*, 100434, doi:10.1016/j.ijcip.2021.100434.

Tucciarelli, T.; Criminisi, A.; Termini, D. Leak Analysis in Pipeline Systems by Means of Optimal Valve Regulation. *Journal of Hydraulic Engineering* **1999**, *125*, 277–285, doi:10.1061/(asce)0733-9429(1999)125:3(277.

UN-DESA, United Nations Department of Economic and Social Affairs, 2018. World Urbanization Prospects: The 2018 Revision, Highlights. United Nations, New York. Retrieved from https://population.un.org/wup/Publications/Files/WUP2018-KeyFacts.pdf.

Van Zyl, J.; Cassa, A. Linking the power and FAVAD equation for modelling the effect of pressure on leakage. *Eleventh International Conference on Computing and Control for Water Industry (CCWI)* **2011**, University of Exeter, United Kingdom.

Vreeburg, J.H.G.; Blokker, E.J.M.; Horst, P.; Van Dijk, J.C. Velocity-Based Self-Cleaning Residential Drinking Water Distribution Systems. *Water Science & Technology Water Supply* **2009**, *9*, 635–641, doi:10.2166/ws.2009.689.

Wagner, J.M.; Shamir, U.; Marks, D.H. Water Distribution Reliability: Simulation Methods. *Journal of Water Resources Planning and Management* **1988**, 114, 276–294, doi:10.1061/(asce)0733-9496(1988)114:3(276.

Walski, T.M.; Pelliccia, A. Economic Analysis of Water Main Breaks. *American Water Works Association* **1982**, *74*, 140–147, doi:10.1002/j.1551-8833.1982.tb04874.x.

Wasserman, S.; Faust, K. *Social Network Analysis: Methods and Applications*; 1994.

Wood, D.J.; Charles, C.O.A. Hydraulic Network Analysis Using Linear Theory. *Journal of the Hydraulics Division* **1972**, *98*, 1157–1170, doi:10.1061/jyceaj.0003348.

Yang, E.; Faust, K.M. Quantifying the Impact of Population Dynamics on the Structural Robustness of Water Infrastructure Using a Structural Hole Influence Matrix Approach. *ACS ES&T Water* **2022**, *2*, 1161–1173, doi:10.1021/acsestwater.1c00433.

Zhu, C.; Wang, X.; Zhu, L. A Novel Method of Evaluating Key Nodes in Complex Networks. *Chaos Solitons & Fractals* **2017**, *96*, 43–50, doi:10.1016/j.chaos.2017.01.007.